Available online at www.sciencedirect.com
ScienceDirect
Geochimica et Cosmochimica Acta 73 (2009) 4963–4997
Geochimica et Cosmochimica Acta
www.elsevier.com/locate/gca

Origin and chronology of chondritic components: A review

A.N. Krot [a,*], Y. Amelin [b], P. Bland [c], F.J. Ciesla [d], J. Connelly [e,f], A.M. Davis [g], G.R. Huss [a], I.D. Hutcheon [h], K. Makide [a], K. Nagashima [a], L.E. Nyquist [i], S.S. Russell [j], E.R.D. Scott [a], K. Thrane [e], H. Yurimoto [k], Q.-Z. Yin [l]

[a] *Hawai'i Institute of Geophysics and Planetology, School of Ocean and Earth Science and Technology, University of Hawai'i at Manoa, Honolulu, HI 96822, USA*
[b] *Planetary Science Institute and Research School of Earth Sciences, The Australian National University, Canberra, ACT 0200, Australia*
[c] *Impacts and Astromaterials Research Centre, Department of Earth Science and Engineering, Imperial College London, South Kensington Campus, London SW7 2AZ, UK*
[d] *Department of Geophysical Sciences, The University of Chicago, 5734 South Ellis Avenue, Chicago, IL 60637, USA*
[e] *Geological Museum, Øster Voldgade 5-7, DK-1350, University of Copenhagen, Denmark*
[f] *Jackson School of Geosciences, The University of Texas at Austin, TX, USA*
[g] *University of Chicago, Chicago, USA*
[h] *Glenn T. Seaborg Institute, Lawrence Livermore National Laboratory, Livermore, CA 94451, USA*
[i] *NASA Johnson Space Center, 2101 NASA Parkway, Houston, TX 77058-3696, USA*
[j] *Department of Mineralogy, The Natural History Museum, Cromwell Road, London SW7 5BD, UK*
[k] *Division of Earth and Planetary Sciences, Hokkaido University, Sapporo 060-0810, Japan*
[l] *Department of Geology, University of California Davis, Davis, CA 95616, USA*

Received 17 March 2008; accepted in revised form 29 September 2008; available online 30 May 2009

Abstract

Mineralogical observations, chemical and oxygen–isotope compositions, absolute ^{207}Pb–^{206}Pb ages and short-lived isotope systematics (^{7}Be–^{7}Li, ^{10}Be–^{10}B, ^{26}Al–^{26}Mg, ^{36}Cl–^{36}S, ^{41}Ca–^{41}K, ^{53}Mn–^{53}Cr, ^{60}Fe–^{60}Ni, ^{182}Hf–^{182}W) of refractory inclusions [Ca,Al-rich inclusions (CAIs) and amoeboid olivine aggregates (AOAs)], chondrules and matrices from primitive (unmetamorphosed) chondrites are reviewed in an attempt to test (i) the *x*-wind model *vs.* the shock-wave model of the origin of chondritic components and (ii) irradiation *vs.* stellar origin of short-lived radionuclides. The data reviewed are consistent with an external, stellar origin for most short-lived radionuclides (^{7}Be, ^{10}Be, and ^{36}Cl are important exceptions) and a shock-wave model for chondrule formation, and provide a sound basis for early Solar System chronology. They are inconsistent with the *x*-wind model for the origin of chondritic components and a local, irradiation origin of ^{26}Al, ^{41}Ca, and ^{53}Mn. ^{10}Be is heterogeneously distributed among CAIs, indicating its formation by local irradiation and precluding its use for the early solar system chronology. ^{41}Ca–^{41}K, and ^{60}Fe–^{60}Ni systematics are important for understanding the astrophysical setting of Solar System formation and origin of short-lived radionuclides, but so far have limited implications for the chronology of chondritic components. The chronological significance of oxygen–isotope compositions of chondritic components is limited. The following general picture of formation of chondritic components is inferred. CAIs and AOAs were the first solids formed in the solar nebula ~4567–4568 Myr ago, possibly within a period of <0.1 Myr, when the Sun was an infalling (class 0) and evolved (class I) protostar. They formed during multiple transient heating events in nebular region(s) with high ambient temperature (at or above condensation temperature of forsterite), either throughout the inner protoplanetary disk (1–4 AU) or in a localized region near the proto-Sun (<0.1 AU), and were subsequently dispersed throughout the disk. Most CAIs and AOAs formed in the presence of an ^{16}O-rich ($\Delta^{17}O \sim -24 \pm 2‰$) nebular gas. The ^{26}Al-poor [$(^{26}Al/^{27}Al)_0 < 1 \times 10^{-5}$], ^{16}O-rich ($\Delta^{17}O \sim -24 \pm 2‰$) CAIs – FUN (fractionation and unidentified nuclear effects) CAIs in CV chondrites, platy hibonite

* Corresponding author.
E-mail address: sasha@higp.hawaii.edu (A.N. Krot).

0016-7037/$ - see front matter
doi:10.1016/j.gca.2008.09.039

crystals (PLACs) in CM chondrites, pyroxene–hibonite spherules in CM and CO chondrites, and the majority of grossite- and hibonite-rich CAIs in CH chondrites—may have formed prior to injection and/or homogenization of ^{26}Al in the early Solar System. A small number of igneous CAIs in ordinary, enstatite and carbonaceous chondrites, and virtually all CAIs in CB chondrites are ^{16}O-depleted ($\Delta^{17}O > -10‰$) and have $(^{26}Al/^{27}Al)_0$ similar to those in chondrules ($<1 \times 10^{-5}$). These CAIs probably experienced melting during chondrule formation. Chondrules and most of the fine-grained matrix materials in primitive chondrites formed 1–4 Myr after CAIs, when the Sun was a classical (class II) and weak-lined T Tauri star (class III). These chondritic components formed during multiple transient heating events in regions with low ambient temperature (<1000 K) throughout the inner protoplanetary disk in the presence of ^{16}O-poor ($\Delta^{17}O > -5‰$) nebular gas. The majority of chondrules within a chondrite group may have formed over a much shorter period of time (<0.5–1 Myr). Mineralogical and isotopic observations indicate that CAIs were present in the regions where chondrules formed and accreted (1–4 AU), indicating that CAIs were present in the disk as free-floating objects for at least 4 Myr. Many CAIs, however, were largely unaffected by chondrule melting, suggesting that chondrule-forming events experienced by a nebular region could have been small in scale and limited in number. Chondrules and metal grains in CB chondrites formed during a single-stage, highly-energetic event ~4563 Myr ago, possibly from a gas-melt plume produced by collision between planetary embryos.

1. INTRODUCTION

Chondritic meteorites (chondrites) consist of three major components—chondrules, matrix, and refractory inclusions, which include Ca,Al-rich inclusions (CAIs) and amoeboid olivine aggregates (AOAs). Two kinds of models for the origin and chronology of chondritic components, which propose different origins for short-lived radionuclides (with a half-life of <10 Myr; see Table 1) in the early Solar System, are currently being debated—(i) shock-wave models (Desch et al., 2005 and references therein), often discussed together with external, stellar origin of short-lived radionuclides (e.g., Goswami et al., 2005 and references therein), and (ii) *x*-wind model (Shu et al., 1996, 2001) commonly associated with a local, irradiation origin of short-lived radionuclides (Lee et al., 1998; Gounelle et al., 2001, 2006; Leya et al., 2003). Neither model is necessarily coupled with a specific scenario for the production of short-lived radionuclides.

According to the shock-wave models, CAIs, chondrules and most of the matrix materials formed in the inner (1–4 AU) disk as a result of multiple transient heating events caused by shock waves that thermally processed presolar dust that was initially mostly amorphous (Fig. 1). The nature of shock waves in the protoplanetary disk remains unclear: they could have resulted from fast moving planetesimals (Hood et al., 2005), collisions between planetary embryos (Hood et al., 2008), X-ray flares (Nakamoto et al., 2005), or disk gravitational instability (Boss and Durisen, 2005). Shock-wave models satisfactorily explain the thermal history of chondrules (Desch and Connolly, 2002; Miura and Nakamoto, 2006) and igneous CAIs (Richter et al., 2006), chondrule–matrix relationship (Scott and Krot, 2005), and multistage reprocessing of chondrules and CAIs (e.g., Jones et al., 2005; Russell et al., 2005; Krot et al., 2007a), and therefore are currently favored.

According to one class of models of external origin of short-lived radionuclides (e.g., Hester and Desch, 2005; Ouellette et al., 2005), the Sun formed in an *H II* region with one or several massive stars. One of these stars exploded as a supernova and injected freshly-synthesized, short-lived radionuclides either into the protosolar molecular cloud or the protoplanetary disk. These radionuclides were quickly homogenized and, therefore, can be used for the early Solar System chronology, including chronology of chondritic components. Testable implications of a model of an external origin of short-lived radionuclides include (i) homogeneity of short-lived radionuclides, (ii) correlation of their abundances, and (iii) the existence of consistent cross-calibrations of chronologies based on short-lived (relative) and long-lived (absolute) isotope systematics (e.g., Wadhwa et al., 2007). The timing and mechanism of injection of short-lived radionuclides into the Solar System remain controversial. For example, it was proposed that ^{26}Al had been injected into the molecular cloud with the stellar wind of massive star(s) prior to supernova explosion that introduced ^{60}Fe (Bizzarro et al., 2007a), that ^{60}Fe and ^{26}Al could be due to local enhancement of ^{60}Fe and ^{26}Al in the Sun-forming region as a result of explosion of a single or multiple supernova prior to the collapse of the protosolar molecular cloud (Gounelle et al., 2008), and that ^{53}Mn could have resulted from galactic chemical evolution (e.g., Huss et al., 2009 and references therein).

The fluctuating *x*-wind model of Shu and co-workers (Shu et al., 1996, 1997, 2001; Lee et al., 1998; Gounelle et al., 2001) is based on (i) astronomical observations, including bi-polar outflows (e.g., Reipurth and Bally, 2001) and powerful X-ray flares (Glassgold et al., 2005 and references therein) associated with young stellar objects, (ii) theoretical modeling of the interaction of the magnetic field of a star and its protoplanetary disk (Shu et al., 1996), and (iii) theoretical modeling of the irradiation origin of short-lived radionuclides, which, given a number of assumptions reproduces to within a factor of 10 or so their initial abundances in the Solar System (Gounelle et al., 2001, 2006; Leya et al., 2003; Chaussidon and Gounelle, 2006). The *x*-wind model was originally proposed for the origin of chondritic components, specifically to explain the coexistence of high-temperature chondritic components, CAIs and chondrules, and apparently thermally unprocessed fine-grained matrix material, that accreted together at 1–4 AU into chondrite parent bodies (Shu et al., 1996, 1997). It was later expanded to explain the origin of short-lived radionuclides in the early Solar System (Lee et al., 1998; Shu et al., 2001; Gounelle et al., 2001, 2006). According to this model, schematically illustrated in

Table 1
Short-lived ($t_{1/2} < 10$ Myr) radionuclides detected in chondritic components, their inferred initial abundances and proposed origin.

Isotope	$t_{1/2}$ (Myr)	Daughter isotope	Reference isotope	Initial abundance[a]	Proposed origin
^{41}Ca	0.1	^{41}K	^{40}Ca	$(^{41}Ca/^{40}Ca)_0 \sim 1.5 \times 10^{-8}$	Stellar (AGB, massive stars, WR, ccSN), solar irradiation
^{36}Cl	0.3	^{36}Ar	^{35}Cl	$(^{36}Cl/^{35}Cl)_0 > 1.6 \times 10^{-4*}$	Stellar (AGB, massive stars, WR, ccSN), solar irradiation
^{26}Al	0.74	^{26}Mg	^{27}Al	$(^{26}Al/^{27}Al)_0 \sim 5 \times 10^{-5}$	Stellar (AGB, massive stars, WR, ccSN), solar irradiation
^{7}Be[b]	53 days	^{7}Li	^{9}Be	$(^{7}Be/^{9}Be)_0 \sim 6 \times 10^{-3}$	Solar irradiation
^{10}Be	1.5	^{10}B	^{9}Be	$(^{10}Be/^{9}Be)_0 \sim (0.5–1.2) \times 10^{-3}$	Solar irradiation, trapped galactic cosmic rays
^{60}Fe	1.5	^{60}Ni	^{56}Fe	$(^{60}Fe/^{56}Fe)_0 \sim (0.5–1) \times 10^{-6*}$	Stellar (AGB, massive stars, SNIa)
^{53}Mn	3.7	^{53}Cr	^{55}Mn	$(^{53}Mn/^{55}Mn)_0 \sim 1 \times 10^{-5*}$	Stellar (massive stars, SNIa), solar irradiation
^{182}Hf	9	^{182}W	^{180}Hf	$(^{182}Hf/^{180}Hf)_0 \sim 1 \times 10^{-4}$	Stellar (SN, NS)

Sources of data: Goswami et al. (2005) and references listed therein; see also text.
AGB = Asymptotic Giant Branch star; NS = neutron star; ccSN = core-collapse Supernova; SNIa = type Ia Supernova; WR = Wolf-Rayet star.
[a] The tabulated values are based on analysis of CAIs or are extrapolated (indicated by "*") to the time of CAI formation based on the analyses of chondrules or bulk chondrites.
[b] Suggestive evidence for presence reported; needs confirmation.

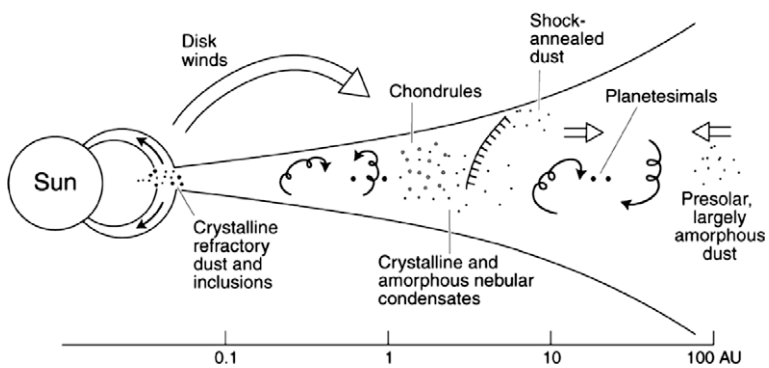

Fig. 1. Schematic diagram showing how amorphous, presolar dust may have been thermally processed in the protoplanetary disk as a result of shocks before accretion into chondritic and cometary planetesimals. Most matrix silicates in primitive chondrites are crystalline, magnesian silicate and amorphous ferromagnesian silicate that condensed when dust aggregates were melted in the disk to form chondrules. Dust that accreted at 2–3 AU into chondrite matrices contains traces of refractory dust ($\sim 10^{-5}$–10^{-4}) that were dispersed from the inner edge of the disk by disk winds and turbulence, and presolar, crystalline silicates and refractory oxides ($\sim 10^{-5}$) and presolar, amorphous silicates and oxides ($\sim 10^{-6}$), which escaped thermal processing. Comets accreted dust at >10 AU containing traces of refractory nebular dust ($\sim 10^{-6}$–10^{-5}) and presolar, crystalline silicates and oxides (~0.1%). Debris from planetesimal collisions at the midplane became increasingly important at later stages (from Scott and Krot (2005)).

Fig. 2, disk accretion at a rate M_D divides at inner disk radius $R_x \sim 0.06$ AU into a funnel flow onto a star and an x-wind outflow. The inner edge of the disk undergoes periodic radial excursions on a short timescale of ~30 yr, perhaps in response to protosolar magnetic cycles. Flares induced by the stressing of magnetic fields threading both the star and the inner edge of the fluctuating disk melt solids in the transition zone between the base of the funnel flow and the reconnection ring, and in the reconnection ring itself. Rocks that fall into the reconnection ring from the funnel flow or that drift into it from the gaseous disk in the reconnection ring are exposed to irradiation by the fast particles (^{1}H, ^{4}He, and ^{3}He) accelerated in gradual and impulsive flares. CAIs formed in the gas-depleted reconnection ring were fully exposed to solar irradiation; chondrules formed contemporaneously with CAIs in the gaseous disk, near the x-region, and were shielded from irradiation to varying degrees. CAIs irradiated in the reconnection ring during a period when R_x is relatively large (because the dipole magnetic moment, μ^*, of the star is strong or the disk accretion rate, M_D, is weak) can later be picked up and launched in the x-wind together with chondrules when a fluctuation (due to decrease in μ^* or increase in M_D) causes the base of the x-wind R_x to migrate to the region previously occupied by such rocks. The magnetocentrifugally-driven x-wind transported chondrules and CAIs to 1–20 AU, where they accreted with thermally unprocessed matrix materials into chondritic and cometary bodies. Since in the x-wind model most short-lived radionuclides, except ^{60}Fe, formed by irradiation near the proto-Sun, they were heterogeneously distributed in the protoplanetary disk, and, as a result, cannot be used for chronology of CAI and chondrule formation.

Several meteorite observations were interpreted as evidence supporting the x-wind model and an irradiation origin of short-lived radionuclides or at least, as consistent with them. These include (i) detection in CAIs of short-lived radionuclides that are not made plentifully in stellar

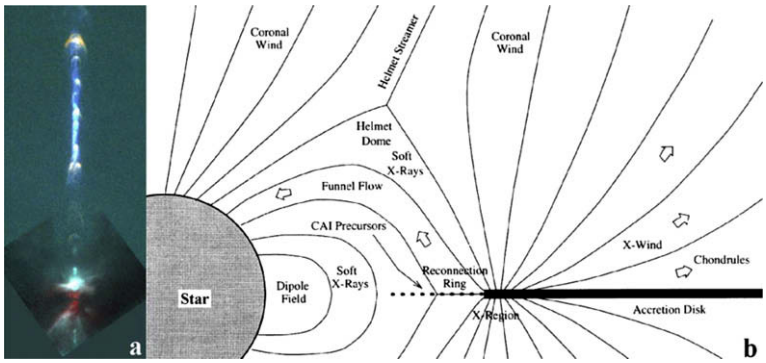

Fig. 2. (a) the HH 111 jet and its source region as imaged by the Hubble Space Telescope in the optical and infrared (from Reipurth and Bally, 2001). (b) A schematic drawing of *x*-wind model for the formation of chondrules and refractory inclusions and local origin of short-lived radionuclides by irradiation in the early Solar System (from Shu et al. (2001)). According to this model, CAIs formed in the gas-depleted reconnection ring and were exposed to solar energetic particle (^{1}H, ^{4}He, and ^{3}He) irradiation that produced all short-lived radionuclides, except ^{60}Fe. Chondrules formed contemporaneously with CAIs in the gaseous disk, near the *x*-region, and were protected from this irradiation to varying degrees. Both chondrules and CAIs were subsequently radially transported by *x*-wind to 1–20 AU where they accreted with thermally unprocessed matrix materials.

interiors: ^{10}Be (McKeegan et al., 2000a), ^{36}Cl (Lin et al., 2005; Hsu et al., 2006), and ^{7}Be (Chaussidon et al., 2006a). Note that ^{7}Be was only tentatively detected and still requires confirmation (see below). (ii) The inferred initial ^{26}Al/^{27}Al ratios [(^{26}Al/^{27}Al)$_0$] in CAIs are significantly higher than those in chondrules (e.g., MacPherson et al., 1995; Kita et al., 2005), suggesting that, in contrast to CAIs, chondrules may have been shielded by the gaseous disk from solar energetic particle irradiation (Lee et al., 1998; Shu et al., 2001). (iii) CAIs appear to have been unaffected by chondrule-forming events, suggesting that they were absent from the chondrule-forming regions. (iv) CAI and chondrule fragments were identified in comet 81P/Wild 2 nucleus samples (McKeegan et al., 2006; Brownlee et al., 2006; Zolensky et al., 2006), as was predicted by Shu et al. (1996, 2001). Note that several other mechanisms of radial transport of solids in protoplanetary disks have been proposed; these mechanisms can also explain the presence of chondrule and CAI fragments in cometary samples (e.g., Boss, 2004, 2006, 2007; Ciesla, 2007a,b).

Participants in two recent workshops on Kauai, Hawai'i—*Chondrites and the Protoplanetary Disk* in 2004 and *Chronology of Meteorites and the Early Solar System* in 2007—attempted to test shock-wave models *vs.* *x*-wind model of the origin of the chondritic components and irradiation *vs.* stellar origin of short-lived radionuclides using chemical, mineralogical and isotopic observations of meteorites and interplanetary dust particles and astronomical observations of active star-forming regions. Here we summarize observations of chondritic meteorites discussed at these meetings and some more recent observations, and show how they can be used to test these competing models.

2. MAJOR CONSTRAINTS ON THE ORIGIN OF CHONDRITIC COMPONENTS

In this section, we summarize major constraints on the origin of refractory inclusions, chondrules and matrices inferred from their textures, mineralogy, major and trace element chemical compositions, isotopic compositions (except short-lived radionuclides, which will be discussed in Section 3) and laboratory simulations. These constraints can be used for testing the *x*-wind model and shock-wave models of their formation.

2.1. Refractory inclusions

Mineralogical differences among CAIs + AOAs and chondrules + matrices are best illustrated on a diagram of mineral stability in a gas of solar composition at 10^{-3} bar total pressure as a function of temperature (Fig. 3). Although there is a weak pressure dependence of condensation temperature of minerals, which will affect the order in which minerals condense in a parcel of cooling nebular gas of solar composition, the variations in condensation sequence are generally minor at total pressure of 10^{-3}–10^{-6} bar (e.g., Yoneda and Grossman, 1995; Ebel and Grossman, 2000; Petaev and Wood, 2005). CAIs and AOAs consist of minerals stable above ~1400 K; chondrules and matrices consist of less refractory minerals.

CAIs are non-igneous (evaporative residues or gas-solid condensates; Fig. 4a and b) or igneous (possibly melted condensates; Fig. 5) objects composed of Ca,Al,Ti,Mg-oxides and silicates. Both types of CAIs are typically surrounded by single- or multilayered rims (called Wark–Lovering rims; Wark and Lovering, 1977), which resulted from high-temperature, gas–solid or gas–melt interaction in the solar nebula (Wark and Boynton, 2001; MacPherson et al., 2005). Some CAIs surrounded by the Wark–Lovering rims are in addition surrounded by forsterite-rich accretionary rims (Fig. 6). The forsterite-rich accretionary rims are texturally and mineralogically similar to AOAs (Krot et al., 2001a, 2004a), suggesting a close genetic relationship between CAIs and AOAs. AOAs are aggregates of mostly forsterite and Fe,Ni-metal, with small enclosed spinel–diopside–anorthite CAIs (Fig. 4c and d; Krot et al., 2004a and references therein). AOAs appear to have avoided significant melting after aggregation.

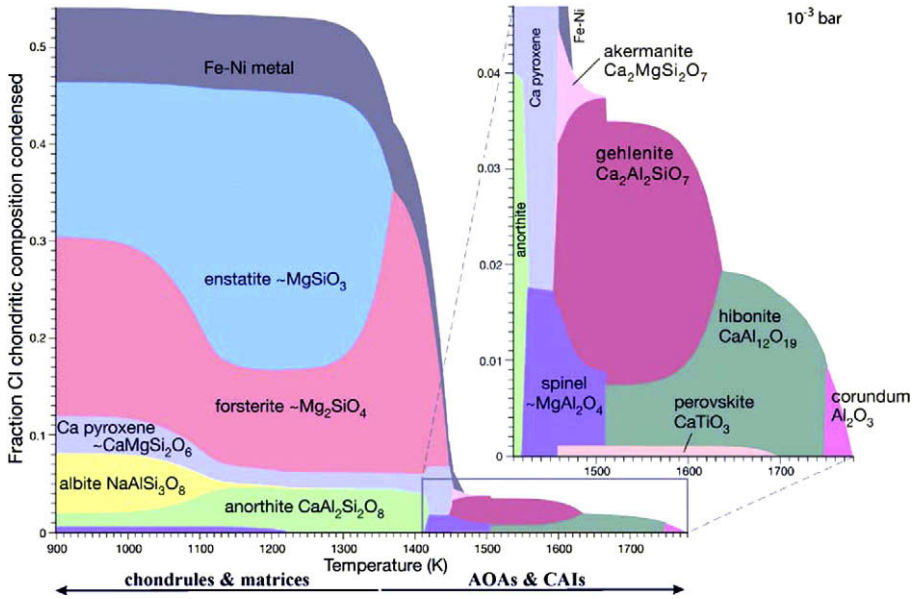

Fig. 3. Equilibrium diagram for a solar nebula at 10^{-3} bar total pressure showing mineral stability above 900 K (Davis and Richter, 2003). Minerals stable above ~1350 K are present in refractory inclusions; minerals stable below 1350 K are found mostly in chondrules and primitive chondrite matrices.

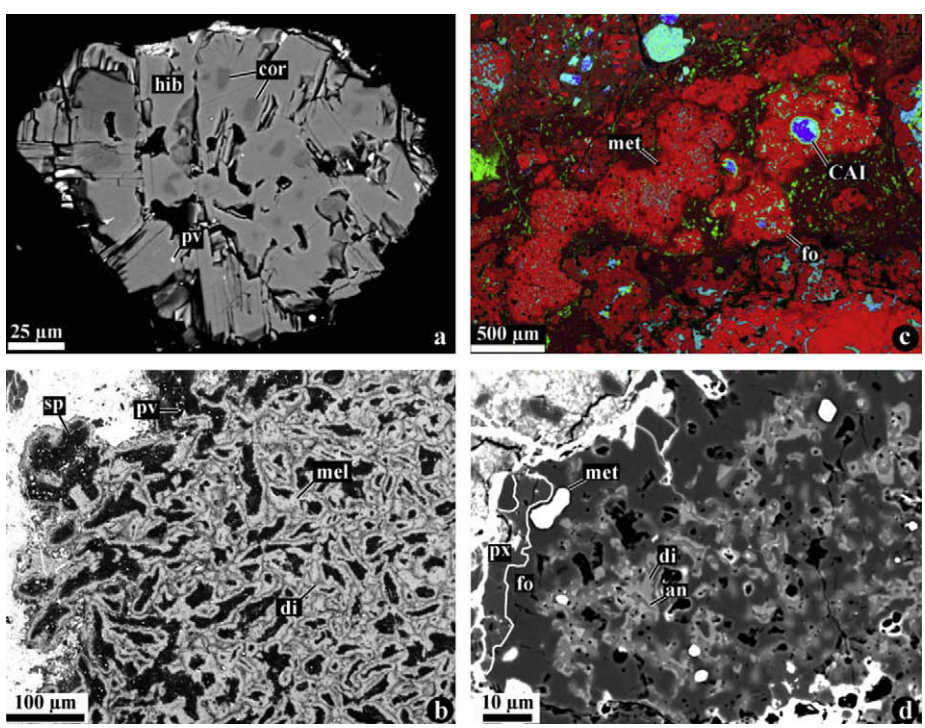

Fig. 4. Backscattered electron (BSE) images (a, b, and d) and combined elemental map in Mg (red), Ca (green) and Al Kα (blue) X-rays showing refractory inclusions which appear to have escaped melting. (a) CAI from Murchison (CM2) consists of corundum, hibonite, and perovskite, which appear to have condensed in the solar nebula above 1650 K (Fig. 3). (b) Fine-grained CAI Efremovka (CV3) consists of concentrically-zoned bodies of spinel, perovskite, melilite, and diopside. (c and d) AOAs from Efremovka (c) and ungrouped carbonaceous chondrite Acfer 094 (d). The AOAs consist of diopside, anorthite and individual CAIs enclosed by forsterite with occasional grains of Fe, Ni-metal Fe,Ni. Forsterite is replaced by low-Ca pyroxene as a result of reaction with SiO gas below 1350 K (Fig. 3). an = anorthite; cor = corundum; di = diopside; fo = forsterite; hib = hibonite; mel = melilite; met = Fe,Ni-metal; pv = perovskite; px = low-Ca pyroxene; sp = spinel. "a" from Simon et al. (2002), "b–d" from Krot et al. (2004a,b). (For interpretation of the references to color in this figure legend, the reader is referred to the web version of this paper.)

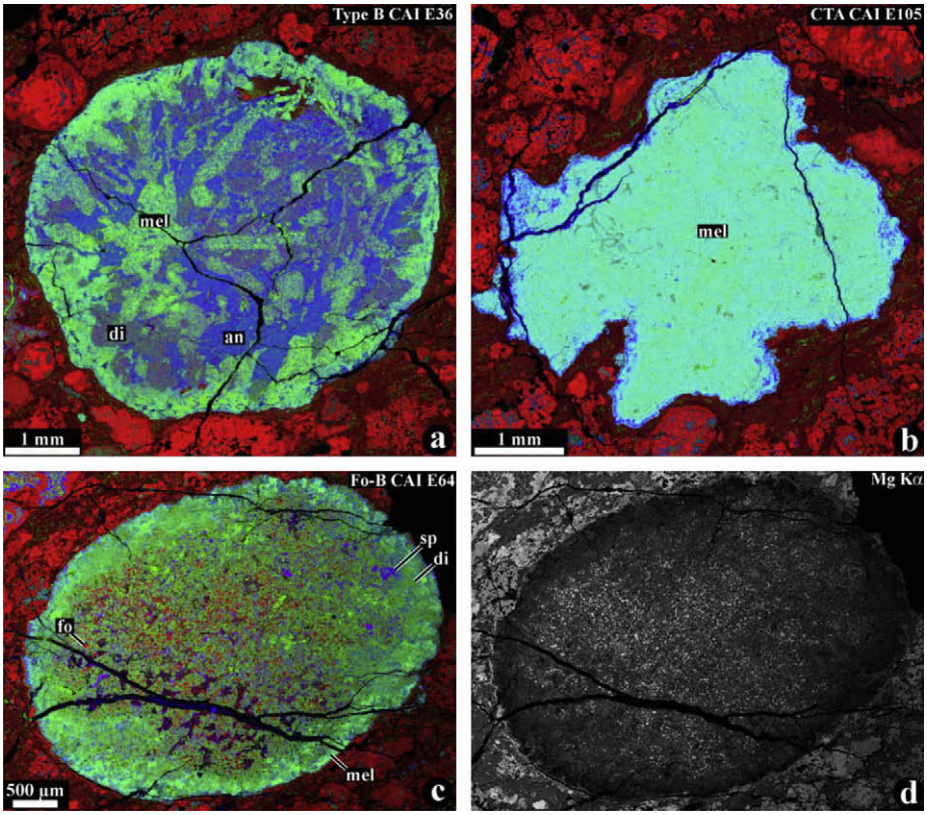

Fig. 5. Combined elemental maps in Mg (red), Ca (green) and Al Kα (blue) X-rays (a–c) and elemental map in Mg Kα (d) of igneous [Type B, compact Type A (CTA), and forsterite-bearing Type B (Fo-B)] CAIs from Efremovka (CV3). CAIs E36 and E64 are surrounded by melilite-rich mantles, which appear to have resulted from volatilization during melt crystallization. an = anorthite; di = diopside; fo = forsterite; mel = melilite; sp = spinel. (For interpretation of the references to color in this figure legend, the reader is referred to the web version of this paper.)

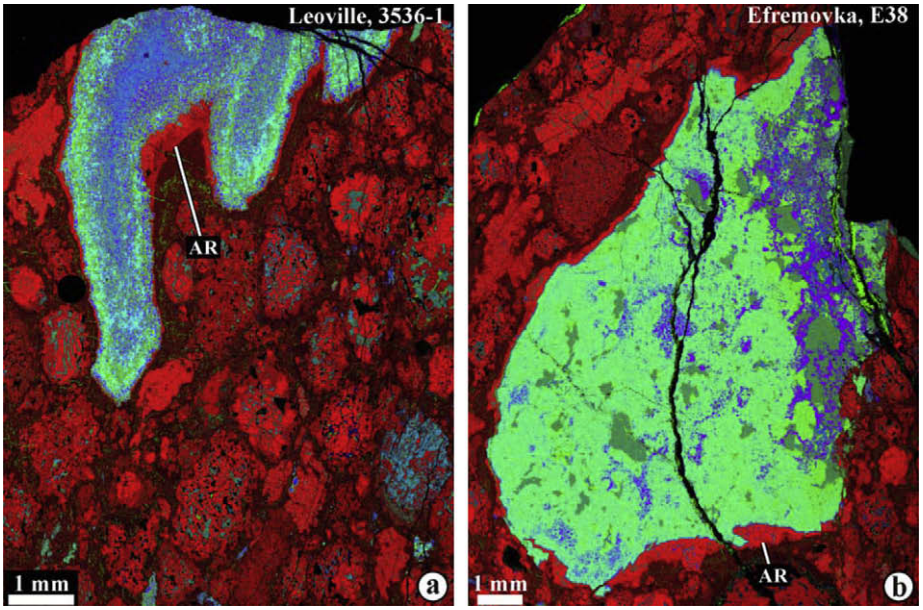

Fig. 6. Combined elemental maps in Mg (red), Ca (green) and Al Kα (blue) X-rays (a–c) and elemental map in Mg Kα (d) of a fine-grained, spinel-rich CAI (a) and a coarse-grained, Type B CAI (b) from CV chondrites Leoville and Efremovka. Both CAIs are surrounded by forsterite-rich accretionary rims (AR), which are texturally and mineralogically similar to AOAs (Fig. 4c and d). "a" from Krot et al. (2004a); "b" from Krot et al. (2004b). (For interpretation of the references to color in this figure legend, the reader is referred to the web version of this paper.)

Many CAIs preserve nucleosynthetic isotopic anomalies in Ca, Ti, Si, Cr, Ni and other elements, possibly indicating incomplete isotopic homogenization in the solar nebula (e.g., Lee, 1988). CAI pyroxenes (Al,Ti-diopside) have high Ti^{3+}/Ti^{4+} ratios (Simon et al., 2007), suggesting formation under approximately solar redox conditions (H_2O/H_2 ratio of $\sim 5 \times 10^{-4}$). Most CAIs have volatility fractionated rare earth element (REE: La, Ce, Pr, Nd, Pm, Sm, Eu, Gd, Tb, Dy, Ho, Er, Tm, Yb, Lu) patterns, indicative of evaporation–condensation processes (e.g., MacPherson et al., 1988; Ireland and Fegley, 2000). Igneous CAIs show chemical (depletion in Mg and Si of CAI mantles; Fig. 5a, c, and d) and isotopic (mass-dependent fractionation of Mg, Si, and O of bulk CAIs) evidence for melt evaporation (Grossman et al., 2002; Davis et al., 2005a and references therein; Richter et al., 2006; Shahar and Young, 2007; Simon and Young, 2007; MacPherson et al., 2008; Krot et al., 2008a).

The majority of CAIs and AOAs from primitive (unmetamorphosed) chondrites (CO3.0, CR2, CH3.0) are uniformly (within an individual inclusion) ^{16}O-rich ($\Delta^{17}O \sim -24 \pm 2‰$) (Fig. 7a and b; Itoh et al., 2004; Makide et al., 2009; Krot et al., 2008b). In these meteorites, only rare, igneous CAIs, typically associated with chondrule materials, are ^{16}O-depleted (Fig. 7a and b; see below). Note that most CAIs in metamorphosed CV and CO chondrites show oxygen–isotope heterogeneity, with spinel and Al,Ti-diopside ^{16}O-enriched and melilite and anorthite ^{16}O-depleted (e.g., Clayton, 1993; Itoh et al., 2004). The nature of this isotope heterogeneity remains controversial; several mechanisms have been proposed: (i) gas–melt exchange during partial or disequilibrium melting in the solar nebula, (ii) gas–solid exchange during transient heating events in the solar nebula, and (iii) exchange during fluid-assisted thermal metamorphism (Clayton, 1993; Ryerson and McKeegan, 1994; Wasson et al., 2001; Fagan et al., 2004; Yurimoto et al., 2007; Nagashima et al., 2007a; Krot et al., 2008a,b,c).

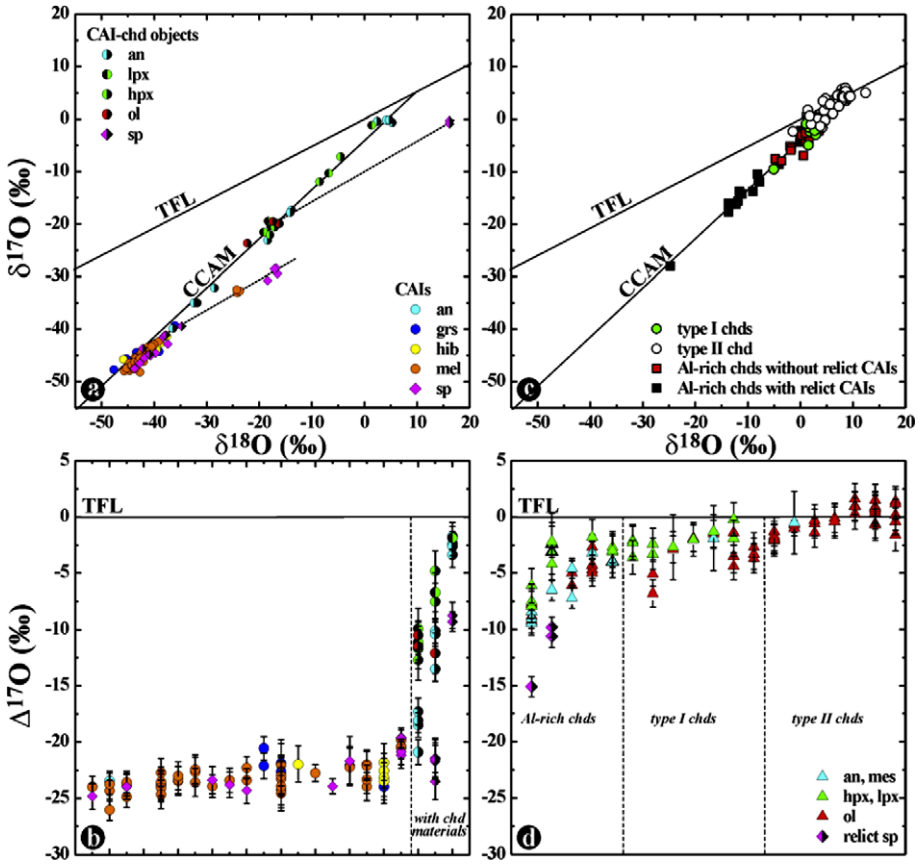

Fig. 7. Oxygen–isotope compositions of individual minerals in CAIs and chondrules in CR chondrites. In "a" and "c", data are plotted as $\delta^{17}O$ *vs.* $\delta^{18}O$. In "b" and "d", the same data are plotted as deviation from the terrestrial fractionation line (TFL), $\Delta^{17}O$; each column represents data for a single CAI or a chondrule. Error bars in "a" and "c" are not shown for clarity; error bars in "b" and "d" are 2σ. Carbonaceous chondrite anhydrous mineral (CCAM) line is shown for reference. Most CAIs are uniformly ^{16}O-rich ($\Delta^{17}O < -20‰$). Chondrule–CAI compound objects are isotopically heterogeneous and ^{16}O-depleted. Two CAIs show large mass-dependent fractionation effects, similar to those observed in FUN (Fractionation and Unidentified Nuclear anomalies) inclusions. Chondrules are ^{16}O-depleted relative to CAIs. Aluminum-rich chondrules with relict CAIs are ^{16}O-enriched compared to those without relict CAIs and ferromagnesian (type I and II) chondrules. an = anorthite; hpx = high-Ca pyroxene; grs = grossite; hib = hibonite; mel = melilite; mes = mesostasis; ol = olivine; lpx = low-Ca pyroxene; sp = spinel. Data for CAIs are from Makide et al. (2009); data for chondrules are from Aléon et al. (2002) and Connolly et al. (2003).

The mineralogical, chemical and isotopic observations summarized above suggest that CAIs formed by evaporation–condensation processes in high-temperature nebular region(s) (at or above condensation temperature of forsterite, >1400 K), under variable, but generally low total pressure ($<10^{-4}$ bar), in the presence of ^{16}O-rich gas, and in reduced environment (Grossman et al., 2000, 2002, 2008; Petaev and Wood, 2005 and references therein). Some CAIs were subsequently melted and behaved as open systems for cumulative timescale of days to weeks (Young et al., 2005; Richter et al., 2006; Shahar and Young, 2007; Simon et al., 2007). Note that formation of CAIs under reduced conditions is inconsistent with the original *x*-wind model (Shu et al., 1996, 2001) that hypothesizes formation of CAIs in a dust-rich, hydrogen-depleted (i.e., highly-oxidized) nebular region, reconnection ring (Desch, 2007), unless dust was highly enriched in carbon (Cuzzi et al., 2005).

2.2. Chondrules

Chondrules are igneous, spherical objects, ~0.01–10 mm in size, composed of ferromagnesian olivine and pyroxene, Fe,Ni-metal, sulfides, and glassy or microcrystalline mesostasis. Chondrules show significant variations in textures, sizes and mineralogy (Fig. 8). Ferromagnesian chondrules with porphyritic textures [magnesian, type I (Fig. 8a) and ferrous, type II (Fig. 8b)], indicative of incomplete melting of chondrule precursors (Hewins, 1997), are dominant in most chondrite groups. In contrast, in the metal-rich (CB and CH) carbonaceous chondrites, magnesian chondrules

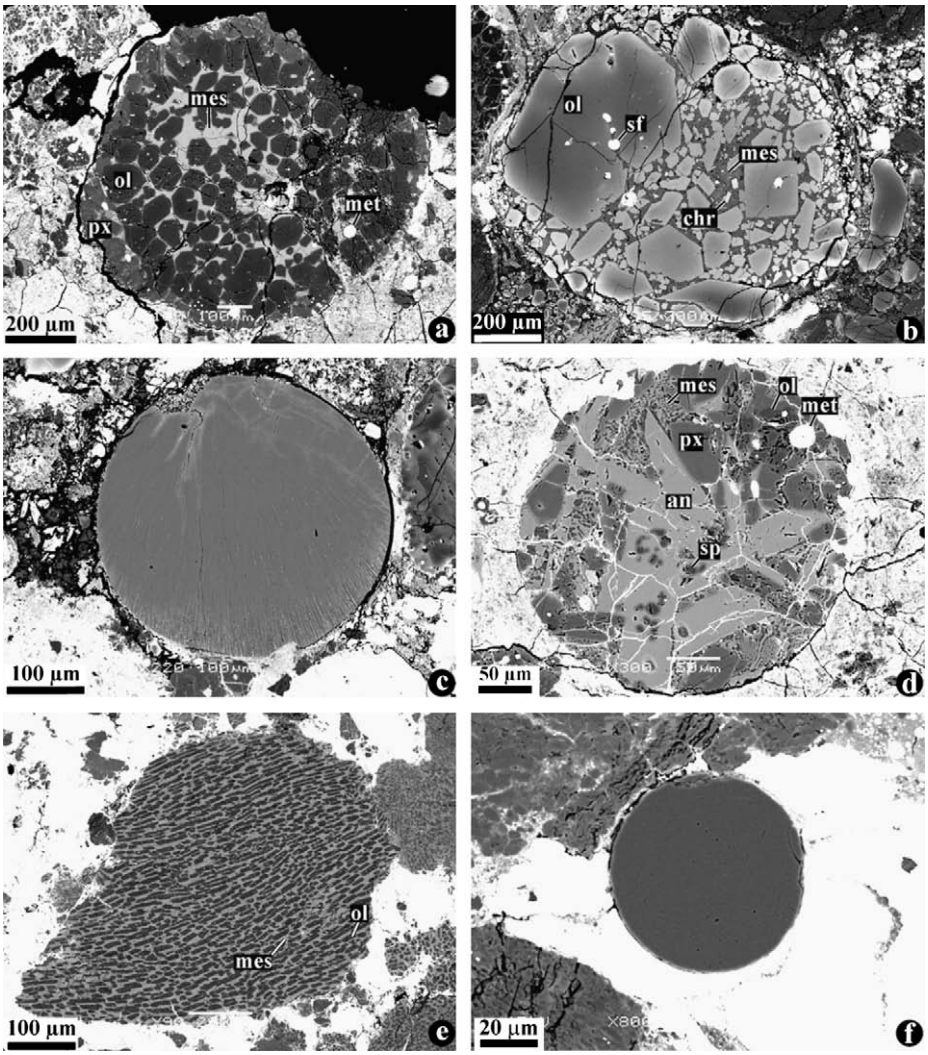

Fig. 8. BSE images of chondrule with different textures and compositions. (a) Magnesian porphyritic-olivine (type I) chondrule composed of magnesian olivine and low-Ca pyroxene, glassy mesostasis, and Fe,Ni-metal. (b) Ferrous porphyritic-olivine chondrule (type II) made of ferrous olivine, fine-grained mesostasis, chromite, and troilite. (c) Ferrous radial-pyroxene chondrule. (d) Aluminous porphyritic-pyroxene chondrule composed of lath-shaped anorthite, low-Ca pyroxene, olivine, spinel, Fe,Ni-metal, and fine-grained mesostasis. (e) Magnesian skeletal chondrule. (f) Magnesian cryptocrystalline chondrule. Chondrules with porphyritic textures, indicative of incomplete melting of chondrule precursors (Hewins, 1997), are dominant in all chondrite groups. Magnesian chondrules with cryptocrystalline and skeletal textures are dominant only in metal-rich (CB and CH) carbonaceous chondrites. an = anorthite; chr = chromite; mes = mesostasis; met = Fe, Ni-metal; ol = olivine; px = low-Ca pyroxene; sf = Fe-sulfide; sp = spinel.

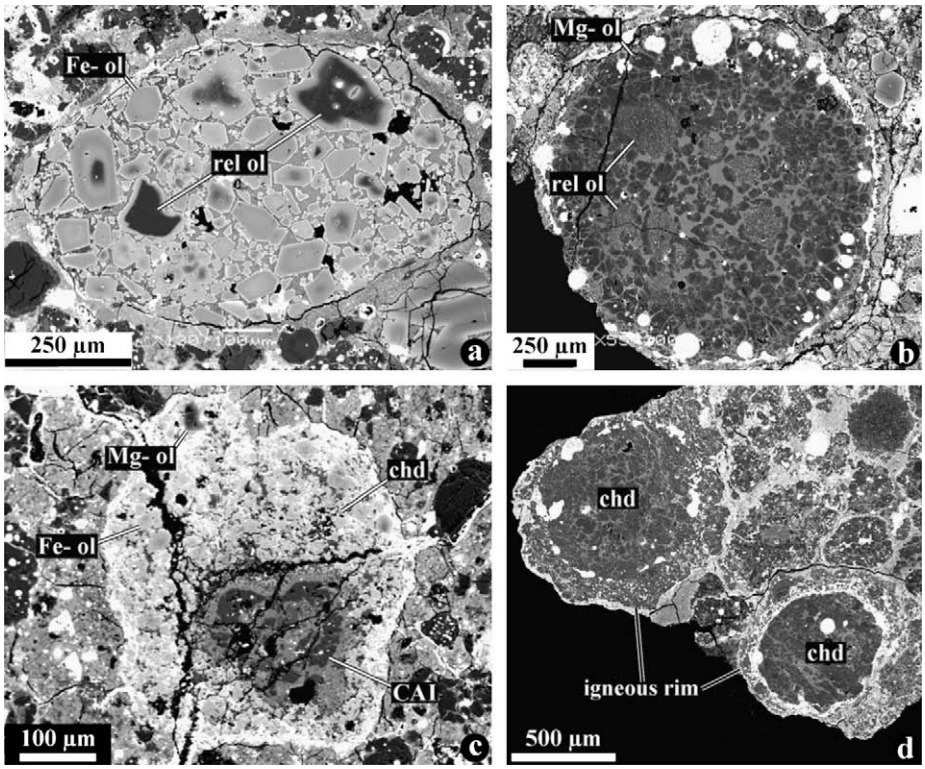

Fig. 9. BSE images of chondrules with relict grains (a–c) and igneous rims (d), indicative of multiplicity of chondrule-forming events. (a) Type II chondrule with relict grains of magnesian olivine. (b) Type I chondrule with relict "dusty" olivines containing numerous inclusions of Ni-poor metal, indicating *in situ* reduction of relict ferrous olivine. (c) Type II chondrule with a relict CAI and a relict magnesian olivine. (d) Type I chondrules surrounded by coarse-grained igneous rims (courtesy of K. Nagashima).

with non-porphyritic (cryptocrystalline and skeletal) textures (Fig. 8e and f) are the most abundant (Krot et al., 2002a). Some chondrules show evidence for multistage melting, including relict fragments of chondrules of earlier generations (Fig. 9a–c), coarse-grained igneous rims around chondrules (Fig. 9d), and independent compound chondrules (Wasson et al., 1994).

It has been recently shown that the abundance of the volatile element sodium remained relatively constant during chondrule formation (Alexander et al., 2008). Prevention of the evaporation of sodium may require that chondrules formed in regions with high dust/gas ratios (Alexander et al., 2008). Alternatively, chondrules may have experienced very fast melting and crystallization, which prevented evaporation of sodium (e.g., Yurimoto and Wasson, 2002).

Based on the bulk chemical compositions of type I chondrules, the chemical compositions of their glasses, and mineralogical observations [presence of low-Ca pyroxene shells around olivine-rich cores (Fig. 8a) and chemical zoning of chondrule mesostasis], Libourel et al. (2006) concluded that type I chondrules experienced open-system behavior during melting and crystallization with some elements condensing into chondrule melts. For example, on the CMAS ($CaO–MgO–Al_2O_3–SiO_2$) phase diagram, bulk chemical compositions of type I chondrules are inside the liquidus fields of olivine and low-Ca pyroxene (Fig. 10). It is expected that crystallization of olivine and pyroxene from melts of such compositions will result in melt evolution along lines of descent. In contrast, glass compositions of type I chondrules define a single, almost linear, compositional trend towards the SiO_2 corner of the CMAS diagram, suggesting that chondrule melts did not evolve by closed-system crystallization, but experienced interaction with silicon-rich nebular gas. Oxygen–isotope disequlibrium between olivine and low-Ca pyroxene grains + glassy mesostasis in type I chondrules from CV and CR chondrites reported by Chaussidon et al. (2008) appears to support this conclusion. However, no differences between the oxygen–isotope compositions of low-Ca pyroxene and olivine (except relict grains) in individual type I chondrules from several primitive (petrologic type <3.2) ordinary chondrites have been observed by Kita et al. (2006, 2008), who interpreted these observations as evidence against gas–melt exchange during chondrule formation. More work is needed to resolve this issue.

Most chondrules are ^{16}O-depleted ($\Delta^{17}O > -10‰$) relative to CAIs and AOAs (Fig. 7c and d; Krot et al., 2006); show no resolvable (<1‰/amu) mass-dependent isotope fractionation effects (Davis et al., 2005a and references therein), and have small/if any nucleosynthetic anomalies (e.g., Niemeyer, 1988).

It is inferred that chondrules formed in isotopically distinct regions, at lower ambient temperature (<1000 K), under more oxidizing conditions, and at higher total pressure and/or dust/gas ratio than CAIs and AOAs (e.g., Scott and Krot, 2005; Jones et al., 2005; Alexander, 2005; Alexander

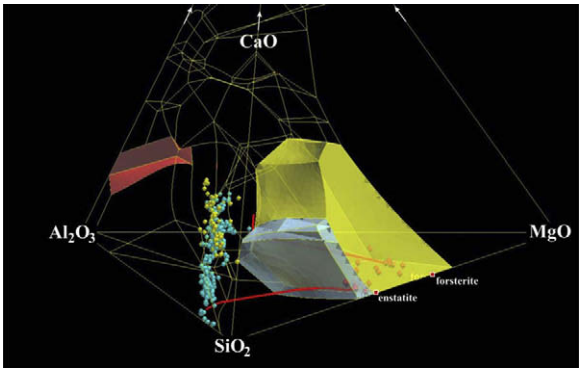

Fig. 10. Open-system behavior of chondrule melts as indicated by glass compositions (in wt%) of melt inclusions in olivine (yellow dots) and glassy mesostases of chondrules (blue dots) in type I chondrules from Semarkona (LL3.0) and CR chondrites plotted on a CaO–MgO–Al_2O_3–SiO_2 phase diagram. Yellow, blue and reddish regions represent the computed stability fields of forsterite, low-Ca pyroxene polymorphs (protoenstatite, orthoenstatite, pigeonite), and hibonite, respectively. Data for bulk compositions of type I chondrules from Semarkona (red balls) are from Jones and Scott (1989) and Jones (1994). Red lines correspond to equilibrium liquid lines of descent calculated from two representative chondrule bulk compositions using the *MAGPOX* code (Longhi, 1991). Chondrule glasses do not follow lines of descent, but define a linear trend towards SiO_2, suggesting that chondrule melts did not evolve by closed-system crystallization, but experienced interaction with SiO nebular gas (from Libourel et al., 2006). (For interpretation of the references to color in this figure legend, the reader is referred to the web version of this paper.)

et al., 2008). Chondrules formed by melting of chondrule precursors—aggregates of fine-grained matrix-like material and coarse-grained components including fragments of CAIs, AOAs and chondrules of earlier generations. Chondrule precursors were heated at 10^4–10^6 K/h (Tachibana and Huss, 2005), reached peak temperatures of 1650–1850 K, and cooled at 100–1000 K/h (Desch and Connolly, 2002). Mass-dependent isotope fractionation in chondrules could have been erased if vaporized gas back reacted with chondrule melt, which requires high number density of chondrules (>10 m^{-3}) (Galy et al., 2000; Cuzzi and Alexander, 2006).

2.3. Matrices

Matrices of primitive chondrites (e.g., Acfer 094, ALHA77307) largely consist of sub-micron crystalline magnesian olivine and pyroxene, Fe,Ni-metal, sulfides, oxides, and amorphous ferromagnesian silicate (Brearley and Jones, 1998). The similarity of the oxygen–isotope compositions of primitive chondrite chondrules and matrices (Fig. 11; Clayton and Mayeda, 1999), the apparent complementarity of chemical compositions of chondrules and matrix materials in an individual chondrite (Palme and Klerner, 2000; Bland et al., 2005), high abundance of crystalline silicates in primitive chondrite matrices, and high cooling rates of matrix pyroxenes inferred from their microstructures, all suggest that a significant fraction of matrix materials was thermally processed during the transient

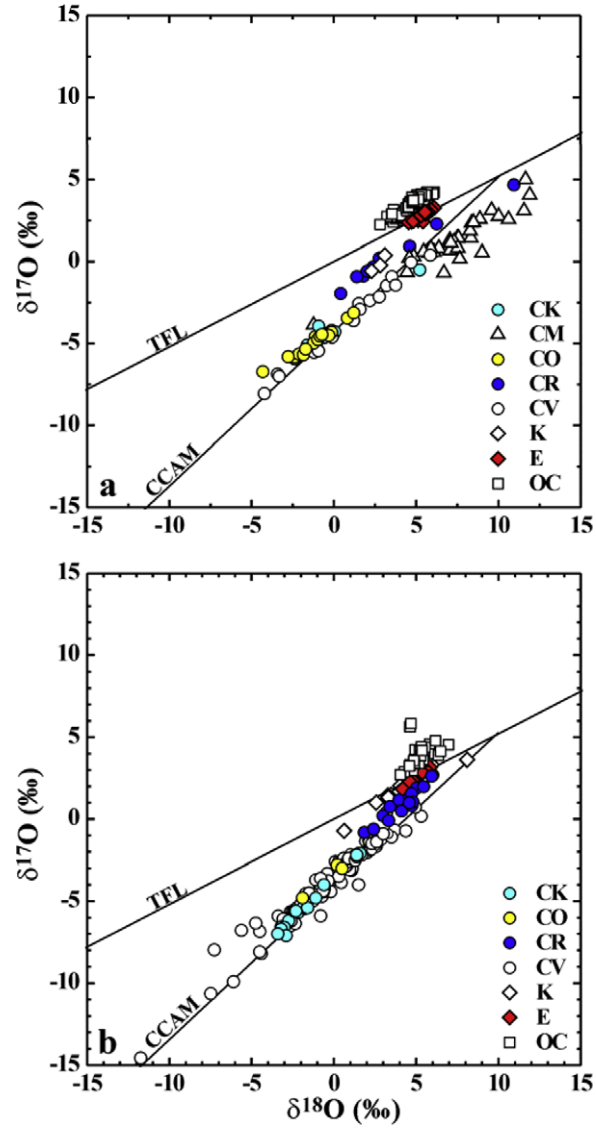

Fig. 11. Whole-rock oxygen–isotope compositions of chondrites (a) and bulk chondrules (b) (data from Clayton and Mayeda, 1999; Ash et al., 1999; Jabeen et al., 1999; Jones et al., 2004). Chondrule compositions are similar to those of their host meteorites. Because chondrules and matrices are the major chondritic components comprising up to 99.5 vol% of a chondrite, these observations suggest that chondrules and matrices have also similar oxygen–isotope compositions.

heating events that formed host chondrite chondrules (Scott and Krot, 2005; Nuth et al., 2005; Wasson, 2008). These observations are generally consistent with the shock-wave model of chondrule formation (Desch et al., 2005), but inconsistent with *x*-wind model, which suggests that matrix escaped thermal processing during chondrule formation (Shu et al., 1996, 2001).

2.4. Chondrite groups

Based on the bulk chemical and oxygen–isotope (Fig. 11) compositions, mineralogy, and petrography (Table 2 and Fig. 12), chondrites are divided into 15

Table 2
Abundances of chondritic components in the chondrite groups.

Class, Group	Refr. incls. (vol%)	Chd. (vol%)*	Chd. avr. diam. (mm)	Fe, Ni metal (vol%)	Matrix (vol%)[a]
Carbonaceous					
CI	<0.01	<5	—	<0.01	95
CM	5	20	0.3	0.1	70
CO	13	40	0.15	1–5	30
CV	10	45	1.0	0–5	40
CK	4	15	0.8	<0.01	75
CR	0.5	50–60	0.7	5–8	30–50
CH	0.1	~70	0.05	20	5
CB_a	<0.1	40	~5	60	<5
CB_b	<0.1	30	~0.5	70	<5
Ordinary					
H	0.01–0.2	60–80	0.3	8	10–15
L	<0.1	60–80	0.5	3	10–15
LL	<0.1	60–80	0.6	1.5	10–15
Enstatite					
EH	<0.1	60–80	0.2	8	<0.1–10
EL	<0.1	60–80	0.6	15	<0.1–10
Other					
K	<0.1	20–30	0.6	6–9	70
R	<0.1	>40	0.4	<0.1	35

Sources of data: Scott and Krot (2003) and references listed therein.
* Includes chondrule fragments and silicates inferred to be fragments of chondrules.
[a] Includes matrix-rich lithic fragments, which account for all the matrix in CH and CB chondrites. CB_a and CB_b are subgroups of CB chondrites.

groups—*carbonaceous*: CI (Ivuna-like), CM (Murchison-like), CR (Renazzo-like), CO (Ornans-like), CV (Vigarano-like), CK (Karoonda-like), CB (Bencubbin-like), CH (high-metal); *ordinary*: H, L and LL; *enstatite*: EH and EL; and *others:* R (Rumuruti-like) and K (Kakangari-like). Each group may represent just one or a few asteroids. There are significant differences in sizes, chemical and textural types of chondrules and chondrule/matrix ratios between different chondrite groups (Table 2 and Fig. 12). These differences and the inferred genetic relationship of chondrules and matrix materials in a chondrite group may require the localized formation of these chondritic components followed by fast accretion into chondrite parent bodies (Alexander, 2005; Scott and Krot, 2005; Alexander et al., 2008). This conclusion is reinforced by astronomical observations (e.g., Watson, 2007) and theoretical modeling, suggesting that radial mixing of solids in protoplanetary disks is a very fast (<<1 Myr) process (Haghighipour and Boss, 2003a,b; Boss, 2004, 2006, 2007, 2008; Ciesla, 2007a,b), and that gravitational instability in locally overdense regions in the midplane of the disk may have played important role in the formation of chondrite planetesimals (Johansen et al., 2007; Alexander et al., 2008).

Although there are also some differences in sizes and mineralogy of CAIs among chondrite groups, one type of CAIs, rich in spinel and pyroxene, dominates in all chondrite groups, except CH chondrites (Krot et al., 2002a and references therein; Lin et al., 2006). These observations can be reconciled with the formation of CAIs in a localized nebular region, possibly near the proto-Sun, followed by outward radial transport in the protoplanetary disk to the accretionary regions of chondrites and comets (Shu et al., 1996, 1997, 2001; Boss, 2004, 2006, 2007; Ciesla, 2007a, b).

3. ABSOLUTE AND RELATIVE CHRONOLOGIES OF CAI AND CHONDRULE FORMATION

3.1. Absolute (^{207}Pb–^{206}Pb) chronology of CAI and chondrule formation

A resolved age difference of a coarse-grained igneous (Type B) CAI from the CV chondrite Efremovka (E49, 4567.17 ± 0.70 Myr) and a set of chondrules from the CR chondrite Acfer 059 (4564.66 ± 0.63 Myr) was first reported by Amelin et al. (2002; Fig. 13a). Subsequently, Amelin et al. (2006) obtained more precise age (4567.11 ± 0.16 Myr) for another Type B CAI from Efremovka, E60. Although this age difference is generally consistent with that inferred from the initial $^{26}Al/^{27}Al$ ratios [$(^{26}Al/^{27}Al)_0$] of the CV CAIs ($\sim 5 \times 10^{-5}$, Amelin et al., 2002) and CR chondrules ($< 5 \times 10^{-6}$, Marhas et al., 2000; Nagashima et al., 2007b, 2008), it could not be used for testing an assumption of the *x*-wind model that CAIs and chondrules in a chondrite group formed contemporaneously, because the measured CAIs and chondrules are from different chondrite groups.

Because CAIs in most chondrite groups are significantly smaller than those in CV chondrites (Fig. 12), all attempts to measure absolute ages of chondrules and CAIs from the same chondrite group were focused on CV chondrites (Chen and Tilton, 1976; Tatsumoto et al., 1976; Amelin and Krot, 2007; Connelly et al., 2008). A resolved age difference (1.66 ± 0.48 Myr) of ^{207}Pb–^{206}Pb ages of Efremovka CAIs and Allende (also CV) chondrules (4565.45 ± 0.45 Myr) has been reported by Connelly et al. (2008) (Fig. 13b); all previous attempts were unsuccessful. This result contradicts the *x*-wind hypothesis of contemporaneous formation of chondrules and CAIs from a single chondrite group. The absolute ages of the CV CAIs and chondrules should be considered cautiously, because all CV chondrites are thermally metamorphosed and altered to varying degrees (Krot et al., 1998; Bonal et al., 2006).

Taking into account published ^{207}Pb–^{206}Pb ages of chondrules from CV (4565.45 ± 0.45 Myr; Connelly et al., 2008), CR (4564.66 ± 0.63 Myr; Amelin et al., 2002) and CB chondrites (4562.7 ± 0.6 Myr; Krot et al., 2005a), we infer that CAIs formed first; chondrule formation started ~1 Myr later and lasted for 3–4 Myr (Table 3). Note that high-precision ^{207}Pb–^{206}Pb ages of sets of chondrules have been reported only for 3 out of 14 known chondrite groups and no absolute ages of individual chondrules have been measured yet. More work is needed to understand the total duration of chondrule formation.

The inferred duration of chondrule formation can be used as a lower limit on the life-time of the protoplanetary disk (Russell et al., 2006). Krot et al. (2005a) proposed that chondrules in CB chondrites formed by collision between

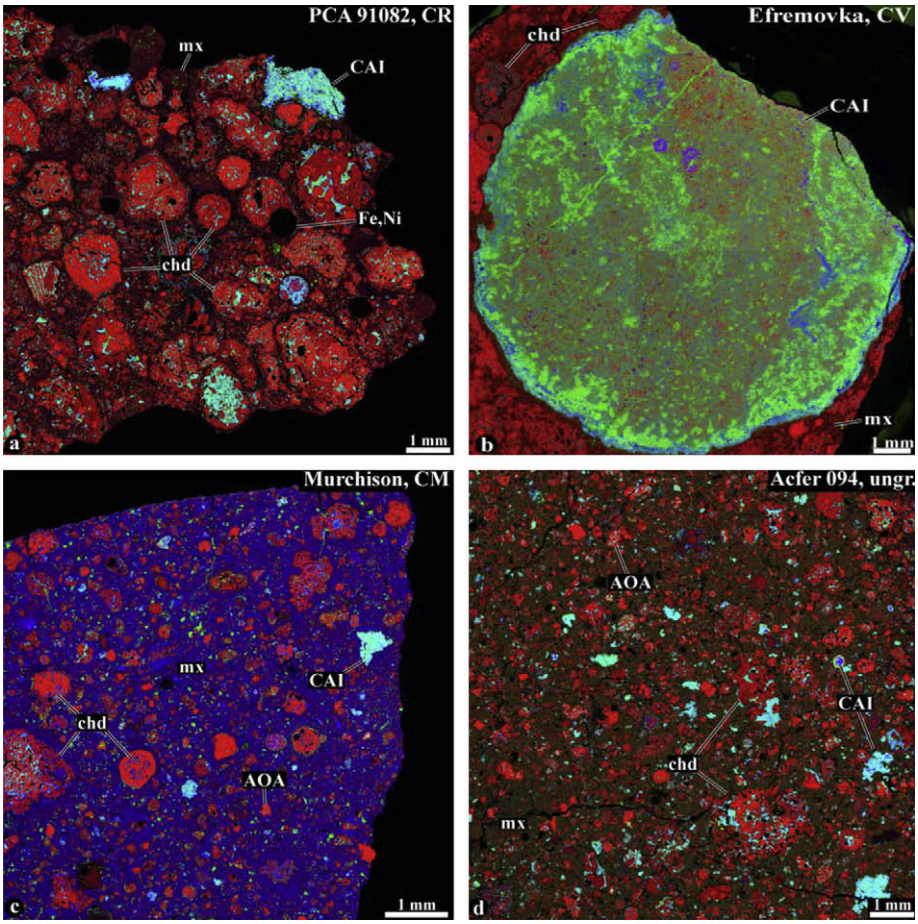

Fig. 12. Combined elemental map in Mg (red), Ca (green) and Al Kα (blue) X-rays of the CR chondrite PCA 91082 (a), CV chondrite Efremovka (b), CM chondrite Murchison (c), and ungrouped carbonaceous chondrite Acfer 094 (d). The meteorites consist of chondrules (chd), refractory inclusions (CAIs and AOAs), and fine-grained interchondrule matrix material (mx). There are significant variations in chondrule/matrix ratio and sizes and textural types of chondrules (Table 2). These characteristics are used as primary classification parameters of chondrite groups (e.g., Krot et al., 2003). Each chondrite group may represent just one or a few asteroids. (For interpretation of the references to color in this figure legend, the reader is referred to the web version of this paper.)

planetary embryos after dissipation of dust in the protoplanetary disk. If this is the case, use of the CB chondrule ages for constraining life-time of the protoplanetary disk may be problematic (see discussion in Section 3.7).

Although an absolute average age of CV CAIs is commonly used as the start of the Solar System formation, there is a disagreement on the exact value of this age, which ranges from ~4567 to ~4570 Myr (e.g., Lugmair and Shukolyukov, 1998; Amelin et al., 2002, 2006; Zinner and Göpel, 2002; Burkhardt et al., 2007; Bouvier et al., 2007, 2008; Jacobsen et al., 2008a,b). For example, by combining several fractions of Allende and Efremovka CAIs, an estimate of the CV CAI formation age of 4568.5 ± 0.5 Myr was obtained by Bouvier et al. (2007); an absolute age of an Allende CAI reported by Bouvier et al. (2008) is 4567.59 ± 0.10 Myr.

3.2. Relative chronology of CAI and chondrule formation

3.2.1. Constraints from mineralogical observations and bulk chemical compositions of CAIs and chondrules

The presence of CAIs in the chondrule-forming regions among chondrule precursors, and, hence, formation of at least some CAIs prior to chondrules, is inferred from petrographic observations: (i) relict CAIs inside chondrules (Figs. 9c and 14), (ii) CAIs surrounded by ferromagnesian silicate, chondrule-like, igneous rims (Fig. EA1a and b), and (iii) igneous CAIs with ferromagnesian silicate, chondrule-like material in their peripheries (Fig. EA1c and d). In addition, some chondrules have CAI-like volatility-fractionated REE patterns, such as Group II and ultrarefractory, suggesting that these chondrules formed by melting of the CAI-like precursors (Rubin and Wasson, 1987; Kring and Boynton, 1990; Misawa and Nakamura, 1996; Pack et al., 2004; Jones and Norman, 2008).

Based on the mineralogical and isotopic studies of the CAI–chondrule compound objects, it was inferred that during remelting these CAIs experienced oxygen–isotope exchange and partial or complete resetting of ^{26}Al–^{26}Mg systematics (Russell et al., 2005 and references therein; Krot et al., 2005b,c). By a process of elimination, some igneous CAIs that were melted during chondrule formation without mixing with chondrule precursors can be identified based on their oxygen– and Al–Mg isotope systematics. For example, a Type C CAI from El Djouf 001 (CR) remelted

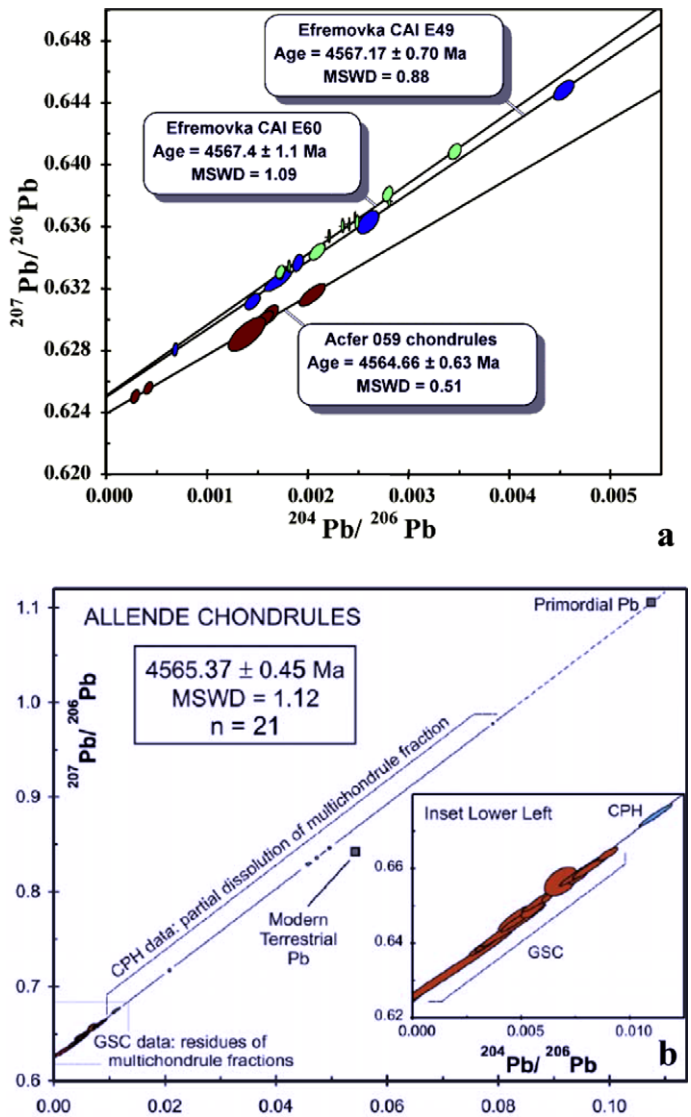

Fig. 13. Pb–Pb isochrons for the six most radiogenic Pb isotopic analyses of acid-washed chondrules from Acfer 059 (CR), for acid-washed fractions from the Efremovka (CV) CAIs E49 and E60 (a) and Allende (CV) chondrules (b) (from Amelin et al., 2002 and Connelly et al., 2008). $^{207}Pb/^{206}Pb$ ratios are not corrected for initial common Pb. Error ellipses are 2σ. Isochron age errors are 95% confidence intervals. MSWD = mean square of weighted deviations. There are resolvable age differences between CV CAIs, CV chondrules and CR chondrules, consistent with those inferred from their ^{26}Al–^{26}Mg systematics.

Table 3
Absolute (^{207}Pb–^{206}Pb) ages of CAIs and chondrules.

Object, chondrite (group and petrologic type)	Age (Myr)	Reference
CAI E49, Efremovka (CV3.1–3.4)	4567.17 ± 0.70	Amelin et al. (2002)
CAI E60, Efremovka	4567.4 ± 1.1	Amelin et al. (2002)
CAI E60, Efremovka	4567.11 ± 0.16	Amelin et al. (2006)
CAIs, Allende (CV > 3.6) and Efremovka	4568.5 ± 0.5	Bouvier et al. (2007)
CAI, Allende	4567.59 ± 0.10	Bouvier et al. (2008)
CAI AJEF, Allende	4567.60 ± 0.36	Jacobsen et al. (2008a)
chondrules, Allende	4565.45 ± 0.45	Connelly et al. (2008)
chondrules, Acfer 059 (CR2)	4564.66 ± 0.63	Amelin et al. (2002)
chondrules, Gujba (CB_a3)	4562.7 ± 0.5	Krot et al. (2005a)
chondrules, Hammadah al Hamra 237 (CB_b3)	4562.8 ± 0.9	Krot et al. (2005a)

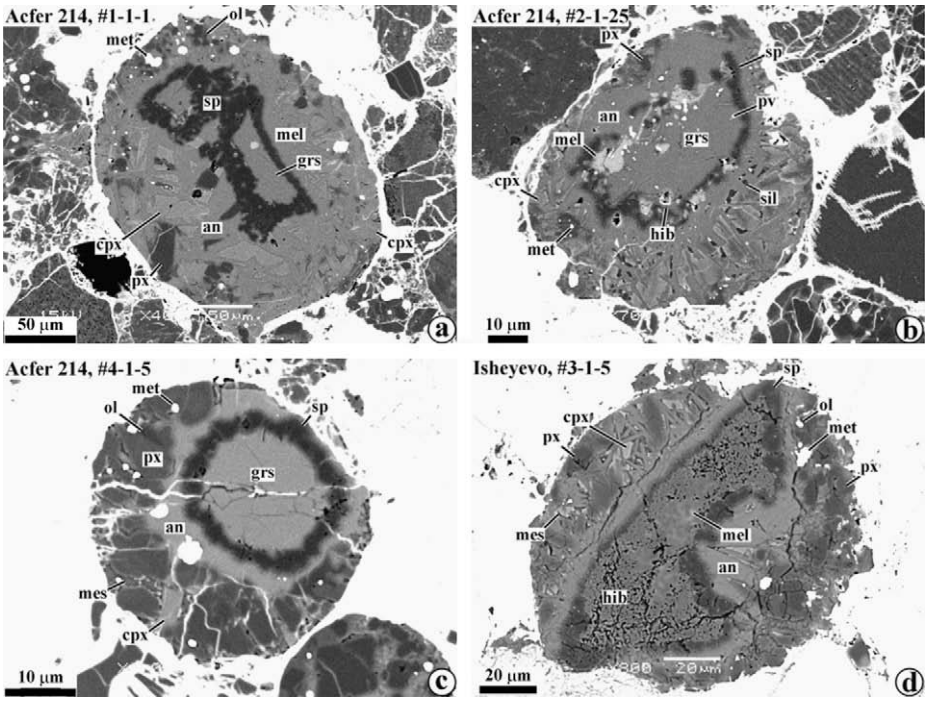

Fig. 14. BSE images of porphyritic chondrules with relict CAIs from the CH chondrite Acfer 214 and CH/CB-like chondrite Isheyevo (from Krot et al., 2007b). The relict CAIs are mineralogically and isotopically similar to those outside chondrules of the host meteorites. an = anorthitic plagioclase; cpx = high-Ca pyroxene; grs = grossite; hib = hibonite; mel = melilite; mes = plagioclase-rich mesostasis; met = Fe,Ni-metal; ol = olivine; pv = perovskite; px = low-Ca pyroxene; sil = silica; sp = spinel.

during chondrule formation (Fig. EA2) shows evidence for isotope exchange with an ^{16}O-poor nebular gas (Δ^{17}O ranges from -18‰ in spinel to -10‰ in Al,Ti-diopside, melilite and anorthite) and has low initial ^{26}Al/^{27}Al ratio [$(1.4 \pm 0.9) \times 10^{-6}$], similar to those in CR chondrules (Aléon et al., 2002; Nagashima et al., 2007b).

CAIs that melted during chondrule formation and those apparently unaffected by chondrule melting are mineralogically similar. For example, the most common type of free-standing CAI (spinel–pyroxene-rich; see above) is also the most common type type of relict CAI found inside carbonaceous chondrite chondrules[1] (Krot and Keil, 2002; Krot et al., 2002b). In addition, there are striking similarities between CAIs melted during chondrule formation and CAIs unaffected by chondrule melting in an individual chondrite group. For example, (i) CAIs in CH chondrites are dominated by mineralogically and isotopically rare types of inclusions: grossite- and hibonite-rich spherules characterized by low initial ^{26}Al/^{27}Al ratios ($<1 \times 10^{-5}$) and ^{16}O-rich (Δ^{17}O < -20‰) compositions (Krot et al., 2008a). Mineralogically and isotopically very similar CAIs are found inside porphyritic chondrules in CH chondrites (Fig. 14). (ii) Coarse-grained igneous CAIs (Type B and Type C) are almost exclusively found in CV chondrites (MacPherson et al., 1988). Some of these CAIs were remelted during chondrule formation (e.g., Fig. EA1). Based on these observations, we infer that the CAIs found in a specific carbonaceous chondrite group were present in a region where chondrules of this chondrite group formed, but many of these CAIs were apparently unaffected by chondrule melting events. We suggest that chondrule-forming events experienced by a nebular region were relatively small in scale and limited in number. Alternatively, it was proposed that accretion of CAIs in intermediate-sized (hundred of meters to kilometers) objects could help to preserve them from being melted during chondrule formation (e.g., Russell et al., 1996; Huss et al., 2001; Hutcheon et al., 2009). Note, however, that no fragments of such hypothetical bodies have been in chondrites so far. In addition, it would require release of some CAIs from these hypothetical bodies to be reprocessed during chondrule melting.

To put a lower limit on a fraction of CAIs affected by chondrule melting (some CAIs could have been completely destroyed during chondrule formation), systematic studies of mineralogy, petrography, oxygen– and magnesium–isotope compositions of CAIs from primitive chondrites are required. For example, based on a very comprehensive study of CAIs from 15 CR chondrites, Makide et al. (2009) showed that at least 8 of 166 CAIs (~5%) identified experienced late-stage melting during chondrule formation.

Note that the presence of CAIs in the chondrule-forming regions is not inconsistent with an *x*-wind astrophysical setting for CAI and chondrule formation (Fig. 2), because some CAIs could have been recycled in the protoplanetary disk, near *x*-region, at the time of low magnetic activity of

[1] Because CAIs in ordinary and enstatite chondrites are very rare, it is difficult to identify CAI-chondrule compound objects in these chondrite groups.

the Sun or low disk accretion rate. However, according to the *x*-wind model, remelting of chondrules in the CAI-forming region should be also expected; no such chondrules have been unambiguously identified yet.[2]

We conclude that mineralogical observations and chemical and oxygen–isotope data support formation of CAIs prior to chondrule formation, which is inconsistent with the *x*-wind model.

3.2.2. ^{26}Al–^{26}Mg systematics of refractory inclusions and chondrules

The use of ^{26}Al ($t_{1/2} = 0.73$ Myr) as a high-resolution chronometer [specifically, inferred $(^{26}Al/^{27}Al)_0$] for dating CAI and chondrule formation requires the assumption of a uniform distribution of ^{26}Al throughout the inner solar nebula, where CAIs and chondrules probably formed (MacPherson et al., 1995). Cross-calibration of ^{26}Al–^{26}Mg and ^{207}Pb–^{206}Pb chronometers (Amelin et al., 2002; Zinner and Göpel, 2002; Jacobsen et al., 2008a,b; Connelly et al., 2008), and high-precision magnesium–isotope measurements of bulk chondrites, Earth, Moon and Mars (Thrane et al., 2006), have validated this assumption and thus confirmed the chronological significance of ^{26}Al–^{26}Mg systematics (Fig. 15).

Before we discuss ^{26}Al–^{26}Mg chronology of CAIs and chondrules, we need to define the term "CAI-formation" used in the paper. There is almost no ambiguity in classifying an object as a CAI or a chondrule (Al-diopside ± spinel ± hibonite spherules could be an exception) based on its mineralogy and/or bulk chemical compositions (see Section 2). However, some igneous CAIs experienced melting during chondrule formation; these CAIs can be recognized based on textures, mineralogy, and/or oxygen–isotope compositions (Figs. 14 and EA1 and 2). Although these objects are true CAIs, they should not be used for constraining the duration of CAI formation, because their ^{26}Al–^{26}Mg systematics could have been reset during chondrule melting.

Note also that oxygen– and Al–Mg isotope systematics of CAIs from many CV chondrites may have been disturbed during fluid-assisted thermal metamorphism and their use for chronological interpretation should be considered cautiously.

3.2.2.1. ^{26}Al–^{26}Mg systematics of CAIs and AOAs. There is converging agreement on the Solar System initial $^{26}Al/^{27}Al$ ratio inferred from recent magnesium–isotope measurements of CAIs (e.g., Baker, 2007; Kita et al., 2007; Jacobsen et al., 2008a) (Table 4 and Fig. 16). Most CAIs and a few AOAs analyzed so far using SIMS (minerals with high $^{27}Al/^{24}Mg$ ratios—anorthite, hibonite, and gehlenitic melilite—are commonly measured) define $(^{26}Al/^{27}Al)_0$ of $\sim(4.5–5) \times 10^{-5}$, referred to as the "*canonical*" value (MacPherson et al., 1995; Weisberg et al., 2007). Higher values

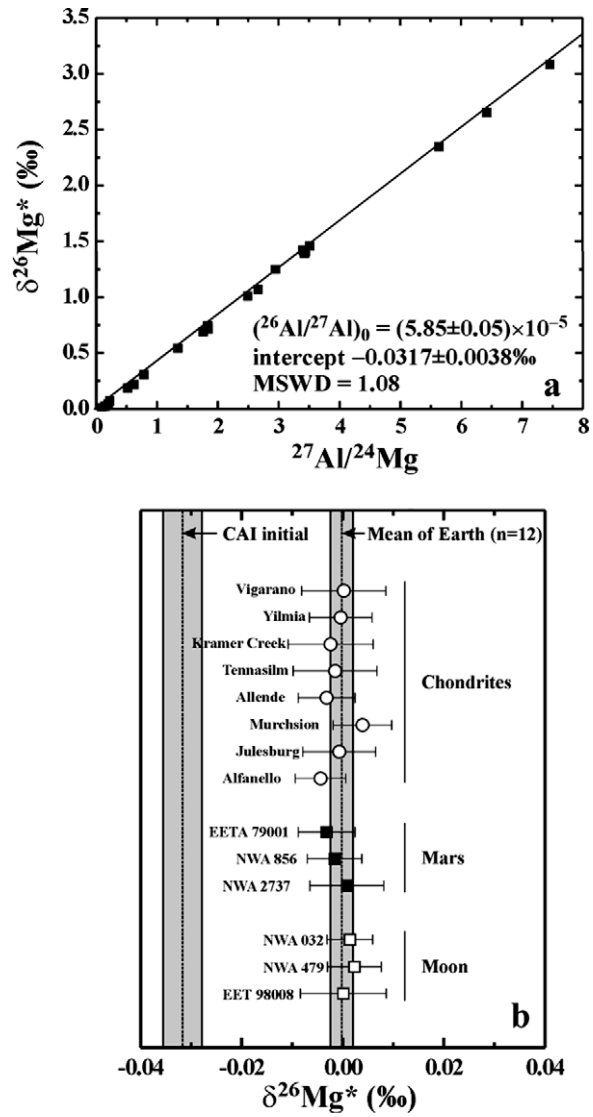

Fig. 15. (a) ^{26}Al–^{26}Mg isochron diagram of "bulk" CV CAIs (sampled by microdrilling) obtained by MC-ICPMS. Error bars are 2σ. MSWD = mean square weighted deviation. The data plot along a slope corresponding to $(^{26}Al/^{27}Al)_0$ of $(5.85 \pm 0.05) \times 10^{-5}$ with an intercept of -0.0317 ± 0.0038‰. The intercept is interpreted as the initial Mg isotope composition at the time of CAI formation. (b) The δ^{26}Mg* values for samples from terrestrial planets and chondrite parent bodies. Error bars are 2σ for individual samples, and 2σ for the mean Earth and CAI initial δ^{26}Mg*. Data are from Bizzarro et al. (2004, 2005), Baker et al. (2005) and Thrane et al. (2006).

called the "*supra-canonical*" that range from 5.85×10^{-5} to 7×10^{-5} have recently been advocated (Galy et al., 2004; Bizzarro et al., 2004, 2005; Young et al., 2005; Taylor et al., 2005; Thrane et al., 2006; Cosarinsky et al., 2007).

The supra-canonical $^{26}Al/^{27}Al$ ratios are obtained largely from bulk-sample magnesium–isotope measurements of CV CAIs using MC-ICPMS (Galy et al., 2004; Bizzarro et al., 2004, 2005; Thrane et al., 2006) or from MC-SIMS and LA-MC-ICPMS measurements of CV CAI minerals with low $^{27}Al/^{24}Mg$ ratios (<3), mainly spinel and Al,

[2] The only controversial CAI-chondrule compound object, A5 from Y-81020 (CO3.0), interpreted as a mixture of CAI and chondrule materials remelted in the CAI-forming region (Itoh and Yurimoto, 2003), is shown in Figure EA3. An explanation for the origin of this object is discussed by Russell et al. (2005) and summarized in caption to the Figure EA3.

Table 4
Initial $^{26}Al/^{27}Al$ ratios in CAIs and chondrules inferred from recent (since 2000) high-precision magnesium-isotope measurements.

Object, chondrite (group and petrologic type)	Analytical technique	$(^{26}Al/^{27}Al)_0$	Reference
11 CAIs, Allende (CV > 3.6), Vigarano (CV3.1–3.4), SAH 98044 (CV), NWA 779 (CV)	MC-ICPMS	$(5.85 \pm 0.05) \times 10^{-5}$	Thrane et al. (2006)
7 CAIs, Allende, Efremovka & Leoville (CV3.1–3.4), Grosnaja (CV3.6)	LA-MC-ICPMS	$<4–7 \times 10^{-5}$	Young et al. (2005)
9 CAIs, Allende	MC-ICPMS, bulk sample isochron	$(5.23 \pm 0.13) \times 10^{-5}$	Jacobsen et al. (2008a)
CAI AJEF, Allende	Mineral separates, internal	$(4.96 \pm 0.25) \times 10^{-5}$	
CAI A44A, Allende	Isochrons	$(5.03 \pm 0.18) \times 10^{-5}$	
CAI A43, Allende	–"–	$(4.47 \pm 0.42) \times 10^{-5}$	
3 Texturally distinct regions in a CAI, Allende	SIMS, internal isochrons	$\sim 5 \times 10^{-5}$ $(4.3 \pm 0.1) \times 10^{-5}$ $(3.3 \pm 0.8) \times 10^{-5}$	Hsu et al. (2000)
12 CAIs, Leoville, Efremovka, Vigarano	SIMS, model & internal isochrons	3.8×10^{-5} to 6.1×10^{-5}	Cosarinsky et al. (2007)
CAI, Leoville	SIMS, internal isochron	$(5.0 \pm 0.3) \times 10^{-5}$	Kita et al. (2007)
CAI, Kaba (CV3.1)	SIMS, internal isochron	$(4.9 \pm 0.6) \times 10^{-5}$	Nagashima et al. (2007a)
CAI in AOA, EET 92105 (CR2)	SIMS, internal isochrons	$(4.7 \pm 0.6) \times 10^{-5}$	Weisberg et al. (2007)
CAIs in AOAs, EET 87770 & 92105 (CR2)		$(5–7) \times 10^{-5}$	
7 CAIs, CR2s	SIMS, internal isochrons SIMS, model isochrons	$(4.43 \pm 0.24) \times 10^{-5}$ to $(5.43 \pm 0.62) \times 10^{-5}$	Makide et al. (2009)
7 CAIs, CR2s		$(4.44 \pm 0.39) \times 10^{-5}$ to $(5.44 \pm 0.60) \times 10^{-5}$	
4 CAIs, Allende	SIMS, model isochrons	$(5.17 \pm 0.24) \times 10^{-5}$	Jacobsen et al. (2008b)
21 Chondrules, Y-81020 (CO3.0)	SIMS, internal isochrons	$(0.29 \pm 0.09) \times 10^{-5}$ to $(1.03 \pm 0.28) \times 10^{-5}$	Kurahashi et al. (2008)
5 Chondrules, Y-81020		$(0.24 \pm 0.17) \times 10^{-5}$ to $(0.65 \pm 0.32) \times 10^{-5}$	Kunihiro et al. (2004)
6 Chondrules, CR2s	SIMS, internal isochron	$(0.13 \pm 0.03) \times 10^{-5}$ to $(0.63 \pm 0.09) \times 10^{-5}$	Nagashima et al. (2007b, 2008)
8 Chondrules, CR2s		No resolved $^{26}Mg^*$	
31 Chondrules, OCs (<3.2)	SIMS, internal isochrons	$(0.48 \pm 0.45) \times 10^{-5}$ to $(2.28 \pm 0.73) \times 10^{-5}$	See Refs. to Fig. 21
8 Chondrules, OCs (<3.2)		No resolved $^{26}Mg^*$	

Ti-diopside (Taylor et al., 2005; Young et al., 2005; Cosarinsky et al., 2007; Simon and Young, 2007). Note that if ^{26}Al was uniformly distributed in the Solar System, ^{26}Al–^{26}Mg isochrons based on bulk-sample magnesium–isotope measurements of igneous CAIs correspond to the time of the last Al–Mg fractionation by evaporation–condensation during formation of these CAIs or their precursors. Internal isochrons based on magnesium–isotope measurements of individual minerals of igneous CAI correspond to their crystallization ages. The internal ^{26}Al–^{26}Mg isochrons in CAIs from even mildly metamorphosed meteorites, including many CVs, are often disturbed and cannot be used to constrain CAI crystallization ages. Note also the importance of using the correct magnesium–isotope mass-fractionation laws (exponential, equilibrium, or experimentally derived) for the correction of magnesium–isotope data for samples with low $^{27}Al/^{24}Mg$ ratios when comparing isochrons for mass-fractionated CAIs (Davis et al., 2005b). The recently published (since 2000) high-precision magnesium-isotope measurements of CAIs, AOAs and chondrules are summarized in Table 4 and shown in Fig. 16, and are discussed below.

High-precision magnesium–isotope measurements of bulk-sample igneous (compact Type A and Type B) Allende CAIs and their mineral separates using MC-ICPMS yield the initial $^{26}Al/^{27}Al$ ratio of $(5.16 \pm 0.09) \times 10^{-5}$ (Jacobsen et al., 2008a), which is inconsistent with $(5.85 \pm 0.05) \times 10^{-5}$ value reported by Thrane et al. (2006) for bulk-sample CV CAIs using a similar analytical technique. Although this apparent discrepancy still needs to be resolved, these data sets suggest a very short (<20–30 kyr) time difference between the formation of precursors of the CV igneous CAIs and their crystallization ages. Thrane et al. (2006) and Jacobsen et al. (2008a) interpreted the small uncertainty in the inferred initial $^{26}Al/^{27}Al$ ratio as the maximum duration of CAI formation. We note that this conclusion is limited at present only to CAIs from several CV chondrites. In order to constrain the *total* duration of CAI formation, high precision measurements of both bulk sample and internal ^{26}Al–^{26}Mg isochrons in CAIs from primitive meteorites of other chondrite groups are required.

Different estimates of crystallization age of CV CAIs were reported using *in situ* SIMS (Hsu et al., 2000; Kita et al., 2007; Nagashima et al., 2007a; Makide et al., 2009)

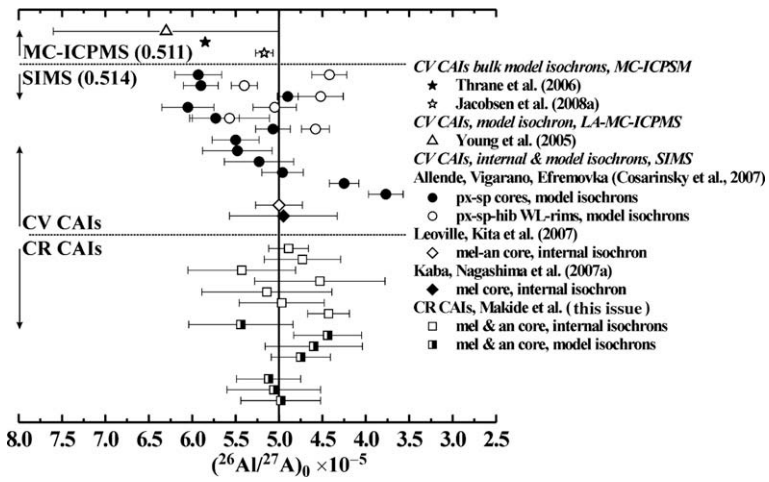

Fig. 16. Distribution of $(^{26}Al/^{27}Al)_0$ in CV and CR CAIs inferred from magnesium–isotope measurements of bulk CAIs and mineral separates (Thrane et al., 2006; Jacobsen et al., 2008a) using MC-ICPMS, in mixed mineral phases and bulk CAIs using LA-MC-ICPMS (Young et al., 2005), and from internal and model isochrons using SIMS (Cosarinsky et al., 2007; Kita et al., 2007; Nagashima et al., 2007a; Makide et al., 2009). $(^{26}Al/^{27}Al)_0$ in CAIs measured by SIMS and ICPMS were calculated using exponential fractionation laws with experimentally derived fractionation factor 0.514 and kinetic fractionation factor 0.511, respectively. For SIMS measurements, each line represents single CAI. CAIs and their Wark–Lovering (WL) rims from Allende (CV > 3.6), Efremovka (CV3.1–3.4) and Vigarano (CV3.1–3.4) show large range of $(^{26}Al/^{27}Al)_0$ [(3.7–6.1) × 10^{-5}]. The $(^{26}Al/^{27}Al)_0$ in CAIs from Leoville (CV3.1–3.4) and Kaba (CV3.1) and CRs are consistent with the canonical value of ~(4.5–5) × 10^{-5}. an = anorthite; hib = hibonite; mel = melilite; px = Al,Ti-diopside; sp = spinel.

and LA-MC-ICPMS measurements (Young et al., 2005). Hsu et al. (2000) obtained three internal isochrons in an Allende Type B CAI composed of three texturally distinct regions (Fig. EA4) and concluded that this CAI recorded multiple heating events during 300,000 years of its evolution.

Magnesium–isotope measurements of mixed phases and bulk sample of eight coarse-grained CAIs from CV chondrites Allende, Efremovka, Grosnaja, Leoville and Vigarano measured by Young et al. (2005) show a range of $(^{26}Al/^{27}Al)_0$ from <4 to 7 × 10^{-5}; 79% of all measurements plot above the canonical value (Fig. 1 in Young et al., 2005). Young et al. (2005) concluded that CV CAIs experienced prolonged thermal history (~300,000 years) in the solar nebula.

Cosarinsky et al. (2007) measured ^{26}Al–^{26}Mg systematics of 14 igneous (Type B and compact Type A) and non-igneous (fluffy Type A) CAIs from Allende (CV > 3.6), Vigarano (CV3.1–3.4) and Efremovka (CV3.1–3.4) (petrologic types according to Bonal et al., 2006), as well as their Wark–Lovering rims, using MC-SIMS. Because melilite in these CAIs often shows evidence for re-distribution of magnesium isotopes, internal isochrons were constructed using only spinel, Al,Ti-diopside and hibonite grains, and the isochron lines were forced through the origin (i.e., these are model isochrons). The inferred $(^{26}Al/^{27}Al)_0$ ratios range from 3.8 to 6.1 × 10^{-5}. In 5 out of 6 CAIs measured, there are resolvable age differences between the formation of the CAI interiors and their Wark–Lovering rims (Fig. 16). Cosarinsky et al. (2007) concluded that formation and thermal processing of CV CAIs lasted for at least 0.5 Myr, supporting earlier conclusions of Hsu et al. (2000) and Young et al. (2005). In contrast, a Type B CAI from Leoville (CV3.1–3.4) and a compact Type A CAI Kaba (CV3.1) (petrologic types according to Bonal et al., 2006) show no disturbance of ^{26}Al–^{26}Mg systematics in any of the minerals studied, including melilite and anorthite; the inferred values of $(^{26}Al/^{27}Al)_0$ are (5.0 ± 0.3) × 10^{-5} (Kita et al., reported at the Workshop in Kauai, 2007) and (4.9 ± 0.6) × 10^{-5} (K. Nagashima, personal communication, 2007), respectively.

To constrain the duration of formation and subsequent thermal processing of CAIs and identify inclusions melted during chondrule formation, Makide et al. (2009) measured *in situ* oxygen–isotope compositions and internal ^{26}Al–^{26}Mg isochrons in the mineralogically pristine CAIs from CR chondrites using SIMS. Makide et al. found that CAIs showing no evidence for being recycled during chondrule formation have uniformly ^{16}O-rich ($\Delta^{17}O$ = −23.3 ± 1.9‰, 2 standard deviations) compositions and $(^{26}Al/^{27}Al)_0$ ratios consistent with the canonical value of ~(4.5 ± 5.0) × 10^{-5} (Table 4 and Fig. 16). The observed range in $(^{26}Al/^{27}Al)_0$, largely due to uncertainties of measurements, suggests formation of CR CAIs lasted between 0.1 and 0.4 Myr.

3.2.2.2. Chronology of ^{26}Al-poor CAIs. Some CAIs show either no excess of ^{26}Mg due to decay of ^{26}Al (deficit of ^{26}Mg or excess of ^{25}Mg is observed instead) or have much lower $(^{26}Al/^{27}Al)_0$ ratio (<1 × 10^{-5}) than the canonical value. These include FUN (fractionation and unidentified nuclear effects) CAIs in Allende (Lee, 1988), some platy hibonite crystals (PLACs) in CM chondrites (e.g., Sahijpal and Goswami, 1998; Ireland and Fegley, 2000; Liu et al., 2007), pyroxene–hibonite spherules in CM and CO chondrites (Ireland et al., 1991; Russell et al., 1998), some corundum-rich CAIs (Simon et al., 2002), most grossite- and hibonite-rich inclusions in CH chondrites (Kimura et al., 1993; Weber et al., 1995; Krot et al., 2008b), and a few CAIs measured in CB chondrites (Gounelle et al., 2007).

FUN CAIs, PLACs and pyroxene–hibonite spherules have large nucleosynthetic isotopic anomalies in many elements (e.g., Ca, Ti, Si) and volatility-fractionated REE patterns. Based on these observations and the refractory nature of many of these inclusions, it is hypothesized that they formed early, prior to injection and/or homogenization of ^{26}Al in the Solar System, before or contemporaneously with CAIs having the canonical ^{26}Al/^{27}Al ratio (Sahijpal and Goswami, 1998). The ^{16}O-rich ($\Delta^{17}O \sim -24 \pm 2‰$) compositions of FUN CAIs (Fig. 17; Thrane et al., 2008), PLACs (Goswami et al., 2001) and corundum-rich CAIs (Simon et al., 2002), which are similar to those of CAIs with the canonical ^{26}Al/^{27}Al ratio (Makide et al., 2009; MacPherson et al., 2008), are generally consistent with this hypothesis, but do not prove it. Measurements of ^{207}Pb–^{206}Pb ages of such CAIs are required to test it.

Most of the ^{26}Al-poor [$(^{26}Al/^{27}Al)_0) < 1 \times 10^{-5}$] grossite- and hibonite-rich CAIs in CH chondrites are ^{16}O-rich ($\Delta^{17}O < -20‰$; Fig. 18) and show no large nuclear isotopic anomalies or mass-dependent fractionation effects (Kimura et al., 1993; Weber et al., 1995; Srinivasan et al., 2007; Krot et al., 2008b). These CAIs may have formed either very early, as hypothesized for FUN CAIs and PLACs (Sahijpal and Goswami, 1998), or very late, after decay of ^{26}Al.

CAIs in CB chondrites are ^{26}Al-poor, $(^{26}Al/^{27}Al)_0)$ $<4.6 \times 10^{-6}$ (only three CAIs have been measured so far) and uniformly ^{16}O-depleted ($\Delta^{17}O > -10‰$; Fig. 19); most of them have igneous textures (Krot et al., 2001b, 2005a; Gounelle et al., 2007). These observations may indicate that CB CAIs experienced isotope exchange during late-stage melting. Since chondrules in CB chondrites formed during a highly-energetic, single-stage event ~4563 Myr ago and have ^{16}O-depleted compositions (Krot et al., 2005a), this event may have resulted in melting and isotope exchange of CB CAIs as well.

3.2.2.3. ^{26}Al–^{26}Mg systematics of primitive chondrite chondrules. High-precision, internal ^{26}Al–^{26}Mg isochrons in chondrules (Fig. 20a and b) are reported for primitive meteorites of two groups of carbonaceous (CO3.0 and CR2) and two groups of ordinary chondrites (L and LL3.0–3.2, Fig. 21) (Kita et al., 2000, 2005; Mostefaoui et al., 2001; Kunihiro et al., 2004; Kurahashi et al., 2004, 2008; Rudraswami and Goswami, 2007; Nagashima et al., 2007b, 2008). In the CO3.0 chondrite Y-81020, the initial ^{26}Al/^{27}Al ratios range from $(0.24 \pm 0.17) \times 10^{-5}$ to $(1.03 \pm 0.28) \times 10^{-5}$, which corresponds to an age difference of 1.3–3.2 Myr after CAIs with the canonical $(^{26}Al/^{27}Al)_0$ (Table 4 and Figs. 20a and 21b). No systematic differences were found between the inferred ages of chondrules from CO and ordinary chondrites; the initial ^{26}Al/^{27}Al ratios in ordinary chondrite chondrules range from $(0.48 \pm 0.45) \times 10^{-5}$ to $(2.28 \pm 0.73) \times 10^{-5}$ (Table 4 and Fig. 21a).[3] In contrast, most chondrules from CR2 chondrites have

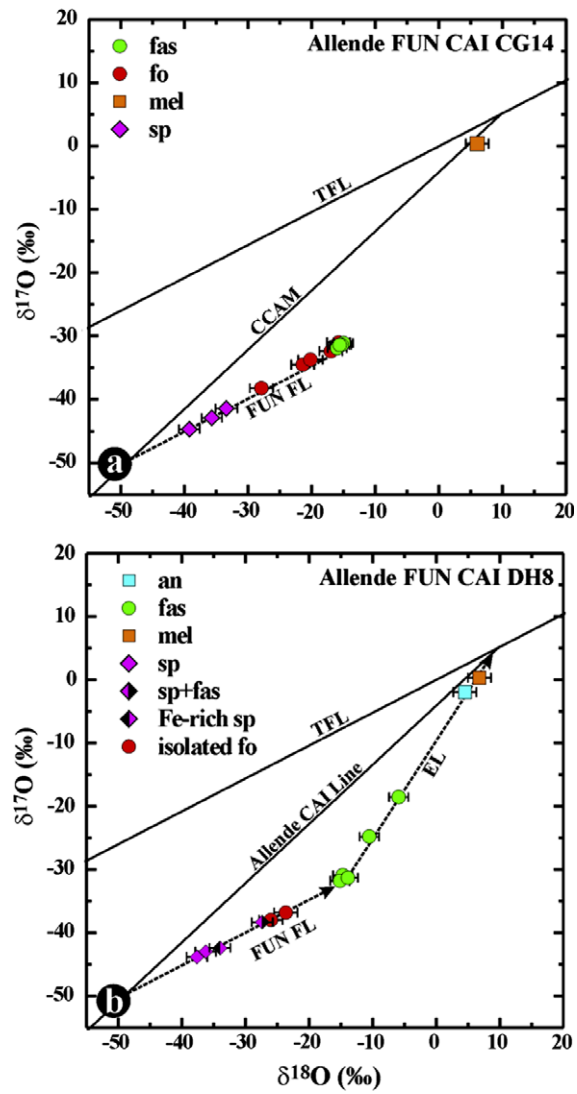

Fig. 17. Oxygen–isotope compositions of individual minerals in the Allende FUN CAIs CG14 and DH8 (data from Krot et al., 2008a). Both CAIs experienced mass-dependent fractionation of oxygen isotopes as a result of melt evaporation: degree of fractionation increases from spinel to forsterite to Al,Ti-diopside, consistent with the inferred crystallization sequence of the CAI melts (Stolper, 1983). Subsequently, melilite, anorthite and some Al,Ti-diopside grains experienced oxygen–isotope exchange with an ^{16}O-poor reservoir. The $\Delta^{17}O$ values of spinel, forsterite and most Al,Ti-diopside grains in the FUN CAI ($\sim -24 \pm 2‰$) are similar to those of non-FUN CAIs. an = anorthite; fas = Al,Ti-diopside; fo = forsterite; mel = melilite; sp = spinel. EL = exchange line; FUN FL = FUN fractionation line.

$(^{26}Al/^{27}Al)_0 < 0.3 \times 10^{-5}$ (Table 4 and Fig. 21c), consistent with their young ^{207}Pb–^{206}Pb absolute ages (Amelin et al., 2002).

The young crystallization ages of primitive chondrite chondrules inferred from the internal ^{26}Al–^{26}Mg isochrons are in apparent conflict with the model ^{26}Al–^{26}Mg isochrons [$(^{26}Al/^{27}Al)_0 \sim (3–5) \times 10^{-5}$] inferred from the bulk-sample magnesium–isotope compositions of CV chondrules (Fig. 20c), which overlap with those of CV CAIs (Bizzarro

[3] Note that a fraction of chondrules with $(^{26}Al/^{27}Al)_0 < 0.5 \times 10^{-5}$ is higher in CO than in ordinary chondrites, which may suggest some systematic differences in ages of the CO and ordinary chondrite chondrules.

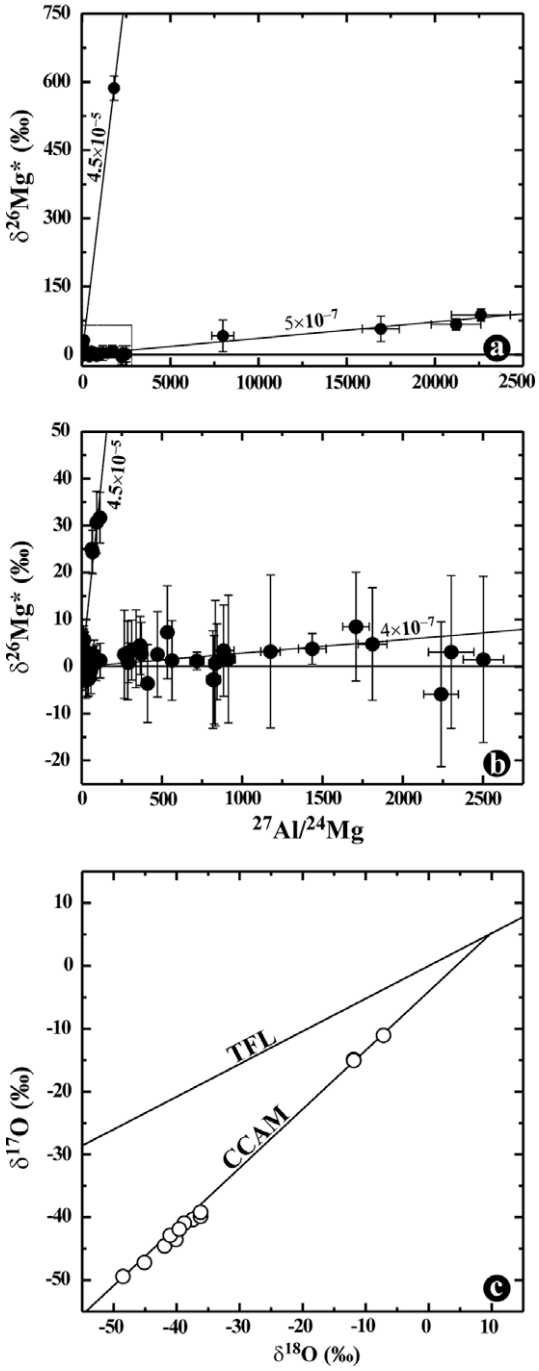

Fig. 18. ^{26}Al–^{26}Mg evolution diagrams (a and b) and oxygen–isotope compositions (c) of CAIs from the CH chondrite Acfer 214 and CH/CB-like chondrite Isheyevo (data from Krot et al., 2008b). Region outlined by dashed line in "a" is shown in "b". Two kinds of CAIs can be recognized based on the ^{26}Al–^{26}Mg isotope systematics: with the canonical $(^{26}Al/^{27}Al)_0$ of ~(4.5–5) × 10^{-5} and with either unresolved or small excesses of ^{26}Mg corresponding to the $(^{26}Al/^{27}Al)_0$ < (4–5) × 10^{-7}. The ^{26}Al-poor CAIs are dominant. Most CAIs of both kinds are ^{16}O-rich. The ^{16}O-depleted CAIs are rare and show no excess of ^{26}Mg. In "a" and "b" errors are 2σ; in "c" 2σ errors correspond size of the symbols.

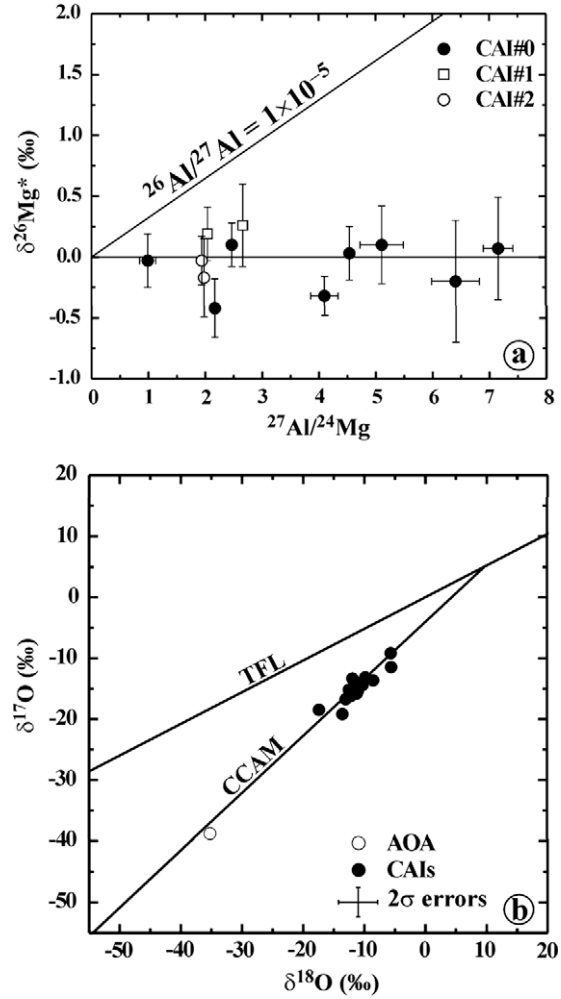

Fig. 19. (a) ^{26}Al–^{26}Mg evolution diagram for CAIs from the CB chondrites Hammadah al Hamra 237 (CAI #0) and QUE 94411 (CAIs #1 and #2) (data from Gounelle et al., 2007). None of the CAIs show resolvable δ^{26}Mg*; errors are 2σ. An upper limit for the initial ^{26}Al/^{27}Al ratio in combined three CAIs is 4.6 × 10^{-6}. Isochron with slope 1 × 10^{-5} is shown for reference. (b) Oxygen–isotope compositions of AOA and CAIs from Hammadah al Hamra 237 and QUE 94411/94627 (data from Krot et al., 2001b). The CB CAIs are uniformly ^{16}O-depleted compared to typical CAIs from primitive chondrites.

et al., 2004; Thrane et al., 2006). The latter data were interpreted as an evidence for contemporaneous formation of chondrules and CAIs (Bizzarro et al., 2004; Bouvier and Wadhwa, 2007), and thus cited as an evidence supporting *x*-wind model (Gounelle et al., 2006). Note, however, that (i) *x*-wind model excludes chronological interpretation of ^{26}Al–^{26}Mg systematics, and (ii) large excesses of ^{26}Mg in CV chondrules are in conflict with *x*-wind model for irradiation origin of ^{26}Al; according to this model, chondrules formed in the gaseous disk and were better shielded from irradiation than CAIs. (iii) The bulk-sample ^{26}Al–^{26}Mg isochrons for chondrules may correspond to the formation time of chondrule precursors, not chondrule crystallization ages. The latter can be inferred unambiguously only from the internal ^{26}Al–^{26}Mg isochrons provided there was no metamorphic resetting since the chondrule crystallization, a condition may have been fulfilled given the low degree

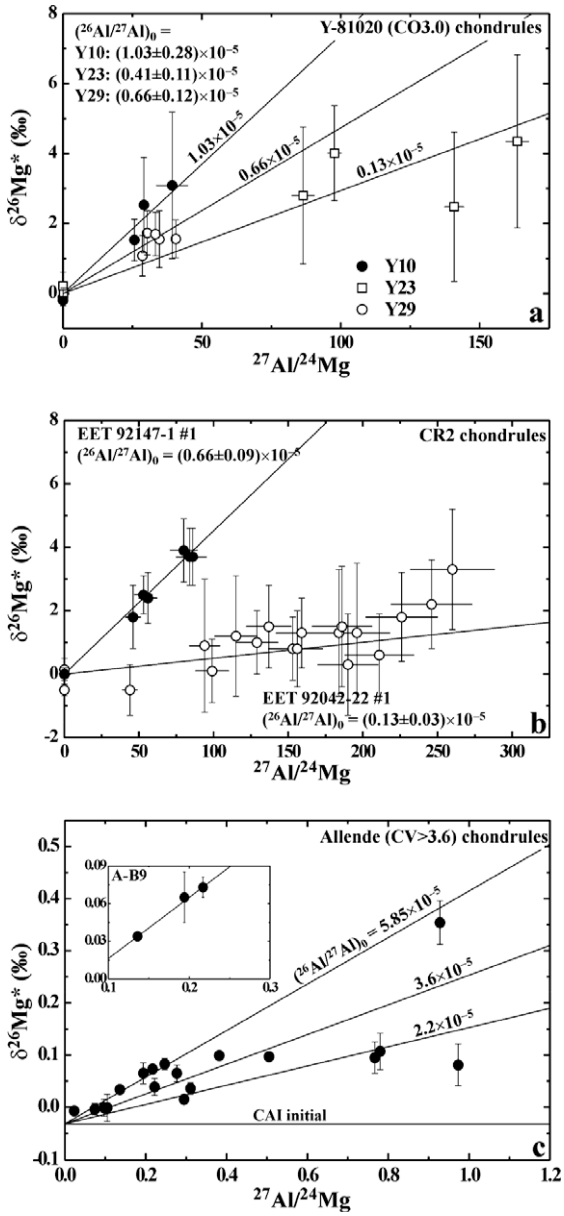

Fig. 20. (a and b) ^{26}Al–^{26}Mg internal isochrons for representative chondrules from Y81020 (CO3.0; Kurahashi et al., 2008) and CR chondrites EET 92147 and EET 92042 (Nagashima et al., 2007b). (c) ^{26}Al–^{26}Mg evolution diagram for "bulk" (samples were drilled out) Allende chondrules obtained by MC-ICPMS (Bizzarro et al., 2004, 2005). Error bars for δ^{26}Mg* are 2σ external reproducibility. Isochrons with slopes 5.85, 3.6 and 2.2×10^{-5} correspond 0, 0.5 and 1 Myr after formation of CAIs with the supra-canonical $(^{26}Al/^{27}Al)_0 = (5.85 \pm 0.05) \times 10^{-5}$. The inset shows the internal isochron for chondrule A-B9, corresponding to an $(^{26}Al/^{27}Al)_0 = (6.2 \pm 2.4) \times 10^{-5}$.

of metamorphism in these primitive meteorites. (iv) Finally, if ^{26}Al was uniformly distributed in the CAI- and chondrule-forming regions, as predicted from models of its stellar origin and argued by Thrane et al. (2006), and if there was no significant Al–Mg fractionation during chondrule formation, bulk-sample isochrons of chondrules and CAIs

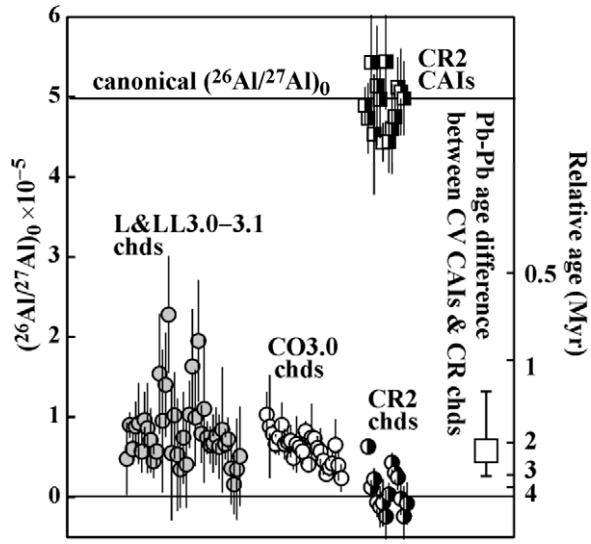

Fig. 21. Distribution of $(^{26}Al/^{27}Al)_0$ in chondrules from primitive (petrologic type 3.0 and 3.1) ordinary (L and LL) and carbonaceous (CO3.0 and CR2) chondrites and in CAIs from CR chondrites. All data were obtained by *in situ* SIMS measurements. Chondrules from ordinary and CO chondrites have similar range of the initial $(^{26}Al/^{27}Al)_0$ ratios; chondrules from CR chondrites have lower values of $(^{26}Al/^{27}Al)_0$. The inferred ^{26}Al–^{26}Mg ages of CR chondrules are consistent with ^{206}Pb–^{207}Pb ages (square) reported by Amelin et al. (2002). Data for chondrules are from Kita et al. (2000), McKeegan et al. (2000b), Huss et al. (2001, 2007), Mostefaoui et al. (2001), Kunihiro et al. (2004), Kurahashi et al. (2008), Rudraswami and Goswami (2007), and Nagashima et al. (2007b, 2008). Data for CAIs are from Makide et al. (2009).

should be similar. The observed spread in slopes of bulk-sample ^{26}Al–^{26}Mg isochrons of CV chondrules (Fig. 20c) may be due to unrepresentative sampling of chondrules by microdrilling used by Bizzarro et al., 2004. This hypothesis can be tested by measurements of magnesium–isotope compositions of whole chondrule samples.

3.2.3. ^{53}Mn-^{53}Cr systematics of CAIs and chondrules

^{53}Mn–^{53}Cr systematics [^{53}Mn decays to ^{53}Cr with $t_{1/2} \sim 3.7$ Myr] of CAIs and chondrules were measured in a very limited number of samples, which are mainly from metamorphosed chondrites and do not provide any firm conclusion on the chronology of CAI and chondrule formation yet (Birck and Allégre, 1985; Nyquist et al., 2001; Yin et al., 2007). In addition, the initial Solar System ^{53}Mn/^{55}Mn ratio [$(^{53}Mn/^{55}Mn)_0$] is uncertain: estimates range from 0.84 to 4.4×10^{-5} (Birck and Allégre, 1988; Lugmair and Shukolyukov, 1998, 2001; Nyquist et al., 2001; Shukolyukov and Lugmair, 2006; Moynier et al., 2007). The most recent value of $(8.5 \pm 1.5) \times 10^{-6}$ has been inferred from whole-rock carbonaceous chondrites, which may correspond to global, high-temperature Mn–Cr fractionation in the solar nebula (Shukolyukov and Lugmair, 2006; Moynier et al., 2007). ^{53}Mn–^{53}Cr systematics of CAIs from CV chondrites, the only group where they were measured, are disturbed, which compromise their chronological significance (e.g., Bogdanovski et al., 2002). Manganese–

chromium isotope measurements of the Chainpur (LL3.4) chondrules yield $(^{53}Mn/^{55}Mn)_0 = (9.4 \pm 1.7) \times 10^{-6}$ (Nyquist et al., 2001). A significantly lower value $[(5.1 \pm 1.6) \times 10^{-6}]$ has been recently reported for the Chainpur chondrules by Yin et al. (2007); the similar $(^{53}Mn/^{55}Mn)_0$ ratio was reported for chondrules from Semarkona (LL3.0) $(5.8 \pm 1.9) \times 10^{-6}$ (Kita et al., 2005).

3.2.4. ^{60}Fe–^{60}Ni systematics of CAIs and chondrules

In spite of very important role of ^{60}Fe ($t_{1/2} \sim 1.5$ Myr) for understanding the origin of short-lived radionuclides in the early Solar System (a stellar, probably supernova source of ^{60}Fe is required) and its astrophysical environment of the Solar System formation (Tachibana and Huss, 2003; Tachibana et al., 2006; Bizzarro et al., 2007a,b; Gounelle et al., 2008), ^{60}Fe–^{60}Ni systematics of chondritic components are too poorly studied to have important implication for the chronology of CAI and chondrule formation. There are several additional reasons which restrict chronological implication of ^{60}Fe–^{60}Ni systematics. (i) The initial $^{60}Fe/^{56}Fe$ ratio $[(^{60}Fe/^{56}Fe)_0]$ in the Solar System is poorly constrained. Although the presence of ^{60}Ni excesses ($^{60}Ni^*$) has been reported in CV CAIs (Quitté et al., 2007), the nucleosynthetic origin of these anomalies cannot be excluded (Bizzarro et al., 2007b). (ii) ^{60}Fe–^{60}Ni systematics has not been anchored yet to other short-lived (^{26}Al–^{26}Mg, ^{53}Mn–^{53}Cr, ^{182}Hf–^{182}W) or long-lived (^{207}Pb–^{206}Pb) isotope systematics. (iii) Uniform distribution of ^{60}Fe in the solar nebula is being debated (e.g., Bizzarro et al., 2007a; Dauphas et al., 2008). (iv) Measurements of ^{60}Fe–^{60}Ni systematics in individual chondritic components are very difficult, because the initial abundance of ^{60}Fe in the Solar System appears to be low, $<1 \times 10^{-6}$ (Tachibana et al., 2006), and minerals suitable for the *in situ* ^{60}Fe–^{60}Ni measurements by SIMS (i.e., 20–30 μm grains with Fe/Ni ratio $>10^6$) are rare. Below is a brief summary of the published data.

The presence of ^{60}Ni excess due to decay of ^{60}Fe was reported in ordinary chondrite sulfides and chondrule silicates (Tachibana and Huss, 2003; Mostefaoui et al., 2005; Tachibana et al., 2006; Bizzarro et al., 2007a; Quitté et al., 2007; Goswami and Mishra, 2007; Guan et al., 2007). The inferred $(^{60}Fe/^{56}Fe)_0$ in sulfides (Mostefaoui et al., 2005) may be compromised by Fe–Ni redistribution between metal and sulfides during aqueous alteration and/or thermal metamorphism experienced by ordinary chondrites (Tachibana et al., 2006; Guan et al., 2007). The inferred $^{60}Fe/^{56}Fe$ ratio in ferromagnesian silicates from Semarkona (LL3.0) and Bishunpur (LL3.1) chondrules, which most likely represents $(^{60}Fe/^{56}Fe)_0$ during crystallization of chondrule melts, ranges from $(2.2 \pm 1.0) \times 10^{-7}$ to $(3.7 \pm 1.9) \times 10^{-7}$ (Tachibana et al., 2006). By applying the time difference of 1.5–2.0 Myr between formation of CAIs and ordinary chondrite chondrules, which can be inferred from their ^{26}Al–^{26}Mg systematics (Fig. 21c; note that only few chondrules with measured ^{26}Al–^{26}Mg systematics were studied for ^{60}Fe–^{60}Ni systematics), a Solar System initial $^{60}Fe/^{56}Fe$ of $(5–10) \times 10^{-7}$ is estimated (Tachibana et al., 2006). Correlated studies of ^{60}Fe–^{60}Ni and ^{26}Al–^{26}Mg systematics in primitive chondrite chondrules can potentially help to establish ^{60}Fe–^{60}Ni chronology of chondrule formation. This work is currently in progress (e.g., Huss et al., 2007; Goswami and Mishra, 2007).

3.2.5. ^{182}Hf–^{182}W systematics of CAIs

^{182}Hf decays to ^{182}W with $t_{1/2} \sim 9$ Myr. There are very few data on ^{182}Hf–^{182}W systematics of chondritic components to draw any firm conclusions of their chronology. Hafnium–tungsten isotope data of four bulk CAIs and mineral separates (melilite, Al,Ti-diopside) of two CAIs from Allende measured using MC-ICPMS yield an isochron with initial $^{182}Hf/^{180}Hf$ ratio $[(^{182}Hf/^{180}Hf)_0]$ of $(1.01 \pm 0.05) \times 10^{-4}$ and initial ε_W (deviation of $^{182}W/^{184}W$ from the terrestrial value) of -3.34 ± 0.14 (Burkhardt et al., 2007), consistent with a $(^{182}Hf/^{180}Hf)_0$ of $(1.00 \pm 0.08) \times 10^{-4}$ and initial ε_W of -3.45 ± 0.25 inferred from Hf–W data for two bulk CAIs, various fragments of a single CAI, and whole-rock carbonaceous chondrites (Kleine et al., 2005). Using the $(^{182}Hf/^{180}Hf)_0$ in angrite D'Orbigny $[(7.4 \pm 0.2) \times 10^{-5}$; Markowski et al., 2008) and its ^{207}Pb–^{206}Pb age (4564.42 ± 0.12 Myr; Amelin, 2008), the $(^{182}Hf/^{180}Hf)_0$ in CAIs corresponds to an absolute age of 4568.0 ± 0.8 Myr, which is barely consistent with the measured ^{207}Pb–^{206}Pb age of the CV CAIs (Amelin et al., 2002)[4]. Note that many CV CAIs experienced alteration resulting in open-system behavior of tungsten (Humayun et al., 2007) and the obtained isochron should be considered with precautious. No hafnium–tungsten isotope data have been reported for chondrules yet.

3.2.6. ^{41}Ca–^{41}K systematics of CAIs

The excess of ^{41}K ($^{41}K^*$) correlated with $^{40}Ca/^{39}K$, indicative for the presence of ^{41}Ca ($t_{1/2} \sim 0.1$ Myr), was reported in CV and CM CAIs with the canonical $^{26}Al/^{27}Al$ ratio (Srinivasan et al., 1994). No evidence for ^{41}Ca was found in FUN CAIs, CH CAIs, corundum and hibonite grains characterized by lower than the canonical $^{26}Al/^{27}Al$ ratio (1×10^{-5} to 5×10^{-8}) (Sahijpal et al., 1998; Sahijpal and Goswami, 1998; Srinivasan and Bischoff, 2001). The apparent correlation between the initial abundances of ^{41}Ca and ^{26}Al (CAIs with resolvable $^{41}K^*$ have the canonical $^{26}Al/^{27}Al$ ratio, whereas CAIs with lower than the canonical $^{26}Al/^{27}Al$ ratio show no $^{41}K^*$) implies a common stellar origin for these radionuclides (Sahijpal et al., 1998). It is proposed that CAIs devoid of ^{41}Ca and with much lower than the canonical $^{26}Al/^{27}Al$ ratio represent some of the first solids that formed in the solar nebula prior to injection and/or homogenization of ^{26}Al and ^{41}Ca (Sahijpal and Goswami, 1998); however, the later formation of such CAIs, after decay of ^{26}Al and ^{41}Ca, cannot be entirely excluded).

Although the presence of ^{41}Ca has an important implication for understanding the origin of short-lived radionuc-

[4] The absolute age of CV CAIs estimated from their $^{182}Hf^{182}W$ systematics and the angrite anchor is inconsistent with the higher-precision $^{207}Pb^{206}Pb$ ages of CV CAIs reported by Amelin et al. (2006), Jacobsen et al. (2008a,b), and Bouvier et al. (2008) (Table 3).

lides in the Solar System, its short half-life and very low initial $^{41}Ca/^{40}Ca$ ratio $[1.5 \pm 0.3) \times 10^{-8}]$, limits its wider applications despite its great chronological significance. It can be potentially used to constrain the early Solar System events with the highest time resolution; *in situ* measurements of ^{41}Ca–^{41}K systematics, however, are very challenging.

3.2.7. ^{36}Cl–^{36}S systematics of CAIs and chondrules

^{36}S excess correlated with $^{35}Cl/^{34}S$ ratio, indicative of the presence of ^{36}Cl ($t_{1/2} \sim 0.3$ Myr), was reported in sodalite replacing anorthite in CAIs and chondrules from the CV chondrites Ningqiang (Lin et al., 2005) and Allende (Hsu et al., 2006). The inferred initial $^{36}Cl/^{35}Cl$ ratio in sodalite is $\sim 5 \times 10^{-6}$. None of the sodalite grains analyzed shows $^{26}Mg^*$, suggesting late-stage origin of sodalite. Assuming formation of sodalite >1.5 Myr after crystallization of the host CAIs, the solar initial $^{36}Cl/^{35}Cl$ ratio is estimated $>1.6 \times 10^{-4}$. The origin of ^{36}Cl, remains controversial; two mechanisms are proposed: injection from a nearby supernova (Lin et al., 2005) and local irradiation origin (Hsu et al., 2006). Since ^{36}Cl has been detected only in sodalite postdating formation of CAIs and chondrules, it has limited significance for the chronology of CAIs and chondrules.

3.2.8. ^{10}Be–^{10}B and ^{7}Be–^{7}Li systematics of CAIs and chondrules

Excesses of ^{10}B correlated with $^{9}Be/^{11}B$, indicative for the presence of ^{10}Be ($t_{1/2} \sim 1.5$ Myr), were reported in many CAIs from CV and CM chondrites (McKeegan et al., 2000a; Sugiura et al., 2001; Marhas et al., 2002; MacPherson et al., 2002). Data for ^{10}Be–^{10}B systematics in CAIs from other chondrite groups are limited (Srinivasan et al., 2007). Since ^{10}Be is not produced in stars, its irradiation origin is required. This is consistent with the observations that ^{10}Be is decoupled from short-lived radionuclides of probably stellar origin—^{26}Al and ^{41}Ca; there is no chronological correlation between the inferred $(^{10}Be/^{9}Be)_0$ and $(^{26}Al/^{27}Al)_0$ or $(^{41}Ca/^{40}Ca)_0$ in CAIs measured (Marhas et al., 2002; MacPherson et al., 2002; Liu et al., this volume).

Two models for the irradiation origin of ^{10}Be were proposed: spallation reactions near the proto-Sun (McKeegan et al., 2000a) and magnetic trapping of galactic cosmic rays in the protosolar molecular cloud (Desch et al., 2004). If ^{10}Be was produced in the molecular cloud, it is expected to be uniformly distributed in the early Solar System, which would make it a very important chronometer for dating early Solar System processes (Desch et al., 2004). The existing data appear to be inconsistent with uniform distribution of ^{10}Be—the inferred initial $^{10}Be/^{9}Be$ ratios in CAIs range from $(12.4 \pm 2.7) \times 10^{-4}$ to $(5.3 \pm 2.4) \times 10^{-4}$ (McKeegan et al., 2000a; Sugiura et al., 2001; Marhas et al., 2002; MacPherson et al., 2002; Srinivasan et al., 2007)—and may support local irradiation origin of ^{10}Be. This precludes use of ^{10}Be–^{10}B systematics for the chronology of CAI and chondrule formation.

Recently, Chaussidon et al. (2006a) reported the possible presence of ^{7}Be ($t_{1/2} = 53$ days) in an Allende CAI having high initial $^{10}Be/^{9}Be$ ratio (excess of ^{7}Li in some melilite grains positively correlates with $^{9}Be/^{6}Li$ ratio). This tentative presence of ^{7}Be has been challenged by Desch and Ouellette (2006). For detailed replies to Desch and Quellette (2006) see Chaussidon et al. (2006b). More measurements are needed to confirm presence of ^{7}Be in CAIs.

Although chondrules show variations in Li–Be–B isotopic compositions, which can be explained as a result of mixing of protosolar and solar sources, the low Be/B and Be/Li ratios in chondrule minerals prevent detection of ^{10}Be and ^{7}Be (Chaussidon and Robert, 1998; Hoppe et al., 2001; Robert and Chaussidon, 2003).

3.3. Chronological significance of oxygen isotopes

It has been recently proposed that (i) oxygen–isotope composition of the protosolar molecular cloud, and, hence of the Sun (yet to be measured on Genesis samples), is ^{16}O-rich ($\Delta^{17}O < -20‰$), and (ii) the oxygen–isotope composition of the nebular gas evolved with time due to variations in the amount of $^{17,18}O$-enriched water in the inner Solar System (Clayton, 2002; Yurimoto and Kuramoto, 2004; Hashizume and Chaussidon, 2005; Lyons and Young, 2005). According to these CO self-shielding models, the absolute and relative chronologies of refractory inclusions and chondrules, and the differences in oxygen–isotope compositions of most chondrules ($\Delta^{17}O > -10‰$) and most refractory inclusions ($\Delta^{17}O < -20‰$), these differences can be interpreted in terms of isotopic self-shielding during UV photolysis of CO either in the parent molecular cloud or in the peripheral part of the protoplanetary disk (Krot et al., 2005d). The UV photolysis of CO preferentially dissociates $C^{17}O$ and $C^{18}O$. The released atomic ^{17}O and ^{18}O are incorporated into water ice, while the residual CO gas becomes enriched in ^{16}O. During the earliest stages of evolution of the protoplanetary disk, the inner disk had a solar H_2O/CO ratio and was ^{16}O-rich. During this time, the ^{16}O-rich refractory inclusions and, possibly, chondrules formed. Subsequently, the inner disk became H_2O-enriched and ^{16}O-depleted, because water–ice-rich dust particles, which were depleted in ^{16}O, agglomerated outside the snowline, drifted rapidly towards the Sun and evaporated. During this time, which may have lasted for ~4 Myr, most chondrules formed and some of the CAIs were melted.

There are several caveats in these models, which reduce possible chronological significance of oxygen isotopes. (i) The origin of ^{16}O-rich reservoir in the early Solar System and oxygen–isotope composition of the Sun remain controversial (Yurimoto et al., 2007 and references therein). (ii) ^{16}O-rich and ^{16}O-poor gaseous reservoirs may have coexisted during the formation of igneous CAIs having nearly canonical $(^{26}Al/^{27}Al)_0$ (Yurimoto et al., 1998; Aléon et al., 2007; Itoh and Yurimoto, 2007). (iii) There is no clear correlation between the degree of ^{16}O-enrichment in chondrules and their crystallization ages (Krot et al., 2006). For example, chondrules from CO and LL chondrites have different oxygen–isotope compositions (Fig. 11), but similar ^{26}Al–^{26}Mg ages (Fig. 21). The apparently young CR chondrules are ^{16}O-enriched relative to the apparently older ordinary chondrite chondrules (Figs. 11 and 21). Note also that the differences in oxygen–isotope compositions of

chondrules from different chondrite groups are relatively small compared to those between CAIs + AOAs and chondrules (e.g., Figs. 7 and 11). This is not predicted in the self-shielding models, because temporal and spatial variations of the water vapor content are expected to be present during chondrule formation epoch and large variations in oxygen–isotope compositions of chondrules are expected (Fukui and Kuramoto, 2008). The relatively small fluctuation in oxygen–isotope compositions of chondrules may reflect local and temporal variations in silicate dust/gas ratio and abundance of water in chondrule-forming regions (Fukui and Kuramoto, 2008), as well as a position of chondrule-forming region relative to the position of snow–line, which may change with time (Ciesla, 2008).

If the differences in oxygen–isotope compositions of CAIs + AOAs and chondrules do reflect evolution of oxygen isotopes of the inner disk with time, oxygen isotopes can be potentially important for searching "old" chondrules (see Section 3.4).

Finally we note that oxygen isotopes can potentially play a very important role for understanding the origin, stellar *vs.* irradiation, of short-lived radionuclides in the early Solar System (Gounelle and Meibom, 2007; Krot et al., 2008b) and distinguishing early *vs.* late formation of ^{26}Al-poor CAIs (Krot et al., 2008a). The importance of oxygen isotopes as an evidence for pollution of the Solar System by a supernovae has been recently explored by Young et al. (2008).

3.4. On the nature of age gap between CAIs and chondrules

An age gap of ~1 Myr between CAI and chondrules formation (i.e., lack of "old" chondrules with age similar to that of CAIs) inferred from the existing ^{207}Pb–^{206}Pb and ^{26}Al–^{26}Mg data is not understood. This gap could be an artifact if (i) old chondrules were all accreted into planetesimals that experienced melting and differentiation, (ii) chondrule recycling was very efficient and reset internal ^{26}Al–^{26}Mg isochrons of chondrules of earlier generations, or (iii) thermal metamorphism reset internal ^{26}Al–^{26}Mg isochrons in chondrules. All these explanations seem unlikely, because CAIs and AOAs, which are older than chondrules, survived in the protoplanetary disk. In addition, peak metamorphic temperatures of CO3.0, CR2 and ordinary chondrites of petrologic type <3.2 are too low to reset ^{26}Al–^{26}Mg systematics of chondrules (LaTourrette and Wasserburg, 1998). This is consistent with the lack of evidence for disturbance of ^{26}Al–^{26}Mg systematics in CAIs of these meteorites (e.g., Makide et al., 2009). (iv) The apparent lack of old chondrules might be a result of small number of primitive chondrite chondrules with measured internal ^{26}Al–^{26}Mg isochrons (Fig. 21). High-precision measurements of internal ^{26}Al–^{26}Mg isochrons in a statistically significant number of chondrules from primitive chondrites are required to test this hypothesis. If oxygen isotopes have chronological significance, they can be used to search for old chondrules, i.e., chondrules with uniformly ^{16}O-rich ($\Delta^{17}O < -20‰$) compositions. This approach may be more efficient than measuring ^{26}Al–^{26}Mg systematics in chondrules, which is very time-consuming and requires the presence of relatively coarse-grained (>10 μm) minerals with high Al/Mg ratios (>20). (v) The observed gap could reflect the chondrule-forming mechanism(s); e.g., if generation of chondrule-forming shock waves requires formation of Jupiter (Boss and Durisen, 2005) and/or planetesimals were involved in chondrule formation (Weidenschilling et al., 1998; Sanders and Taylor, 2005; Hood et al., 2005, 2008; Scott and Sanders, 2008). The latter hypothesis is based on the observations that chondrule formation overlapped and probably postdated accretion and differentiation of some planetesimals (Bizzarro et al., 2004; Kleine et al., 2005; Halliday and Kleine, 2006), and that asteroidal fragments may have been present among chondrule precursors (Libourel and Krot, 2006). An additional argument for a role for planetesimals in the formation of chondrules is based on the ^{53}Mn–^{53}Cr whole-rock isochron for carbonaceous chondrites, which dates Mn–Cr fractionation between carbonaceous chondrites at 4568 ± 1 Myr (Shukolyukov and Lugmair, 2006; Moynier et al., 2007). To understand how whole-rock chondrite compositions reflect Mn–Cr fractionation that may have occurred several Myr before chondrule formation, Scott and Sanders (2008) proposed that chondrules and fine-grained matrices formed out of a mixture of volatile-rich nebular dust and refractory material derived from planetesimals that formed early and melted.

3.5. Preservation of CAIs in the protoplanetary disk

The confirmed age difference between CAIs and chondrules within a single chondrite group and the much shorter duration of CAI formation (may be less than 0.1 Myr) compared to that of chondrule formation (up to 4 Myr) requires an explanation for the preservation of CAIs for millions of years before being accreted into the chondritic meteorite parent bodies despite dynamical arguments that these objects would be lost to the Sun due to gas drag on much shorter timescales (Weidenschilling, 1977). The preservation of CAIs in the disk could have occurred in one of two ways: (*i*) CAIs were stored in an early generation of planetesimals that were not affected by gas drag and were subsequently disrupted, allowing the CAIs to be re-accreted into a later generation of planetesimals that would become the chondritic meteorite parent bodies (e.g., Hutcheon et al., 2009) or (ii) some dynamical process operated in the solar nebula that offset the effects of gas drag, allowing the CAIs to survive as free floating objects until they were accreted into the meteorite parent bodies (e.g., Cuzzi et al., 2003; Haghighipour and Boss, 2003a,b; Boss, 2004; Ciesla, 2007a,b).

The planetesimal storage hypothesis is problematic as the large amount of live ^{26}Al that they would incorporate along with the CAIs would lead to thermal processing, if not total differentiation, of the sizable planetesimals (Hevey and Sanders, 2006). Because there is no clear evidence that CAIs experienced thermal processing in an asteroidal setting prior to incorporation into asteroid-sized bodies, this hypothesis has largely fallen out of favor. Although CAIs stored within a few km-sized planetesimals could have avoided significant thermal processing, no fragments of

such hypothetic CAI-rich planetesimals have been found yet. Note also that since relict CAIs are commonly found inside chondrules (see section 3.2.1), some CAIs must have been released from such hypothetic bodies prior to chondrule formation.

A variety of nebular processes have been proposed to counteract gas drag, allowing small CAI-sized particles to be preserved in the nebula for timescales of millions of years. The *x*-wind model proposed by Shu et al. (1996) argues that CAIs were launched on ballistic trajectories from near the Sun and then rained back down onto the solar nebula at distances that were dependent on the size of the particles. However, prior to being launched, the CAIs would have resided in a highly-oxidizing environment (Desch, 2007), which is inconsistent with their mineralogy (e.g., Simon et al., 2007). Alternatively, it has been suggested that gravitational torques (Boss, 2008) or turbulent diffusion (Cuzzi et al., 2003) could have served to carry CAIs

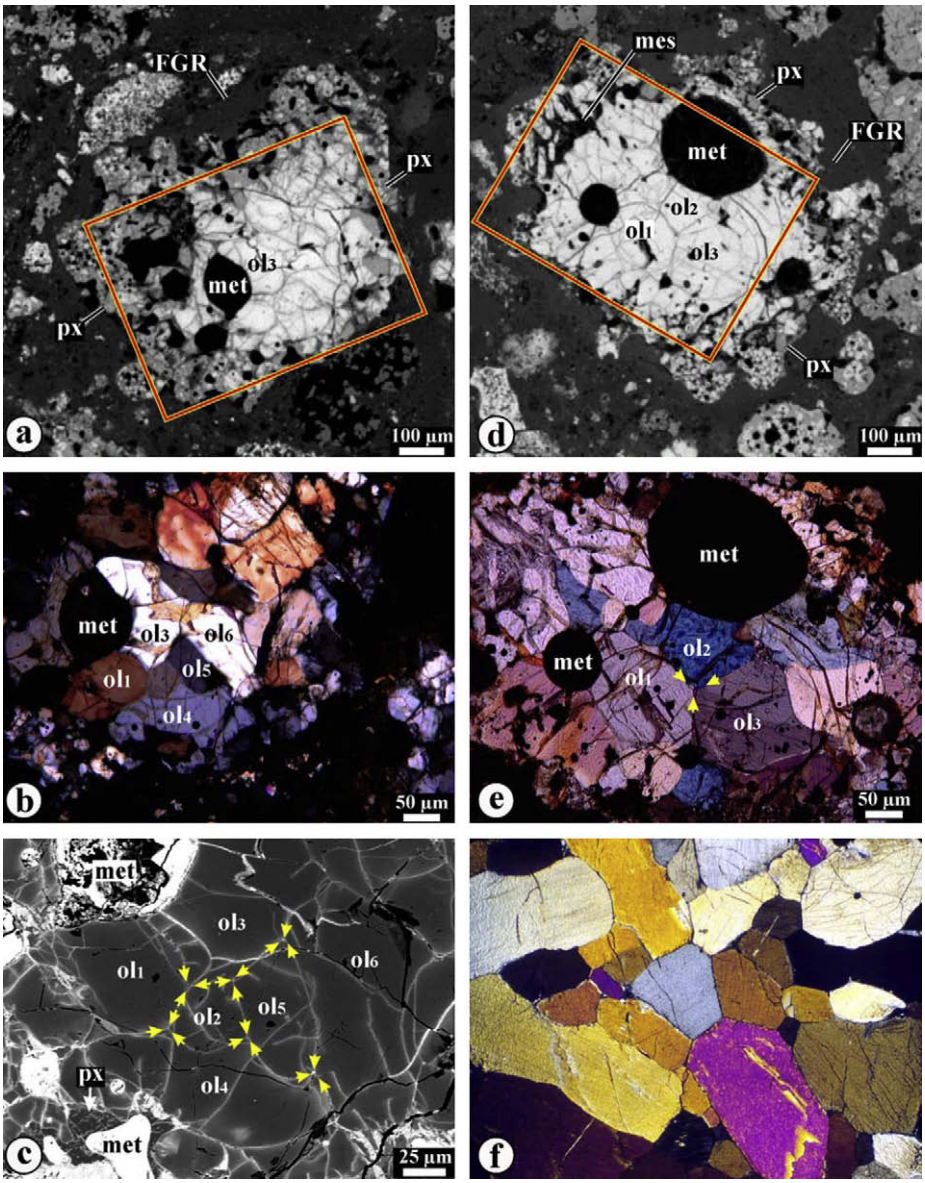

Fig. 22. X-ray elemental maps in Mg Kα (a and d), optical micrographs in crossed-polarized light (b, e, and f), and back-scattered electron image of two Type I chondrules in the CV carbonaceous chondrite Vigarano (a–e) and a terrestrial dunite (f). Regions outlined in (a) and (d) are shown in details in (b) and (e), respectively. The chondrules contain coarse-grained, aggregates composed of Fe,Ni-metal (met; replaced by terrestrial weathering products) and magnesian olivines (ol) surrounded by the igneous shells composed of low-Ca pyroxene (px) and glassy mesostasis (mes) and by the fine-grained, matrix-like rims (FGR). Olivine grains in the aggregates show triple junctions with interfacial angles of ~120° (yellow arrows in c and e), indicative of granoblastic equilibrium textures; such textures cannot be produced by crystallization from chondrule melts. It is inferred that these olivine dominated (dunite-like) aggregates are relict grains resulting from fragmentation of differentiated planetesimals (from Libourel and Krot (2006)). (For interpretation of the references to color in this figure legend, the reader is referred to the web version of this paper.)

outward within the solar nebula. In the case of gravitational torques, simulations were only carried out for $\sim 10^3$ years, and it is unclear whether the CAIs would be preserved for timescales $(1–4) \times 10^3$ times longer. In order for turbulent diffusion to preserve the needed number of CAIs, Cuzzi et al. (2003) found that hot nebula region, where CAIs formed, would have to be enriched in silicates by factors of $>10^3$, which is unlikely based on the work of Ciesla and Cuzzi (2006). While each of these mechanisms has questions surrounding it, a variation on the turbulent diffusion model offers a possible solution. Ciesla (2007a,b) demonstrated that during the earliest stages of disk evolution, the net inward movement of mass would be accompanied by outward flows around the disk mid-plane that would allow for more effective outward transport than found by Cuzzi et al. (2003).

Another way to keep CAIs in the protoplanetary disk without loss to inward gas drag is having disk with rings and spiral arms, which force the solids to the centers of the rings and spiral arms, where they can survive indefinitely, as shown by Haghighipour and Boss (2003a,b). Spiral arms are a natural feature of a marginally gravitationally unstable disk, which may to be required in order to form Jupiter, by either core accretion or disk instability (Boss, 2006).

3.6. Presence of asteroidal material among chondrule precursors

If there is a $\sim$1 Myr age gap between CAIs and chondrules, and accretion and differentiation of planetesimals predated or overlapped with chondrule formation and

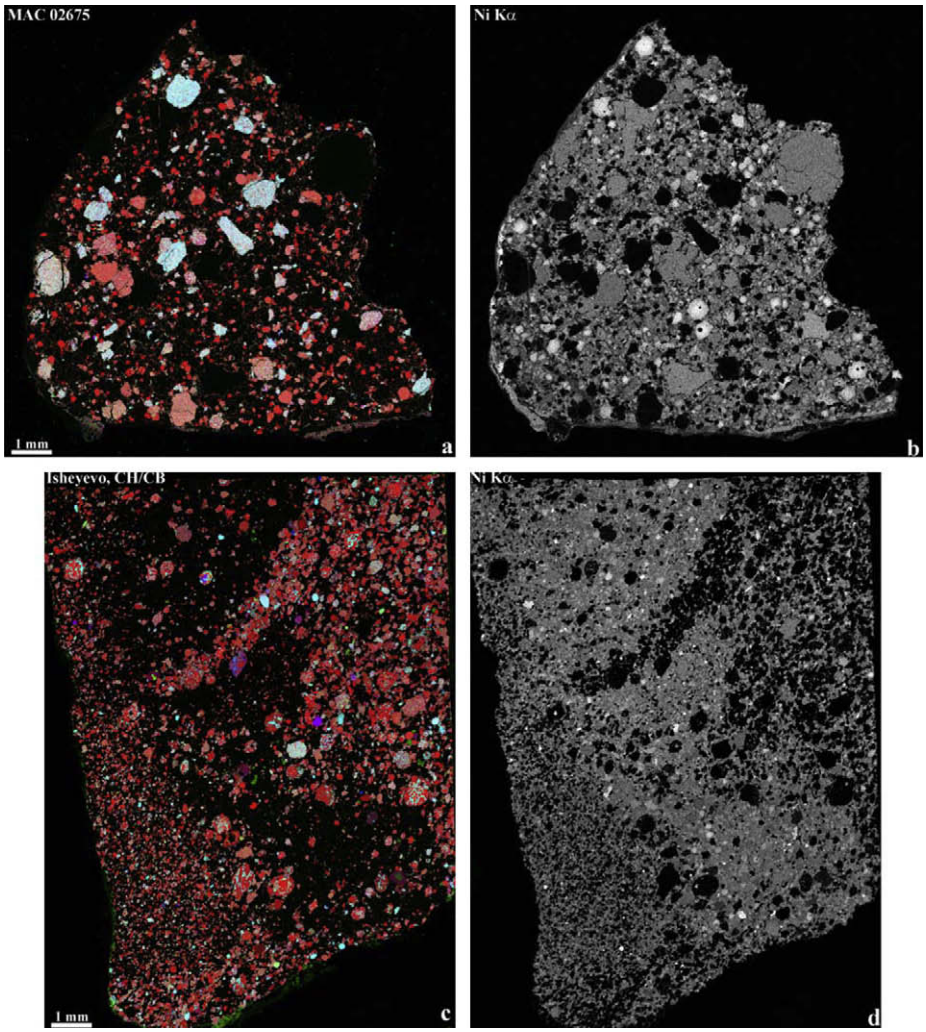

Fig. 23. Combined X-ray elemental maps in Mg (red), Ca (green) and Al Kα (blue) (a and c) and Ni Kα map (b and d) of the CB carbonaceous chondrite MAC 02675 and CH/CB-like carbonaceous chondrite Isheyevo. Both meteorites contain abundant chemically-zoned metal grains and magnesium-rich cryptocrystalline chondrules, which could have resulted from a single-stage process, possibly from a gas-melt plume formed by collision between planetary embryos (Krot et al., 2005a). In addition, Isheyevo contains ferromagnesian porphyritic chondrules formed by melting of dust in the solar nebula and CAIs formed by evaporation-condensation processes. (For interpretation of the references to color in this figure legend, the reader is referred to the web version of this paper.)

accretion of chondrite parent bodies, fragments of these early differentiated planetesimals may be expected within chondrites or even among chondrule precursors. Libourel and Krot (2006) described coarse-grained lithic clasts of forsteritic olivine with granoblastic textures inside type I chondrules from CV chondrites (Fig. 22) and concluded that these clasts are relict and may represent fragments of thermally processed, metamorphosed or differentiated, asteroids. The relict origin of the clasts has been confirmed by oxygen–isotope measurements, which revealed lack of isotope equilibrium between olivine of the clasts and host chondrule pyroxenes (Chaussidon et al., 2008).

High-temperature annealing experiments of Whattam et al. (2008) showed that formation of granoblastic textures requires sintering and prolonged (several days), high-temperature (>1000 °C) annealing, conditions which are not expected in the protoplanetary disk during chondrule formation (e.g., Desch and Connolly, 2002), but could have been achieved in planetesimals. If these clasts are indeed fragments of thermally processed planetesimals, which were present among chondrule precursors, it will place important constraints on the early Solar System chronology. More work is required to test this hypothesis.

3.7. Metal-rich carbonaceous (CB and CH) chondrites and their chronological significance

Chondrules and metal grains in CB chondrites are mineralogically, chemically and isotopically unique. (i) A high proportion of metal grains in the CB chondrites Hammadah al Hamra 237, QUE 94411 and MAC 02675 are chemically-zoned and appear to have formed by gas-solid condensation followed by some annealing (Meibom et al., 2001; Campbell et al., 2001; Petaev et al., 2001; Zipfel and Weyer, 2007). (ii) The CB chondrules are Fe,Ni-metal-free and have exclusively magnesian compositions ($Fa_{<3}$ and $Fs_{<3}$) and non-porphyritic (cryptocrystalline or skeletal) textures, flat REE patterns, young ^{207}Pb–^{206}Pb ages and show no evidence for repeatable melting (lack of relict grains, igneous rims, and independent compound chondrules). Some cryptocrystalline chondrules occur as inclusions inside chemically-zoned metal condensates (Krot et al., 2001c, 2005a). (iii) In contrast to other chondrite groups, chondrules and metal grains in CB chondrites show mass-dependent fractionation effects in Mg, Fe and Ni isotopes (Gounelle et al., 2007; Zipfel and Weyer, 2007). Based on these observations, it was suggested that CB chondrules and metal grains formed during a single-stage, highly-ener-

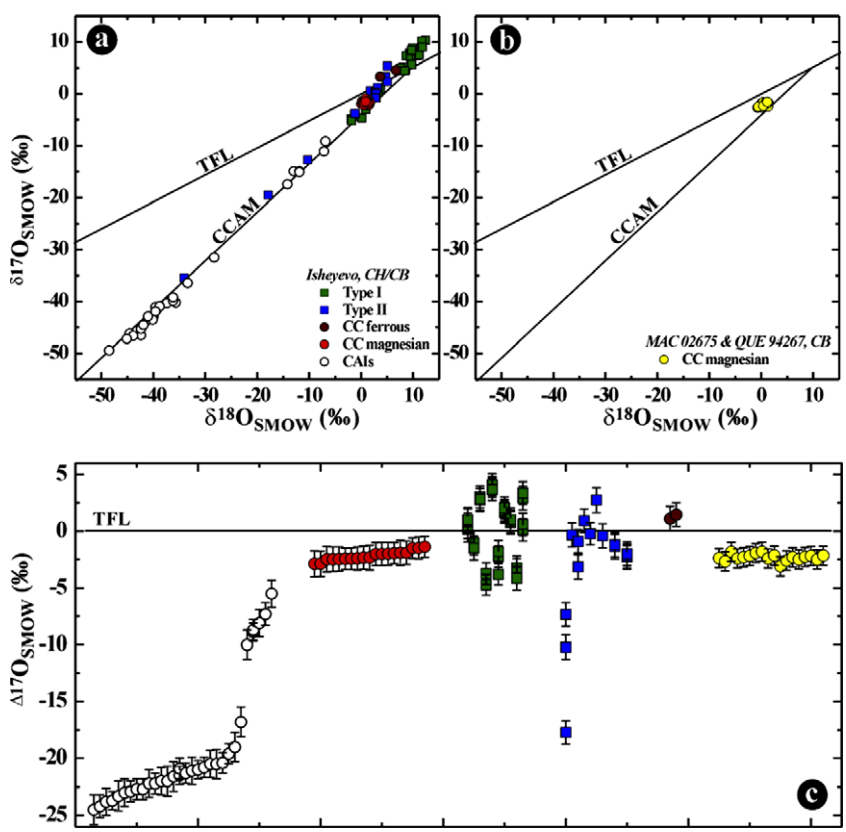

Fig. 24. Oxygen–isotope compositions of chondrules and CAIs in the CH/CB-like chondrite Isheyevo and CB chondrites MAC 02675 and QUE 94627. In "a" and "b", data are plotted as $\delta^{17}O$ *vs.* $\delta^{18}O$. In (c), the same data are plotted as deviation from the TF line, as $\Delta^{17}O$; each column represents data for a single chondrule or a refractory inclusion. Error bars in "a" and "b" are not shown for clarity; error bars in "c" are 2σ. Magnesian cryptocrystalline (CC) chondrules in Isheyevo, MAC 02675 and QUE 94627 have nearly identical oxygen–isotope compositions ($\Delta^{17}O = -2.2 \pm 0.9‰$ and $-2.3 \pm 0.6‰$, respectively), consistent with an impact-plume origin as gas-liquid condensates. Ferromagnesian chondrules (Type I and Type II) show large variations in oxygen–isotope compositions, consistent with their origin by melting of isotopically diverse precursors. Most Isheyevo CAIs are ^{16}O-rich.

getic event, possibly from a gas-melt plume generated by a collision between planetary embryos (Campbell et al., 2002; Rubin et al., 2003; Krot et al., 2005a).

A single-stage formation mechanism and measured ^{207}Pb–^{206}Pb ages of CB chondrules provide a unique opportunity for anchoring short-lived isotope systematics, such as ^{60}Fe–^{60}Ni, ^{182}Hf–^{182}W, and ^{53}Mn–^{53}Cr, to an absolute timescale. For example, (i) Bizzarro et al. (2007b) reported a preliminary ^{60}Fe–^{60}Ni isochron for chondrules and metal grains from the CB chondrite Gujba with the initial $^{60}Fe/^{56}Fe$ ratio of 5×10^{-8}, which allows to put upper limit on the initial $^{60}Fe/^{56}Fe$ ratio in the Solar System as (4–6) $\times 10^{-7}$, consistent with the estimates by Tachibana et al. (2006). (ii) Kleine et al. (2005) reported tungsten–isotope composition (ε_W) of CB metal, which, however, has a large error bar and overlaps with the inferred initial solar value (Fig. 3 in Kleine et al., 2005). Since CB metal and silicates are co-genetic, this can be used to obtain precise ^{182}Hf–^{182}W isochron for the CB chondrules and metal grains. (*iii*) Chondrules in CB chondrites show large variations in Al/Mg ratio: cryptocrystalline chondrules have olivine–pyroxene normative compositions and are highly depleted in Al_2O_3 (<0.1 wt%) whereas skeletal chondrules composed of olivine, Al-rich pyroxenes and anorthitic glass are enriched in Al_2O_3 (up to 10–12 wt%). The large range in Al/Mg ratios between these co-genetic chondrules can be potentially used to obtain a precise ^{26}Al–^{26}Mg isochron for CB chondrules by MC-ICPMS.

^{207}Pb–^{206}Pb ages of chondrules from CV (Connelly et al., 2008), CR (Amelin et al., 2002) and CB chondrites (Krot et al., 2005a) indicate that chondrule formation started ~1 Myr after CAIs and lasted for 3–4 Myr. The inferred duration of chondrule formation can be used to constrain a lower limit on the life-time of the protoplanetary disk (Russell et al., 2006). Based on the nearly complete lack of fine-grained matrix material and porphyritic chondrules, Krot et al. (2005a) suggested that CB chondrules formed after dissipation of dust (gas could have been still present) of the protoplanetary disk. If this is the case, the use of the CB chondrule ages for constraining life-time of the protoplanetary disk could be problematic. This hypothesis, however, is inconsistent with the recently inferred genetic relationship between the CB and CH chondrites (Krot et al., 2008d; Krot and Nagashima, 2008). Both groups contain abundant Fe,Ni-metal grains and magnesian non-porphyritic chondrules having similar textures, mineralogy (Fig. 23) and oxygen–isotope compositions (Fig. 24). In addition, CH chondrites contain ^{16}O-rich refractory inclusions, some with the canonical $^{26}Al/^{27}Al$ ratio (Krot et al., 2008a), and abundant porphyritic chondrules formed by melting of the mineralogically diverse solid precursors, including CAIs (Fig. 14; Krot et al., 2008d). Krot and Nagashima (2008) concluded that non-porphyritic magnesian chondrules in CH chondrites formed during the same event that resulted in formation of CB chondrules. They were subsequently size sorted and accreted together with other chondritic components (porphyritic chondrules and refractory inclusions) formed by different processes into CH parent body. These observations may indicate that some solids were still present in the protoplanetary disk at the time of the CB chondrule formation. As a result, ^{207}Pb–^{206}Pb ages of CB chondrules can be used to constrain life-time of the protoplanetary disk.

4. CONCLUSIONS

(1) Mineralogical observations, chemical and oxygen–isotope compositions, and absolute (^{207}Pb–^{206}Pb) and relative (^{26}Al–^{26}Mg) chronologies of primitive chondrite components are consistent with shock-wave models of their formation and with an external, stellar origin of ^{26}Al; they are inconsistent with the *x*-wind model of the origin of chondritic components and a local, irradiation origin of ^{26}Al.

(2) CAIs and AOAs were the first solids formed in the solar nebula ~4567 Myr ago, possibly within a period of <0.1 Myr. CAIs and AOAs formed during multiple transient heating events in a nebular reservoir with ^{16}O-rich ($\Delta^{17}O \sim -24 \pm 2‰$) composition and high ambient temperature, either throughout the inner protoplanetary disk (1–4 AU) or in a localized nebular region near the proto-Sun (<0.1 AU) and were subsequently dispersed throughout the disk.

(3) The ^{26}Al-poor [$(^{26}Al/^{27}Al)_0 < 1 \times 10^{-5}$), ^{16}O-rich CAIs may have formed prior to injection and/or homogenization of ^{26}Al in the early Solar System.

(4) A small number of igneous CAIs in ordinary, enstatite and carbonaceous chondrites, and a large number of CAIs in metal-rich, CB and CH, chondrites are ^{16}O-depleted ($\Delta^{17}O > -10‰$) and have initial $^{26}Al/^{27}Al$ ratios similar to those in chondrules ($<1 \times 10^{-5}$). These CAIs could have experienced melting and isotope exchange during chondrule formation.

(5) Chondrules and most of the matrix materials in primitive chondrites formed during multiple transient heating events throughout the inner protoplanetary disk 1–3 Myr after CAIs in the presence of ^{16}O-poor ($\Delta^{17}O > -5‰$) nebular gas. The majority of chondrules within a chondrite group may have formed over a much shorter period of time (<0.5–1 Myr), but the data are inconclusive.

(6) The existing data indicate that there is an age gap of at least 1 Myr between the formation of CAIs and chondrules. This gap may reflect the nature of chondrule-forming mechanism(s); e.g., if generation of chondrule-forming shock waves requires formation of Jupiter and/or planetesimals were involved in chondrule formation. Both may require time delay of chondrule formation.

(7) CAIs and AOAs were present in the regions where chondrules formed, probably close to the accretion regions of the chondrite parent bodies (1–4 AU), indicating that CAIs were present in the protoplanetary disk as free-floating objects for at least 4 Myr. Many CAIs, however, were largely unaffected by chondrule melting, suggesting the chondrule-forming events experienced by a nebular region were small in scale and limited in number.

(8) Chondrules and metal grains in CB chondrites formed during a single-stage, highly-energetic event ~4563 Myr ago, possibly from a gas-melt plume produced by collision between planetary embryos. A unique, single-stage origin of chondrules and metal grains in CB chondrites, about 5 Myr after CAIs, can potentially link several relative chronometers (e.g., ^{60}Fe–^{60}Ni, ^{182}Hf–^{182}W) to an absolute (^{207}Pb–^{206}Pb) time–scale.

(9) ^{7}Be–^{7}Li, ^{10}Be–^{10}B, ^{41}Ca–^{41}K, and ^{60}Fe–^{60}Ni systematics of CAIs and chondrules are important for understanding of astrophysical setting of Solar System formation and origin of short-lived radionuclides, but so far have limited implications for the chronology of the chondritic components.

(10) The chronological implication of oxygen–isotope compositions of chondritic components are limited at the moment. Oxygen isotopes can potentially play a very important role for understanding the origin, stellar *vs.* irradiation, of short-lived radionuclides in the early Solar System and distinguishing early *vs.* late formation of ^{26}Al-poor CAIs.

ACKNOWLEDGMENTS

We thank Alan Boss, Marc Chaussidon, Gregory Herzog and anonymous reviewer for critical comments and suggestions which helped to improve the manuscript. This work was supported by NASA Grants NNX07AI81G (A.N. Krot, PI), NNG05GG48G (G.R. Huss, PI), NAG5-10523 (I.D. Hutcheon, PI), and NAG5-11591 (K. Keil, PI), and was performed under the auspices of the Department of Energy by LLNL under Contract W-7405-ENG-48. The UCLA ion microprobe laboratory is partially supported by a grant from the NSF Instrumentation and Facilities program. This is Hawai'i Institute of Geophysics and Planetology publication 1796 and School of Ocean and Earth Science and Technology publication 7726.

APPENDIX A. SUPPLEMENTARY DATA

Supplementary data associated with this article can be found, in the online version, at doi:10.1016/j.gca.2008.09.039.

REFERENCES

Aléon J., Krot A. N. and McKeegan K. D. (2002) Ca–Al-rich inclusions and amoeboid olivine aggregates from the CR carbonaceous chondrites. *Meteorit. Planet. Sci.* **37**, 1729–1755.

Aléon J., El Goresy A. and Zinner E. (2007) Oxygen–isotope heterogeneities in the earliest protosolar gas recorded in a meteoritic calcium–aluminum-rich inclusion. *Earth Planet Sci. Lett.* **263**, 114–127.

Alexander C. M. O'D. (2005) From supernovae to planets: the view from meteorites and interplanetary dust particles. In *Chondrites and the Protoplanetary Disk*, vol. 341 (eds. A. N. Krot, E. R. D. Scott and B. Reipurth). ASP Conference Series, pp. 974–1004.

Alexander C. M. O', Grossman J. N., Ebel D. S. and Ciesla F. (2008) The formation conditions of chondrules and chondrites. *Science* **320**, 1617–1620.

Amelin Y. (2008) U–Pb ages of angrites. *Geochim. Cosmochim. Acta* **72**, 221–232.

Amelin Y., Krot A. N., Hutcheon I. D. and Ulyanov A. A. (2002) Lead isotopic ages of chondrules and calcium–aluminum-rich inclusions. *Science* **297**, 1678–1683.

Amelin Y., Wadhwa M. and Lugmair G. (2006) Pb-isotopic dating of meteorites using ^{202}Pb–^{205}Pb double-spike: comparison with other high-resolution chronometers (abstract). *Lunar Planet. Sci.* **37**, 1970.

Amelin Y. and Krot A. N. (2007) Pb isotopic age of the Allende chondrules. *Meteorit. Planet. Sci.* **42**, 1321–1337.

Ash R. D., Young E. D., Rumble, III, D., Alexander C. M. O' and MacPherson G. J. (1999) Oxygen isotope systematics in Allende chondrules (abstract). *Lunar Planet. Sci.* **30**, 1836.

Baker J. A. (2007) ^{26}Al–^{26} Mg dating solid formation and planetesimal accretion and differentiation in the early Solar System (abstract). In *Workshop on the Chronology of Meteorites and the Early Solar System*, pp. 28–29.

Baker J., Bizzarro M., Wittig N., Connelly J. and Haack H. (2005) Early planetesimal melting from an age of 4.5662 Gyr for differentiated meteorites. *Nature* **436**, 1127–1131.

Birck J.-L. and Allégre C. J. (1985) Evidence for the presence of ^{53}Mn in the early solar system. *Geophys. Res. Lett.* **12**, 745–748.

Birck J.-L. and Allégre C. J. (1988) Manganese–chromium isotope systematics and the development of the early solar system. *Nature* **331**, 579–584.

Bizzarro M., Baker J. A. and Haack H. (2004) Mg isotope evidence for contemporaneous formation of chondrules and refractory inclusions. *Nature* **431**, 275–278.

Bizzarro M., Baker J. A. and Haack H. (2005) Mg isotope evidence for contemporaneous formation of chondrules and refractory inclusions. *Nature* **435**, 1280.

Bizzarro M., Ulfbeck D., Trinquier A., Thrane K., Connelly J. N. and Meyer B. S. (2007a) Evidence for a late supernova injection of ^{60}Fe into the protoplanetary disk. *Science* **316**, 1178–1181.

Bizzarro M., Birck J.-L., Chen J., Lugmair G., Mostefaoui S., Papanastassiou D., Shukolyukov A., Quitté G., Tachibana S. and Wadhwa M. (2007b) Nickel isotope anomalies in meteorites and the ^{60}Fe–^{60} Ni clock (abstract). In *Workshop on the Chronology of Meteorites and the Early Solar System*, pp. 29–30.

Bland P. A., Alard O., Benedix G. K., Kearsley A. T., Menzies O. N., Watt L. E. and Rogers N. W. (2005) Volatile fractionation in the early solar system and chondrule/matrix complementarity. *Proc. Nat. Acad. Sci.* **102**, 13755–13760.

Bogdanovski O., Papanastassiou D. A. and Wasserburg G. J. (2002) Cr isotopes in Allende Ca–Al-rich inclusions (abstract). *Lunar Planet. Sci.* **32**, 1802.

Bonal L., Quirico E., Bourot-Denise M. and Montagnac G. (2006) Determination of the petrologic type of CV3 chondrites by Raman spectroscopy of included organic matter. *Geochim. Cosmochim. Acta* **70**, 1849–1863.

Boss A. P. and Durisen R. H. (2005) Sources of shock waves in the protoplanetary disk. In *Chondrites and the Protoplanetary Disk*, vol. 341 (eds. A. N. Krot, E. R. D. Scott and B. Reipurth). ASP Conference Series, pp. 821–839.

Boss A. P. (2004) Evolution of the solar nebula. VI. Mixing and transport of isotopic heterogeneity. *Astrophys. J.* **616**, 1265–1277.

Boss A. P. (2006) Spatial heterogeneity of ^{26}Al/^{27}Al and of stable oxygen isotopes in the solar nebula. *Meteorit. Planet. Sci.* **41**, 1695–1703.

Boss A. P. (2007) Evolution of the solar nebula. VIII. Spatial and temporal heterogeneity of short-lived radioisotopes and stable oxygen isotopes. *Astrophys. J.* **660**, 1707–1714.

Boss A. P. (2008) Mixing in the solar nebula: implications for isotopic heterogeneity and large-scale transport of refractory grains. *Earth Planet. Sci. Lett.* **268**, 102–109.

Bouvier A. and Wadhwa M. (2007) An appraisal of ^{207}Pb–^{206}Pb and ^{26}Al–^{26}Mg chondrologies in CAIs from chondrules (abstract). In *Workshop on the Chronology of Meteorites and the Early Solar System*, pp. 36–37.

Bouvier A., Blichert-Toft J., Moynier F., Vervoort J. D. and Albarède F. (2007) Pb–Pb dating constraints on the accretion and cooling history of chondrites. *Geochim. Cosmochim. Acta* **71**, 1583–1604.

Bouvier A., Wadhwa M. and Janney P. (2008) ^{26}Al–^{26}Mg and ^{207}Pb–^{208}Pb systematics in an Allende inclusion (abstract). *Meteorit. Planet. Sci.* **43**(Suppl.), A28.

Brearley A. J. and Jones R. H. (1998) Chondritic meteorites. In *Planetary Materials*, vol. 36 (ed. J. J. Papike). *Rev. Mineral*, pp. 3.1–3.398.

Brownlee D. et al. (2006) Comet 81P/Wild 2 under a microscope. *Science* **314**, 1711–1716.

Burkhardt C., Kleine T., Palme H., Bourdon B., Friedrich J., Zipfel J. and Ebel D. (2007) ^{182}Hf–^{182}W chronometry of CAIs and the age of the Solar System (abstract). *Meteorit. Planet. Sci.* **42**(Suppl.), 5189.

Campbell A. J., Humayun M., Meibom A., Krot A. N. and Keil K. (2001) Origin of metal grains in the QUE 94411 chondrite. *Geochim. Cosmochim. Acta* **65**, 163–180.

Campbell A. J., Humayun M. and Weisberg M. K. (2002) Siderophile element constraints on the formation of metal in the metal-rich chondrites Bencubbine, Weatherford, and Gujba. *Geochim. Cosmochim. Acta* **66**, 647–660.

Chaussidon M. and Robert F. (1998) ^{7}Li/^{6}Li and ^{11}B/^{10}B variations in chondrules from the Semarkona unequilibrated chondrite. *Earth Planet Sci. Lett.* **164**, 577–589.

Chaussidon M., Robert F. and McKeegan K. D. (2006a) Li and B isotopic variations in an Allende CAI: evidence for the *in situ* decay of short-lived ^{10}Be and for the possible presence of the short-lived nuclide ^{7}Be in the early solar system. *Geochim. Cosmochim. Acta* **70**, 224–245.

Chaussidon M., Robert F. and McKeegan K. D. (2006b) Reply to the comment by Desch and Ouellette on "Li and B isotopic variations in an Allende CAI: evidence for the in situ decay of short-lived ^{10}Be and for the possible presence of the short-lived nuclide ^{7}Be in the early solar system". *Geochim. Cosmochim. Acta* **70**, 5433–5436.

Chaussidon M. and Gounelle M. (2006) Irradiation processes in the early solar system. In *Meteoritics and the Early Solar System II* (eds. D. S. Lauretta and H. Y. McSween, Jr.). University of Arizona Press, Tucson, pp. 323–340.

Chaussidon M., Libourel G. and Krot A. N. (2008) Oxygen isotopic constraints on the origin of magnesian chondrules and on the gaseous reservoirs in the early Solar System. *Geochim. Cosmochim. Acta.* **72**, 1724–1738.

Chen J. H. and Tilton G. R. (1976) Isotopic lead investigations on the Allende carbonaceous chondrite. *Geochim. Cosmochim. Acta* **40**, 635–643.

Ciesla F. J. and Cuzzi J. N. (2006) The evolution of the water distribution in a viscous protoplanetary disk. *Icarus* **181**, 178–204.

Ciesla F. J. (2007a) Outward transport of high-temperature materials around the midplane of the solar nebula. *Science* **318**, 613–615.

Ciesla F. J. (2007b) Two-dimensional dynamics of CAIs in the solar nebula (abstract). In *Workshop on the Chronology of Meteorites and the Early Solar System*, pp. 44–45.

Ciesla F. J. (2008) Enhancement of water near the snowline: two-dimensional considerations (abstract). *Lunar Planet. Sci.* **39**, 1046.

Clayton R. N. (1993) Oxygen isotopes in meteorites. *Ann. Rev. Earth Planet. Sci.* **21**, 115–149.

Clayton R. N. (2002) Self-shielding in the solar nebula. *Nature* **415**, 860–861.

Clayton R. N. and Mayeda T. K. (1999) Oxygen isotope studies of carbonaceous chondrites. *Geochim. Cosmochim. Acta* **63**, 2089–2104.

Connelly J. N., Amelin Y., Krot A. N. and Bizzarro M. (2008) Chronology of the Solar System's oldest solids. *Astrophys. J.* **675**, L121–L124.

Connolly H. C., Weisberg M. K. and Huss G. R. (2003) On the nature and origins of FeO-rich chondrules in CR2 chondrites: a preliminary report (abstract). *Lunar Planet. Sci.* **34**, 1770.

Cosarinsky M., Taylor D. J., Liu M.-C., McKeegan K. D. and Krot A. N. (2007) Distribution of aluminum-26 in refractory inclusions from CV chondrites (abstract). In *Workshop on the Chronology of Meteorites and the Early Solar System*, pp. 48–49.

Cuzzi J. N. and Alexander C. M. O'D. (2006) Chondrule formation in particle-rich nebular regions at least hundreds of kilometres across. *Nature* **441**, 483–485.

Cuzzi J. N., Davis S. S. and Dobrovolskis A. R. (2003) Blowing in the wind II. Creation and redistribution of refractory inclusions in a turbulent protoplanetary nebula. *Icarus* **166**, 385–402.

Cuzzi J. N., Ciesla F. J., Petaev M. I., Krot A. N., Scott E. R. D. and Weidenschilling S. J. (2005) Nebula evolution of thermally processed solids: reconciling models and meteorites. In *Chondrites and the Protoplanetary Disk*, vol. 341 (eds. A. N. Krot, E. R. D. Scott and B. Reipurth). ASP Conference Series, pp. 732–774.

Dauphas N., Cook D. L., Sacarabany A., Frohlich C., Davis A. M., Wadhwa M., Pourmand A., Rauscher T. and Gallino R. (2008) Iron-60 evidence for early injection and efficient mixing of stellar debris in the protosolar nebula. *Astrophys. J.* **686**, 560–569.

Davis A. M. and Richter F. M. (2003) Condensation and evaporation of solar system materials. In *Meteorites, Comets and Planets*, vol. 1 (ed. A.M. Davis), *Treatise on Geochemistry*, vol. 341 (eds. H. D. Holland and K. K. Turekian). Elsevier, 1935, Oxford, pp. 407–430.

Davis A. M., Alexander C. M. O'D., Nagahara H. and Richter F. M. (2005a) Evaporation and condensation during CAI and chondrule formation. In *Chondrites and the Protoplanetary Disk*, vol. 341 (eds. A. N. Krot, E. R. D. Scott and B. Reipurth). ASP Conference Series, pp. 432–456.

Davis A. M., Richter F. M., Mendybaev R. A., Janney P. E., Wadhwa M. and McKeegan K. D. (2005b) Isotopic mass fractionation laws and the initial Solar System ^{26}Al/^{27}Al ratio (abstract). *Lunar Planet. Sci.* **35**, 2334.

Desch S. J. (2007) Inti did not form in an *x*-wind (and neither did most CAIs) (abstract). *Meteorit. Planet. Sci.* **42**(Suppl.), 5073.

Desch S. J. and Connnolly, Jr., H. C. (2002) A model of the thermal processing of particles in solar nebula shocks: application to the cooling rates of chondrules. *Meteorit. Planet. Sci.* **37**, 183–207.

Desch S. J., Connolly H. C. and Srinivasan, Jr., G. (2004) An interstellar origin for the ^{10}Be in calcium-rich, aluminum-rich inclusions. *Astrophys. J.* **602**, 528–542.

Desch S. J., Ciesla F. J., Hood L. L. and Nakamoto T. (2005) Heating of chondritic materials in solar nebula shocks. In *Chondrites and the Protoplanetary Disk*, vol. 341 (eds. A. N. Krot, E. R. D. Scott and B. Reipurth). ASP Conference Series, pp. 849–873.

Desch S. J. and Ouellette N. (2006) Comment on "Li and Be isotopic variations in an Allende CAI: evidence for the in situ decay of short-lived Be and for the possible presence of the short-lived nuclide Be in the early solar system", by M. Chaussidon, F. Robert, and K.D. McKeegan. *Geochim. Cosmochim. Acta* **70**, 5426–5432.

Ebel D. S. and Grossman L. (2000) Condensation in dust-enriched systems. *Geochim. Cosmochim. Acta* **64**, 339–366.

Fagan T. J., Krot A. N., Keil K. and Yurimoto H. (2004) Nebular setting of oxygen isotopic alteration in a coarse-grained Ca–Al-rich inclusion from Efremovka. *Meteorit. Planet. Sci.* **39**, 1257–1272.

Fukui T. and Kuramoto K. (2008) Simultaneous enhancement of water vapor and silicate dust in the inner solar nebula: implication for the small oxygen isotopic variation of chondrules (abstract). *Meteorit. Planet. Sci.* **43**(Suppl.), A46.

Galy A., Young E. D., Ash R. D. and O'Nions R. K. (2000) The formation of chondrules at high gas pressures in the solar nebula. *Science* **290**, 1751–1754.

Galy A., Hutcheon I. D. and Grossman L. (2004) $(^{26}Al/^{27}Al)_0$ of the solar nebula inferred from Al–Mg systematic in bulk CAIs from CV3 chondrites (abstract). *Lunar Planet. Sci.* **35**, 1790.

Glassgold A. E., Feigelson E. D., Montmerle T. and Wolk S. (2005) X-ray flares of Sun-like young stellar objects and their effects on protoplanetary disks. In *Chondrites and the Protoplanetary Disk*, vol. 341 (eds. A. N. Krot, E. R. D. Scott and B. Reipurth). ASP Conference Series, pp. 165–181.

Goswami J. N., McKeegan K. D., Marhas K. K., Sinha N. and Davis A. M. (2001) Isotopic records in Murray and Murchison hibonites: implications for the oxygen isotopic reservoirs in the early Solar System (abstract). *Lunar Planet. Sci.* **32**, 1576.

Goswami J. N., Marhas K. K., Chaussidon M., Gounelle M. and Meyer B. S. (2005) Origin of short-lived radionuclides in the early solar system. In *Chondrites and the Protoplanetary Disk*, vol. 341 (eds. A. N. Krot, E. R. D. Scott and B. Reipurth. ASP Conference Series. pp. 485–527.

Goswami J. N. and Mishra R. (2007) Fe-Ni isotope systematics in silicate phases of UOC chondrules (abstract). *Lunar Planet. Sci.* **38**, 5088.

Gounelle M. and Meibom A. (2007) The oxygen isotopic composition of the Sun as a test of the supernova origin of ^{26}Al and ^{41}Ca. *Astrophys. J.* **664**, L123–L125.

Gounelle M., Shu F. H., Shang H., Glassgold A. E., Rehm K. E. and Lee T. (2001) Extinct radioactivities and protosolar cosmic rays: self-shielding and light elements. *Astrophys. J.* **548**, 1051–1070.

Gounelle M., Shu F. H., Shang H., Glassgold A. E., Rehm K. E. and Lee T. (2006) The irradiation origin of beryllium radioisotopes and other short-lived radionuclides. *Astrophys. J.* **640**, 1163–1170.

Gounelle M., Young E. D., Shahar A., Tonui E. and Kearsley A. (2007) Magnesium isotopic constraints on the origin of CB_b chondrites. *Earth Planet Sci. Lett.* **256**, 521–533.

Gounelle M., Meibom A. and Hennebelle P. (2008) The unlikely formation of the Sun in an Orion-like setting (abstract). *Lunar Planet. Sci.* **39**, 1601.

Grossman L., Ebel D. S., Simon S. B., Davis A. M., Richter F. M. and Parsad N. M. (2000) Major element chemical and isotopic compositions of refractory inclusions in C3 chondrites: the separate roles of condensation and evaporation. *Geochim. Cosmochim. Acta* **64**, 2879–2894.

Grossman L., Ebel D. S. and Simon S. B. (2002) Formation of refractory inclusions by evaporation of condensate precursors. *Geochim. Cosmochim. Acta* **66**, 145–161.

Grossman L., Beckett J. R., Fedkin A. V., Simon S. B. and Ciesla F. J. (2008) Redox conditions in the solar nebula: orservational, experimental and theoretical constraints. In *Oxygen in Earliest Solar System Materials and Processes*, vol. 68 (eds. G. J. MacPherson, D. W. Mittlefehldt, J. H. Jones and S. B. Simon), *Rev. Miner. Geochem.*, pp. 93–141.

Guan Y., Huss G. R. and Leshin L. A. (2007) ^{60}Fe–^{60}Ni and ^{53}Mn–^{53}Cr isotopic systems in sulfides from unequilibrated enstatite chondrites. *Geochim. Cosmochim. Acta* **71**, 4082–4091.

Haghighipour N. and Boss A. P. (2003a) On pressure gradients and rapid migration of solids in a nonuniform solar nebula. *Astrophys. J.* **583**, 996–1003.

Haghighipour N. and Boss A. P. (2003b) On gas-drag induced rapid migration of solids in a non-uniform solar nebula. *Astrophys. J.* **598**, 1301–1311.

Halliday A. N. and Kleine T. (2006) Meteorites and the timing, mechanisms, and conditions of terrestrial planet accretion and early differentiation. In *Meteoritics and the Early Solar System II* (eds. D. S. Lauretta and H. Y. McSween, Jr.). University of Arizona Press, Tucson, pp. 775–801.

Hashizume K. and Chaussidon M. (2005) A non-terrestrial ^{16}O-rich isotopic composition for the protosolar nebula. *Nature* **434**, 619–622.

Hester J. J. and Desch S. J. (2005) Understanding our origins: star formation in H II region environments. In *Chondrites and the Protoplanetary Disk*, vol. 341 (eds. A. N. Krot, E. R. D. Scott and B. Reipurth). ASP Conference Series, pp. 107–131.

Hevey P. J. and Sanders I. S. (2006) A model for planetesimal meltdown by ^{26}Al and its implications for meteorite parent bodies. *Meteoritics Meteorit Planet. Sci.* **41**, 95–106.

Hewins R. H. (1997) Chondrules. *Ann. Rev. Earth Planet. Sci.* **25**, 61–83.

Hood L. L., Ciesla F. J. and Weidenschilling S. J. (2005) Chondrule formation in planetesimal bow shocks: heating and cooling rates. In *Chondrites and the Protoplanetary Disk*, vol. 341 (eds. A. N. Krot, E. R. D. Scott and B. Reipurth). ASP Conference Series, pp. 873–883.

Hood L. L., Ciesla F. J., Artemieva N. A. and Weidenschilling S. J. (2008) Nebular shock waves generated by large-scale impacts: possible sites for chondrule formation (abstract). *Lunar Planet. Sci.* **39**, 2147.

Hoppe P., Goswami J. N., Krähenbühl U. and Marti K. (2001) Boron in chondrules. *Meteorit. Planet. Sci.* **36**, 1331–1343.

Hsu W., Wasserburg G. J. and Huss G. R. (2000) High time resolution by use of the ^{26}Al chronometer in the multistage formation of a CAI. *Earth Planet. Sci. Lett.* **182**, 15–29.

Hsu W., Guan Y., Leshin L. A., Ushikubo T. and Wasserburg G. J. (2006) A late episode of irradiation in the early solar system: evidence from extinct ^{36}Cl and ^{26}Al in meteorites. *Astrophys. J.* **640**, 525–529.

Humayun M., Simon S. B. and Grossman L. (2007) Tungsten and hafnium distribution in calcium aluminum inclusions (CAIs) from Allende and Efremovka. *Geochim. Cosmochim. Acta* **71**, 4609–4627.

Huss G. R., MacPherson G. J., Wasserburg G. J., Russell S. S. and Srinivasan G. (2001) ^{26}Al in CAIs and chondrules from unequilibrated ordinary chondrites. *Meteorit. Planet. Sci.* **36**, 975–997.

Huss G. R., Tachibana S. and Nagashima K. (2007) $_{26}Al$ and ^{60}Fe in chondrules from unequilibrated ordinary chondrites (abstract). *Meteorit. Planet. Sci.* **42**(Suppl.), 5005.

Huss G. R., Meyer B. S., Srinivasan G., Goswami J. N. and Sahijpal S. (2009) Stellar sources of the short-lived radionuclides in the early solar system. *Geochim. Cosmochim. Acta* **73**, 4922–4945.

Hutcheon I. D., Marhas K., Krot A. N., Goswami J. N. and Jones R. H. (2009) ^{26}Al in plagioclase-rich chondrules in carbona-

ceous chondrites: evidence for an extended duration of chondrule formation. *Geochim. Cosmochim. Acta* **73**, 5080–5099.

Ireland T. R., Fahey A. J. and Zinner E. K. (1991) Hibonite-bearing microspherules—A new type of refractory inclusions with large isotopic anomalies. *Geochim. Cosmochim. Acta* **55**, 367–389.

Ireland T. R. and Fegley, Jr., B. (2000) The solar system's earliest chemistry: systematics of refractory inclusions. *Int. Geol. Rev.* **42**, 865–894.

Itoh S. and Yurimoto H. (2003) Contemporaneous formation of chondrules and refractory inclusions in the early Solar System. *Nature* **423**, 728–731.

Itoh S., Kojima H. and Yurimoto H. (2004) Petrography and oxygen isotopic compositions in refractory inclusions from CO chondrites. *Geochim. Cosmochim. Acta* **68**, 183–194.

Itoh S. and Yurimoto H. (2007) Fluctuation frequency of oxygen isotope reservoirs in the early Solar System (abstract). In *Workshop on the Chronology of Meteorites and the Early Solar System*, pp. 78–79.

Jabeen I., Kusakabe M., Nakamura T. and Nagao K. (1999) Parent body processes in Allende: evidence from oxygen isotope study of the Allende chondrules. *Symp. Antarct. Meteorit.* **24**, 59–61.

Jacobsen B., Yin Q.-Z., Moynier F., Amelin Y., Krot A. N., Nagashima K., Huthceon I. D. and Palme H. (2008a) ^{26}Al–^{26}Mg and ^{207}Pb–^{206}Pb systematics of Allende CAIs: canonical solar initial ^{26}Al/^{27}Al ratio reinstated. *Earth Planet Sci. Lett.* **272**, 353–364.

Jacobsen B., Cosarinsky M., Wasserburg G. J., Yin Q.-Z., McKeegan K. D., Hutcheon I. D., Krot A. N., Nagashima K. and Palme H. (2008b) Mg isotopic composition of low Al/Mg phases in CAIs: the initial solar ^{26}Mg/^{24}Mg? (abstract). *Lunar Planet. Sci.* **39**, 2387.

Johansen A., Oishi J. S., Low M.-M. , Klahr H., Henning T. and Youdin A. (2007) Rapid planetesimal formation in turbulent circumstellar disks. *Nature* **448**, 1022–1025.

Jones R. H. (1994) Petrology of FeO-poor, porphyritic pyroxene chondrules in the Semarkona chondrite. *Geochim. Cosmochim. Acta* **58**, 5325–5340.

Jones R. H. and Scott E. R. D. (1989) Petrology and thermal history of type IA chondrules in the Semarkona (LL3.0) chondrite. *Proc. Lunar Planet Sci. Conf.* **19**, 523–536.

Jones R. H., Leshin L. A., Yunbin G., Sharp Z., Durakiewicz T. and Schilk A. J. (2004) Oxygen isotope heterogeneity in chondrules from the Mokoia CV3 carbonaceous chondrites. *Geochim. Cosmochim. Acta* **68**, 3423–3438.

Jones R. H., Grossman J. N. and Rubin A. E. (2005) Chemical, mineralogical and isotopic properties of chondrules: clues to their origin. In *Chondrites and the Protoplanetary Disk*, vol. 341 (eds. A. N. Krot, E. R. D. Scott and B. Reipurth). ASP Conference Series, pp. 251–286.

Jones R. H. and Norman M. D. (2008) Trace elements in aluminum-rich chondrules from the Mokoia CV chondrite (abstract). *Lunar Planet. Sci.* **39**, 2051.

Kimura M., El Goresy A., Palme H. and Zinner E. (1993) Ca–Al-rich inclusions in the unique chondrite ALH85085—Petrology, chemistry, and isotopic compositions. *Geochim. Cosmochim. Acta* **57**, 2329–2359.

Kita N. T., Nagahara H., Togashi S. and Morishita Y. (2000) A short duration of chondrule formation in the solar nebula: evidence from ^{26}Al in Semarkona ferromagnesian chondrules. *Geochim. Cosmochim. Acta* **64**, 3913–3922.

Kita N. T., Huss G. R., Tachibana S., Amelin Y., Nyquist L. E. and Hutcheon I. D. (2005) Constraints on the origin of chondrules and CAIs from short-lived and long-lived radionuclides. In *Chondrites and the Protoplanetary Disk*, vol. 341 (eds. A. N. Krot, E. R. D. Scott and B. Reipurth). ASP Conference Series, pp. 558–588.

Kita N. T., Nagahara H., Tomomura S., Tachibana S. and Valley J. W. (2006) Systematic Oxygen isotopic variations among chondrules from the least equilibrated ordinary chondrites: improved ion microprobe precision (abstract). *Lunar Planet. Sci.* **37**, 1496.

Kita N. T., Ushikubo T., Knight K. B., Mendybaev R. A., Davis A. M. and Richter F. M. (2007) High precision Al–Mg internal isochron using zoned melilite in CAI (abstract). In *Workshop on the Chronology of Meteorites and the Early Solar System*. pp. 92–93.

Kita N. T., Ushikubo T., Kimura M., Nyquist L. E. and Valley J. W. (2008) Oxygen isotope systematics of chondrules from the least equilibrated H chondrite (abstract). *Lunar Planet. Sci.* **39**, 2059.

Kleine T., Mezger K., Palme H., Scherer E. and Munker C. (2005) Early core formation in asteroids and late accretion of chondrite parent bodies: evidence from ^{182}Hf–^{182}W in CAIs, metal-rich chondrites, and iron meteorites. *Geochim. Cosmochim. Acta* **69**, 5805–5818.

Kring D. A. and Boynton W. V. (1990) Trace-element compositions of Ca-rich chondrules from Allende: relationships between refractory inclusions and ferromagnesian chondrules (abstract). *Meteoritics* **25**, 377.

Krot A. N., Petaev M. I., Scott E. R. D., Choi B.-G., Zolensky M. E. and Keil K. (1998) Progressive alteration in CV3 chondrites: more evidence for asteroidal alteration. *Meteorit. Planet. Sci.* **33**, 1065–1085.

Krot A. N., Ulyanov A. A., Meibom A. and Keil K. (2001a) Forsterite-rich accretionary rims around Ca, Al-rich inclusions from the reduced CV3 chondrite Efremovka. *Meteorit. Planet. Sci.* **36**, 611–628.

Krot A. N., McKeegan K. D., Russell S. S., Meibom A., Weisberg M. K., Zipfel J., Krot T. V., Fagan T. J. and Keil K. (2001b) Refractory Ca, Al-rich inclusions and Al-diopside-rich chondrules in the metal-rich chondrites Hammadah al Hamra 237 and QUE 94411. *Meteorit. Planet. Sci.* **36**, 1189–1217.

Krot A. N., Meibom A., Russell S. S., Alexander C. M. O', Jeffries T. E. and Keil K. (2001c) A new astrophysical setting for chondrule formation. *Science* **291**, 1776–1779.

Krot A. N. and Keil K. (2002) Anorthite-rich chondrules in CR and CH carbonaceous chondrites: genetic link between Ca, Al-rich inclusions and ferromagnesian chondrules. *Meteorit. Planet. Sci.* **37**, 91–111.

Krot A. N., Meibom A., Weisberg M. K. and Keil K. (2002a) The CR chondrite clan: implications for early solar system processes. *Meteorit. Planet. Sci.* **37**, 1451–1490.

Krot A. N., Hutcheon I. D. and Keil K. (2002b) Anorthite-rich chondrules in the reduced CV chondrites: evidence for complex formation history and genetic links between CAIs and ferromagnesian chondrules. *Meteorit. Planet. Sci.* **37**, 155–182.

Krot A. N., Keil K., Goodrich C., Weisberg M. K. and Scott E. R. D. (2003) Classification of meteorites. In *Meteorites, Comets and Planets*, vol. 1 (ed. A.M. Davis), *Treatise on Geochemistry*, vol. 341 (eds. H. D. Holland and K. K. Turekian). Elsevier, Oxford, pp. 83–129.

Krot A. N., Petaev M. I., Russell S. S., Itoh S., Fagan T., Yurimoto H., Chizmadia L., Weisberg M. K., Komatsu M., Ulyanov A. A. and Keil K. (2004a) Amoeboid olivine aggregates in carbonaceous chondrites: records of nebular and asteroidal processes (Invited review). *Chem. Erde* **64**, 185–239.

Krot A. N., MacPherson G. J., Ulyanov A. A. and Petaev M. I. (2004b) Fine-grained, spinel-rich inclusions from the reduced CV chondrites Efremovka and Leoville. I. Mineralogy, petrology, and bulk chemistry. *Meteorit. Planet. Sci.* **39**, 1517–1553.

Krot A. N., Amelin Y., Cassen P. and Meibom A. (2005a) Young chondrules in CB chondrites from a giant impact in the early Solar System. *Nature* **436**, 989–992.

Krot A. N., Yurimoto H., Hutcheon I. D. and MacPherson G. J. (2005b) Relative chronology of CAI and chondrule formation: evidence from chondrule-bearing igneous CAIs. *Nature* **434**, 998–1001.

Krot A. N., McKeegan K. D., Huss G. R., Liffman K., Sahijpal S., Hutcheon I. D., Srinivasan G., Bischoff A. and Keil K. (2005c) Aluminum-magnesium and oxygen isotope study of relict Ca–Al-rich inclusions in chondrules. *Astrophys. J.* **629**, 1227–1237.

Krot A. N., Hutcheon I. D., Yurimoto H., Cuzzi J. N., McKeegan K. D., Scott E. R. D., Libourel G., Chaussidon M., Aléon J. and Petaev M. I. (2005d) Evolution of oxygen isotopic composition in the inner solar nebula. *Astrophys. J.* **622**, 1333–1342.

Krot A. N., Yurimoto H., McKeegan K. D., Leshin L., Chaussidon M., Libourel G., Yoshitake M., Huss G. R., Guan Y. and Zanda B. (2006) Oxygen isotopic compositions of chondrules: implication for understanding oxygen isotope evolution of the solar nebula. *Chem. Erde* **66**, 249–276.

Krot A. N., Yurimoto H., Hutcheon I. D., Libourel G., Chaussidon M., Petaev M. I., MacPherson G. J., Paque-Heather J. and Wark D. (2007a) Anorthite-rich, igneous (Type C) Ca, Al-rich inclusions from the CV carbonaceous chondrite Allende: evidence for multistage formation history. *Geochim. Cosmochim. Acta* **71**, 4342–4364.

Krot A. N., Nagashima K., Huss G. R., Bizzarro M., Ciesla F. J. and Ulyanov A. A. (2007b) Relict refractory inclusions in magnesium porphyritic chondrules from the CH and CH/CB carbonaceous chondrites (abstract). *Meteorit. Planet. Sci.* **42**(Suppl.), A90.

Krot A. N., Nagashima K., Hutcheon I. D., Davis A. M., Thrane K., Bizzarro M., Huss G. R., Papanastassiou D. A. and Wasserburg G. J. (2008a) Oxygen isotopic compositions of individual minerals from FUN CAIs (abstract). *Lunar Planet Sci.* **39**, 2162.

Krot A. N., Nagashima K., Bizzarro M., Huss G. R., Davis A. M., McKeegan K. D., Meyer B. S. and Ulyanov A. A. (2008b) Multiple generations of refractory inclusions in the metal-rich carbonaceous chondrites Acfer 182/214 and Isheyevo. *Astrophys. J.* **672**, 713–721.

Krot A. N., Chaussidon M., Yurimoto H., Sakamoto N., Nagashima K., Hutcheon I. D. and MacPherson G. J. (2008c) Oxygen isotopic compositions of Allende Type C CAIs: evidence for isotopic exchange during nebular melting and asteroidal metamorphism. *Geochim. Cosmochim. Acta.* **72**, 2534–2555.

Krot A. N., Ivanova M. A. and Ulyanov A. A. (2008d) Chondrules in the CB/CH-like carbonaceous chondrite Isheyevo: evidence for various chondrule-forming mechanisms and multiple chondrule generations. *Chem. Erde* **67**, 283–300.

Krot A. N. and Nagashima K. (2008) Oxygen isotopic composition of porphyritic and non-porphyritic chondrules from the CH/CB-like chondrite Isheyevo (abstract). *Meteorit. Planet. Sci.* **43**(Suppl.), A81.

Kunihiro T., Rubin A. E., McKeegan K. D. and Wasson J. T. (2004) Initial ^{26}Al/^{27}Al in carbonaceous chondrite chondrules: too little ^{26}Al to melt asteroids. *Geochim. Cosmochim. Acta* **68**, 2947–2957.

Kurahashi E., Kita N. T., Nagahara H. and Morishita Y. (2004) Contemporaneous formation of chondrules in the^{26}Al–^{26}Mg system for ordinary and CO chondrites (abstract). *Lunar Planet. Sci.* **35**, 1476.

Kurahashi E., Kita N. T., Nagahara H. and Morishita Y. (2008) ^{26}Al–^{26}Mg systematics of chondrules in a primitive CO chondrite. *Geochim. Cosmochim. Acta* **72**, 3865–3883.

Lee T. (1988) Implications of isotopic anomalies for nucleosynthesis. In *Meteorites and the Early Solar System*. University of Arizona Press, Tucson, AZ, pp. 1063–1089.

Lee T., Shu F. H., Shang H., Glassgold A. E. and Rehm K. E. (1998) Protostellar cosmic rays and extinct radioactivities in meteorites. *Astrophys. J.* **506**, 898–912.

LaTourrette T. and Wasserburg G. J. (1998) Mg diffusion in anorthite: implications for the formation of early solar system planetesimals.. *Earth Planet Sci. Lett.* **158**, 91–108.

Leya I., Halliday A. N. and Wieler R. (2003) The predictable collateral consequences of nucleosynthesis by spallation reactions in the early Solar System. *Astrophys. J.* **594**, 605–616.

Libourel G. and Krot A. N. (2006) Evidence for the presence of planetesimal material among the precursors of magnesian chondrules of nebular origin. *Earth Planet Sci. Lett.* **254**, 1–8.

Libourel G., Krot A. N. and Tissandier L. (2006) Role of gas–melt interaction during chondrule formation. *Earth Planet Sci. Lett.* **251**, 232–240.

Lin Y., Guan Y., Leshin L. A., Ouyang Z. and Wang D. (2005) Short-lived ^{36}Cl in a Ca- and Al-rich inclusion from the Ningqiang carbonaceous chondrite. *Proc. Nation. Acad. Sci.* **102**, 1306–1311.

Lin Y., Kimura M., Miao B., Dai D. and Monoi A. (2006) Petrographic comparison of refractory inclusions from different chemical groups of chondrites. *Meteorit. Planet. Sci.* **41**, 67–81.

Liu M.-C., McKeegan K. D., Davis A. M. and Irelandm T. R. (2007) ^{26}Mg deficits in CM hibonite grains: nucleosynthetic, galactic chemical evolution, or spallogenic? (abstract). *Lunar Planet. Sci.* **38**, 2253.

Longhi J. (1991) Comparative liquidus equilibria of hypersthene-normative basalts at low pressure. *Amer. Mineral.* **76**, 785–800.

Lugmair G. W. and Shukolyukov A. (1998) Early solar system timescales according to ^{53}Mn–^{53}Cr systematics. *Geochim. Cosmochim. Acta* **62**, 2863–2886.

Lugmair G. W. and Shukolyukov A. (2001) Early solar system events and timescales. *Meteorit. Planet. Sci.* **36**, 1017–1026.

Lyons J. R. and Young E. D. (2005) CO self-shielding as the origin of oxygen isotope anomalies in the early solar nebula. *Nature* **435**, 317–320.

MacPherson G. J., Wark D. A. and Armstrong J. T. (1988) Primitive material surviving in chondrites: refractory inclusions. In *Meteorites and the Early Solar System* (eds. J. F. Kerridge and M. S. Matthews). University of Arizona Press, Tucson, pp. 746–807.

MacPherson G. J., Davis A. M. and Zinner E. K. (1995) The distribution of ^{26}Al in the early solar system. *Meteoritics* **30**, 365–386.

MacPherson G. J., Huss G. R. and Davis A. M. (2002) Extinct ^{10}Be in Type A calcium–aluminum-rich inclusions from CV chondrites. *Geochim. Cosmochim. Acta* **67**, 3165–3179.

MacPherson G. J., Simon S. B., Davis A. M., Grossman L. and Krot A. N. (2005) Calcium–aluminum-rich inclusions: major unanswered questions. In *Chondrites and the Protoplanetary Disk*, vol. 341 (eds. A. N. Krot, E. R. D. Scott and B. Reipurth). ASP Conference Series, pp. 225–251.

MacPherson G. J., Nagashima K., Bullock E. S. and Krot A. N. (2008) Mass-dependent oxygen isotopic fractionation in non-FUN forsterite-bearing Type B CAIs (abstract). *Linar Planet. Sci.* **39**, 2039.

Makide K., Nagashima K., Krot A. N., Huss G. R., Hutcheon I. D. and Biscoff A. (2009) Oxygen- and magnesium-isotope compositions of calcium–aluminum-rich inclusions from CR

carbonaceous chondrites. *Geochim. Cosmochim. Acta* **73**, 5018–5050.

Marhas K. K., Hutcheon I. D., Krot A. N. and Goswami J. N. (2000) ^{26}Al in carbonaceous chondrite chondrules (abstract). *Meteorit. Planet. Sci.* **35**(Suppl.), A102.

Marhas K. K., Goswami J. N. and Davis A. M. (2002) Short-lived nuclides in hibonite grains from Murchison: evidence for Solar System evolution. *Science* **298**, 2182–2185.

Markowski A., Quitté G., Kleine T., Halliday A. N., Bizzarro M. and Irving A. J. (2008) Hafnium tungsten chronometry of angrites and the earliest evolution of planetary objects. *Earth Planet Sci. Lett.* **262**, 214–229.

McKeegan K. D., Chaussidon M. and Robert F. (2000a) Incopporation of short-lived ^{10}Be in a calicum–aluminum-rich inclusion from the Allende meteorite. *Science* **289**, 1334–1337.

McKeegan K. D., Greenwood J. P., Leshin L. A. and Cosarinsky M. (2000b) Abundance of ^{26}Al in ferromagnesian chondrules of unequilibrated ordinary chondrites (abstract). *Lunar Planet. Sci.* **31**, 2009.

McKeegan K. D. et al. (2006) Isotopic compositions of cometary matter returned by Stardust. *Science* **314**, 1724–1728.

Meibom A., Petaev M. I., Krot A. N., Keil K. and Wood J. A. (2001) Growth mechanism and additional constraints on FeNi-metal condensation in the solar nebula. *J. Geophys. Res.* **104**, 22053–22059.

Misawa K. and Nakamura N. (1996) Origin of refractory precursor components of chondrules from carbonaceous chondrites. In *Chondrules and the Protoplanetary Disk* (eds. R. H. Hewins, R. H. Jones and E. R. D. Scott), pp. 99–105.

Miura H. and Nakamoto T. (2006) Shock-wave heating model for chondrule formation: prevention of isotopic fractionation. *Astrophys. J.* **651**, 1272–1295.

Moynier F., Yin Q.-Z. and Jacobsen B. (2007) Dating the first stage of planet formation. *Astrophys. J.* **671**, L181–L183.

Mostefaoui S., Kita N. T., Togashi S., Tachibana S., Nagahara H. and Morishita Y. (2001) The relative formation ages of ferromagnesian chondrules inferred from their initial ^{26}Al/^{27}Al ratios. *Meteorit. Planet. Sci.* **37**, 421–438.

Mostefaoui S., Lugmair G. W. and Hoppe P. (2005) ^{60}Fe: a heat source for planetary differentiation from a nearby supernova explosion. *Astrophys. J.* **625**, 271–277.

Nagashima K., Krot A. N. and Hua X. (2007a) Common presence of ^{16}O-rich melilite in calcium-aluminum-rich inclusions from the least metamorphosed CV carbonaceous chondrite Kaba (abstract). *Lunar Planet Sci.* **38**, 2059.

Nagashima K., Krot A. N. and Chaussidon M. (2007b) Aluminum–magnesium isotope systematics of chondrules from CR chondrites (abstract). *Meteorit. Planet. Sci.* **42**(Suppl.), A115.

Nagashima K., Krot A. N. and Huss G. R. (2008) ^{26}Al in chondrules from CR carbonaceous chondrites (abstract). *Lunar Planet Sci.* **39**, 2224.

Nakamoto T., Hayashi M. R., Kita N. T. and Tachibana S. (2005) Chondrule-forming shock waves in the solar nebula by X-ray flares. In *Chondrites and the Protoplanetary Disk*, vol. 341 (eds. A. N. Krot, E. R. D. Scott and B. Reipurth). ASP Conference Series, pp. 883–893.

Niemeyer S. (1988) Titanium isotopic anomalies in meteorites. *Geochim. Cosmochim. Acta* **52**, 309–318.

Nuth J. A., III, Brearley A. J. and Scott E. R. D. (2005) Microcrystals and amorphous material in comets and primitive meteorites: keys to understanding processes in the early Solar System. In *Chondrites and the Protoplanetary Disk*, vol. 341 (eds. A. N. Krot, E. R. D. Scott and B. Reipurth). ASP Conference Series, pp. 675–701.

Nyquist L., Lindstrom D., Mittlefehldt D., Shih C.-Y., Wiesmann H., Wentworth S. and Martinez R. (2001) Manganese–chromium formation intervals for chondrules from the Bishunpur and Chainpur meteorites. *Meteorit. Planet. Sci.* **36**, 911–938.

Ouellette N., Desch S. J., Hester J. J. and Leshin L. A. (2005) A nearby supernova injected short-lived radionuclides into our protoplanetary disk. In *Chondrites and the Protoplanetary Disk*, vol. 341 (eds. A. N. Krot, E. R. D. Scott, B. Reipurth). ASP Conference Series, pp. 527–539.

Pack A., Shelley J. M. G. and Palme H. (2004) Rare earth element fractionation in chondrules (abstract). *Lunar Planet Sci.* **35**, 2062.

Palme H. and Klerner S. (2000) Formation of chondrules and matrix in carbonaceous chondrites (abstract). *Meteorit. Planet. Sci.* **35**(Suppl.), A124.

Petaev M. I., Meibom A., Krot A. N., Wood J. A. and Keil K. (2001) The condensation origin of zoned metal grains in QUE94411: implications for the formation of the Bencubbin-like chondrites. *Meteorit. Planet. Sci.* **36**, 93–106.

Petaev M. I. and Wood J. A. (2005) Meteoritic constraints on temperatures, pressures, cooling rates, chemical compositions, and models of condensation in the solar nebula. In *Chondrites and the Protoplanetary Disk*, vol. 341 (eds. A. N. Krot, E. R. D. Scott and B. Reipurth). ASP Conference Series, pp. 373–407.

Quitté G., Halliday A. N., Meyer B. S., Markowski A., Latkoczy C. and Günther D. (2007) Correlated ^{60}Fe, ^{62}Ni, and ^{96}Zr in refractory inclusions and the origin of the Solar System. *Astrophys. J.* **655**, 678–684.

Reipurth B. and Bally J. (2001) Herbig-Haro flows: probes of early stellar evolution. *Ann. Rev. Astron. Astrophys.* **39**, 403–455.

Richter F. M., Mendybaev R. A. and Davis A. M. (2006) Conditions in the protoplanetary disk as seen by the type B CAIs. *Meteorit. Planet. Sci.* **41**, 83–93.

Robert F. and Chaussidon M. (2003) Boron and lithium isotopic composition in chondrules from the Mokoia meteorite (abstract). *Lunar Planet. Sci.* **34**, 1344.

Rubin A. E. and Wasson J. T. (1987) Chondrules, matrix and coarse-grained chondrule rims in the Allende meteorite—Origin, interrelationships, and possible precursor components. *Geochim. Cosmochim. Acta* **51**, 1923–1937.

Rubin A. E., Kallemeyn G. W., Wasson J. T., Clayton R. N., Mayeda T. K., Grady M., Verchovsky A. B., Eugster O. and Lorenzetti S. (2003) Formation of metal and silicate globules in Gujba: a new Bencubbin-like meteorite fall. *Geochim. Cosmochim. Acta* **67**, 3283–3298.

Rudraswami N. G. and Goswami J. N. (2007) ^{26}Al in chondrules from unequilibrated L chondrites: onset and duration of chondrule formation in the early solar system.. *Earth Planet Sci. Lett.* **257**, 231–244.

Russell S. S., Srinivasan G., Huss G. R., Wasserburg G. J. and MacPherson G. J. (1996) Evidence for wide spread ^{26}Al in the solar nebula and constraints for nebula time scales. *Science* **273**, 757–762.

Russell S. S., Huss G. R., Fahey A. J., Greenwood R. C., Hutchison R. and Wasserburg G. J. (1998) An isotopic and petrologic study of calcium-aluminum-rich inclusions from CO3 meteorites. *Geochim. Cosmochim. Acta* **62**, 689–714.

Russell S. S., Krot A. N., MacPherson G. J., Huss G. R., Itoh S., Yurimoto H. and Keil K. (2005) Genetic relationship between refractory inclusions and chondrules. In *Chondrites and the Protoplanetary Disk*, vol. 341 (eds. A. N. Krot, E. R. D. Scott and B. Reipurth). ASP Conference Series, pp. 317–353.

Russell S. S., Hartmann L., Cuzzi J. N., Krot A. N., Gounelle M. and Weidenschilling S. J. (2006) Timescales of the solar protoplanetary disk. In *Meteorites and The Early Solar System II* (eds. D. Lauretta and H. McSween). University of Arizona Press, pp. 233–253.

Ryerson F. J. and McKeegan K. D. (1994) Determination of oxygen self-diffusion in åkermanite, anorthite, diopside, and spinel: implications for oxygen isotopic anomalies and the thermal histories of Ca–Al-rich inclusions. *Geochim. Cosmochim. Acta* **58**, 3713–3734.

Sahijpal S., Goswami J. N., Davis A. M., Lewis R. S. and Grossman L. (1998) A stellar origin for the short-lived nuclides in the early solar system. *Nature* **391**, 559–562.

Sahijpal S. and Goswami J. N. (1998) Refractory phases in primitive meteorites devoid of ^{26}Al and ^{41}Ca: representative samples of first Solar System solids? *Astrophys. J.* **509**, L137–L140.

Sanders I. S. and Taylor G. J. (2005) Implication of ^{26}Al in nebular dust: formation of chondrules by disruption of molten planetesimals. In *Chondrites and the Protoplanetary Disk*, vol. 341 (eds. A. N. Krot, E. R. D. Scott and B. Reipurth). ASP Conference Series, pp. 915–933.

Scott E. R. D. and Krot A. N. (2003) Chondrites and their components. In *Meteorites, Comets and Planets*, vol. 1 (ed. A.M. Davis) *Treatise on Geochemistry* (eds. H.D. Holland and K.K. Turekian), Elsevier, Oxford, pp. 143–200.

Scott E. R. D. and Krot A. N. (2005) Chondritic meteorites and the high-temperature nebular origins of their components. In *Chondrites and the Protoplanetary Disk*, vol. 341 (eds. A. N. Krot, E. R. D. Scott, B. Reipurth). ASP Conference Series, pp. 15–54.

Scott E. R. D. and Sanders I. S. (2008) Carbonaceous chondrite Mn–Cr isochron: implications for chondrule formation and the early fractionation of moderately volatile elements (abstract). *Lunar Planet. Sci.* **39**, 2065.

Shahar A. and Young E. D. (2007) Astrophysics of CAI formation as revealed by silicon isotope LA-MC-ICPMS of an igneous CAI. *Earth Planet Sci. Lett.* **257**, 497–510.

Shu F. H., Shang H. and Lee T. (1996) Towards an astrophysical theory of chondrites. *Science* **271**, 1545–1552.

Shu F. H., Shang H., Glassgold A. E. and Lee T. (1997) X-rays and fluctuating *x*-winds from protostars. *Science* **277**, 1475–1479.

Shu F. H., Shang H., Gounelle M., Glassgold A. E. and Lee T. (2001) The origin of chondrules and refractory inclusions in chondritic meteorites. *Astrophys. J.* **548**, 1029–1050.

Shukolyukov A. and Lugmair G. W. (2006) Manganese–chromium isotope systematics of carbonaceous chondrites.. *Earth Planet Sci. Lett.* **250**, 200–213.

Simon S. B., Davis A. M., Grossman L. and McKeegan K. D. (2002) A hibonite-corundum inclusion from Murchison: a first-generation condensate from the solar nebula. *Meteorit. Planet. Sci.* **37**, 533–548.

Simon J. I. and Young E. D. (2007) Open-system behavior of CAIs: a key component to their 26Al/26Mg chronologies (abstract). In *Workshop on the Chronology of Meteorites and the Early Solar System*, pp. 156–157.

Simon S. B., Sutton S. R. and Grossman L. (2007) Valence of titanium and vanadium in pyroxene in refractory inclusion interiors and rims. *Geochim. Cosmochim. Acta* **71**, 3098–3118.

Srinivasan G. and Bischoff A. (2001) Ca–K and Al–Mg studies of CAIs from CH and CR chondrites (abstract). *Meteorit. Planet. Sci.* **36**(Suppl.), A196.

Srinivasan G., Ulyanov A. A. and Goswami J. N. (1994) ^{41}Ca in the early solar system. *Astrophys. J.* **431**, L67–L70.

Srinivasan G., Chaussidon M. and Bischoff A. (2007) ^{26}Al and ^{10}Be in Efremovka and Acfer CAIs: constraints on the origin of short-lived radionuclides (abstract). *Lunar Planet. Sci.* **38**, 1781.

Stolper E. (1983) Crystallization sequences of Ca–Al-rich inclusions from Allende—an experimental study. *Geochim. Cosmochim. Acta* **46**, 2159–2180.

Sugiura N., Shuzou Y. and Ulyanov A. (2001) Beryllium–boron and aluminum–magnesium chronology of calcium–aluminum-rich inclusions in CV chondrites. *Meteorit. Planet. Sci.* **36**, 1397–1408.

Tachibana S. and Huss G. R. (2003) The initial abundance of ^{60}Fe in the Solar System. *Astrophys. J.* **588**, L41–L44.

Tachibana S. and Huss G. R. (2005) Sulfur isotope composition of putative primary troilite in chondrules from Bishunpur and Semarkona. *Geochim. Cosmochim. Acta* **69**, 3075–3097.

Tachibana S., Huss G. R., Kita N. T., Shimoda G. and Morishita Y. (2006) ^{60}Fe in chondrites: debris from a nearby supernova in the early Solar System? *Astrophys. J.* **639**, L87–L90.

Tatsumoto M., Unruh D. M. and Desborough G. A. (1976) U–Th–Pb and Rb–Sr systematics of Allende and U–Th–Pb systematics of Orgueil. *Geochim. Cosmochim. Acta* **40**, 617–634.

Taylor D. J., Cosarinsky M., Liu M.-C., McKeegan K. D., Krot A. N. and Hutcheon I. D. (2005) Survey of initial ^{26}Al in Type A and B CAIs: evidence for an extended formation period for refractory inclusions (abstract). *Meteorit. Planet. Sci.* **40**(Suppl.), A151.

Thrane K., Bizzarro M. and Baker J. A. (2006) Extremely brief formation interval for refractory inclusions and uniform distribution of ^{26}Al in the early Solar System. *Astrophys. J.* **646**, L159–L162.

Thrane K., Nagashima K., Krot A. N. and Bizzarro M. (2008) Discovery of a new FUN CAI from a CV carbonaceous chondrite: evidence for multistage thermal processing in the protoplanetary disk. *Astrophys. J.* **680**, L141–L144.

Wadhwa M., Amelin Y., Bizzarro M., Kita N., Kleine T., Lugmair G. W. and Yin Q. (2007) Comparison of short-lived and long-lived chronometers: towards a consistent chronology of the early Solar System (abstract). In *Workshop on the Chronology of Meteorites and the Early Solar System,* pp. 173–174.

Wark D. A. and Lovering J. F. (1977) Marker events in the early solar system: evidence from rims on Ca, Al-rich inclusions in carbonaceous chondrites. *Proc. Lunar Planet Sci. Conf.* **8**, 95–112.

Wark D. A. and Boynton W. V. (2001) The formation of rims on calcium–aluminum-rich inclusions: step I—flash heating. *Meteorit. Planet. Sci.* **36**, 1135–1166.

Wasson J. T. (2008) Evaporation of nebular fines during chondrule formation. *Icarus* **195**, 895–907.

Wasson J. T., Krot A. N., Lee M. S. and Rubin A. E. (1994) Compound chondrules in ordinary chondrites: evidence for multiple heating events and for large-scale heterogenieties in the nebula. *Geochim. Cosmochim. Acta* **59**, 1847–1869.

Wasson J. T., Yurimoto H. and Russell S. S. (2001) ^{16}O-rich melilite in CO3.0 chondrites. Possible formation of common, ^{16}O-poor melilite by aqueous alteration. *Geochim. Cosmochim. Acta* **65**(453), 9–4549.

Watson D. M. (2007) Sedimentation, mineralization, planet formation and dissipation in protoplanetary disks (abstract). In *Workshop on the Chronology of Meteorites and the Early Solar System*, p. 175.

Weber D., Zinner E. and Bischoff A. (1995) Trace element abundances and magnesium, calcium, and titanium isotopic compositions of grossite-containing inclusions from the carbonaceous chondrite Acfer 182. *Geochim. Cosmochim. Acta* **59**, 803–823.

Weidenschilling S. J. (1977) Aerodynamics of solid bodies in the solar nebula. *Royal Astronom. Soc. Mon. Notices* **180**, 57–70.

Weidenschilling S. J., Marzari F. and Hood L. L. (1998) The origin of chondrules at Jovian resonances. *Science* **279**, 681–684.

Weisberg M. K., Kita N. T., Ushikubo T., Connolly H. C., Ebel D. S., Spicuzza M. J. and Valley J. W. (2007) Petrologic-isotopic

study of amoeboid olivine aggregates in CR chondrites (abstract). *Lunar Planet. Sci.* **38**, 1588.

Whattam S. A., Hewins R. H., Cohen B. A., Seaton N. C. and Prior D. J. (2008) Granoblastic olivine aggregates in magnesian chondrules: planetesimal fragments or thermally annealed solar nebula condensates? *Earth Planet Sci. Lett.* **269**, 200–211.

Yin Q.-Z., Jacobsen B., Moynier F. and Hutcheon I. D. (2007) Toward consistent chronology in the early Solar System: high-resolution ^{53}Mn–^{53}Cr chronometry for chondrules. *Astrophys. J.* **662**, L43–L46.

Yoneda S. and Grossman L. (1995) Condensation of CaO–MgO–Al_2O_3–SiO_2 liquids from cosmic gases. *Geochim. Cosmochim. Acta* **59**, 3413–3444.

Young E. D., Simon J. I., Galy A., Russell S. S., Tonui E. and Lovera O. (2005) Supra-canonical 26Al/27Al and the residence time of CAIs in the solar protoplanetary disk. *Science* **308**, 223–227.

Young E. D., Gounelle M., Smith R., Morris M. R. and Pontoppiddan K. M. (2008) Solar System oxygen-isotope ratios result from pollution by Type II supernovae (abstract). *Lunar Planet. Sci* **39**, 1329.

Yurimoto H. and Wasson J. T. (2002) Extremely rapid cooling of a carbonaceous-chondrite chondrule containing very ^{16}O-rich olivine and a ^{26}Mg-excess. *Geochim. Cosmochim. Acta* **66**, 4355–4363.

Yurimoto H. and Kuramoto K. (2004) Molecular cloud origin for the oxygen-isotope heterogeneity in the Solar System. *Science* **305**, 1763–1766.

Yurimoto H., Ito M. and Nagasawa H. (1998) Oxygenisotope exchange between refractory inclusion in Allende and solar nebula gas. *Science* **282**, 1874–1877.

Yurimoto H., Kuramoto K., Krot A. N., Scott E. R. D., Cuzzi, J. N., Thiemens M. H. and Lyons J. R. (2007) Origin and evolution of oxygen isotopic compositions of the Solar System. In *Protostars and Planets* (eds. V. B. Reipurth, D. Jewitt and K. Keil). University of Arizona Press, Tucson, pp. 849–862.

Zinner E. and Göpel C. (2002) ^{26}Al in H4 chondrites: implications for its production and its usefulness as a fine-scale chronometer for early solar system events. *Meteorit. Planet. Sci.* **37**, 1001–1013.

Zipfel J. and Weyer S. (2007) *In situ* analyses of Fe isotopes in zoned metal grains of Hammadah al Hamra 237 (abstract). *Lunar Planet. Sci.* **38**, 1927.

Zolensky ME. et al. (2006) Mineralogy and petrology of comet 81P/Wild 2 nucleus samples. *Science* **314**, 1735–1739.

Associate editor: Gregory F. Herzog